IFAC

INTERNATIONAL FEDERATION
OF AUTOMATIC CONTROL

WARSZAWA 1969

Chemical and Allied
Paper-Sugar-Cement Industries

Fourth Congress of the International Federation of Automatic Control
Warszawa 16–21 June 1969

TECHNICAL SESSION
66

Organized by
Naczelna Organizacja Techniczna w Polsce

INTERNATIONAL FEDERATION OF AUTOMATIC CONTROL

Chemical and Allied
Paper-Sugar-Cement Industries

TECHNICAL SESSION No 66

FOURTH CONGRESS OF THE INTERNATIONAL
FEDERATION OF AUTOMATIC CONTROL
WARSZAWA 16 – 21 JUNE 1969

Organized by
Naczelna Organizacja Techniczna w Polsce

Contents

Wydawnictwa Czasopism Technicznych NOT - Polska

Wyk. "Zespół" zam.506.69 n. 1034 +7

PROCESS COMPUTER CONTROLS EUROPE'S LARGEST NEWSPRINT MILL

Auther: Tekn. lic. Henry Sandblom, ASEA, Västerås, Sweden.

Introduction

The paper describes an on-line process computer system installed at Hallsta Paper Mill, belonging to the Holmens Bruks & Fabriks AB, Sweden. The mill, which is the largest in Europe, has an annual capacity of 450,000 tons of newsprint.

The computer controls the co-ordination of, for example:

- the paper production and pulp consumption of the paper machines
- the production of mechanical pulp
- the flow and storage of the pulp broke and the white water

The consumption and production of electrical energy for all the mills and factories within the Holmens Group are also controlled by the computer.

The paper will give details about the control system, including control strategies and programmes. Experience from the start-up and the operation up to the present day will be given. The economic justification for computer control will be discussed in broad terms.

The co-ordination of the units of a newsprint mill is complex

In a newsprint mill the major process units are the paper machines, the wood grinders, the pulp storage tanks and the broke and white water systems. In addition to these there is usually a sulphite (or sulphate) mill (15 - 25 % of the total pulp consumption for newsprint consists of such pulp).

At Holmens Bruks & Fabriks AB, Hallsta Paper Mill, there are 7 paper machines, the largest of which has a capacity of

150,000 tons newsprint a year. The number of wood grinders is 23, the largest of which have an installed power of 4,000 kW. The oldest part of the mill is more than 50 years old, whereas the new larger paper machine and the latest wood grinders were started during 1967. With a total production of close on 450,000 tons a year, this is the largest paper mill in Europe. A schematic diagram of the mill is shown in fig. 1.

Large flows of pulp and white water through the mill make the various operation units very dependent on each other. Large disturbances, e.g., wire changes in the paper machines with sudden interruptions in the flows, make the situation still more complicated. Pulp and paper quality, the consumption of electric power and the fibre loss with the waste water are all related to the quality of the co-ordination of the plants. -If all of these factors are taken into account in a large and progressively built up paper mill like Hallsta, the picture becomes quite complex.

It is, in fact, quite impossible for the operators to run the whole mill in the optimum manner, or even get anywhere near this, with the conventional means used today, i.e., so that the pulp quality is maximized, the electricity consumption minimized, etc. Fig. 2 shows how such a mill may be run without a computer connected to it. To ensure that sufficient pulp is available at every instant for the consumption at the paper machines, the operator tries to maintain a high level in the pulp buffer tank. If the level starts to drop, he switches in a number of grinders. Disturbances in the flow, such as the shut down of a paper machine, which may occur soon after this, will necessitate the stopping of a number of wood grinders again, and so on. A minor loop which introduces disturbances into this main line is the broke system. The starting and stopping of wood grinders may cause an excessive amount of paper breaks. The broke system will then fill up so rapidly that the broke proportion to the paper machines has to be increased, or, in rare cases, the excessive amount of broke has to be pumped into the mechanical pulp system. These disturbances necessitate stopping of wood grinders so as to avoid overfilling of the buffer tanks. In this manner as many as 20 stops and starts of wood grinders may be undertaken during one single day. Fig. 2 shows that the production of mechanical pulp (represented by the consumption of electric power) may come in direct negative phase with the consumption of pulp in the paper mill (represented by the generation of electric power corresponding to the steam consumption).

Since the major stream of pulp has a concentration of 3 % (on dry basis) very large amounts of water, several thousand

cubic metres an hour, are transported through the system. This water is drained on the paper machine wires and is then pumped back to the grinders. Shut down of a paper machine or of wood grinders introduces a step change in this flow and, therefore, sharply alters the condition of eguilibrium in the white water system. During a wire change in a large paper machine the white water content in the system may change by several thousand cubic metres. Fresh water is taken in at low level in the white water buffer tank, introducing the danger of a temperature shock to the system. This water will eventually have to be drained again, by this time, however, the water has taken up heat from the system and also contains fibres. Thus a fresh water intake of this nature means corresponding loss of fibre and heat. The loss of fibres in a newsprint mill usually amounts to 1-2 % of the total production.
It is obvious that it is not possible to achieve satisfactory and even utilization of the electrical power with frequent changes occurring in the operation of the wood grinders, which in turn leads to high electric energy costs.

Control strategies were tried out on a mill simulator

A thorough study of the entire Hallsta Paper Mill was undertaken and using the knowledge acquired,a number of simulations were performed at ASEA's computer centre. Various control strategies were tried out. The computer was programmed to give print-outs, as well as tables of the variables, and diagrams. Fig. 3 illustrates one such diagram. As can be seen, the grinders may be run for two whole days before any changes have to be made. The diagram also shows the flows of broke to the paper machines and the white water drainage, as well as the variation in the storage tank's inventory. Note that the total buffer volume for pulp is used to its limit. The drainage of white water is based, at least to some extent, on the total water content in the system, calculated from the contents in the various white water and pulp tanks, and takes into account where in the system the water is stored as well as the schedule for the mill operation.

Important improvement with simple strategies

Throughout the work for the Hallsta computer project the principal aim was that of simplicity. It is generally rather easier to make a computer project too complex than to accomplish simple and still profitable solutions. All strategies chosen were straightforward and any additions to the original speci-

fications for the computer programme were carefully avoided in order to avoid laborious alterations and to keep the project as far as possible within specified limits. Even so, considerable improvement has been accomplished, which can be seen when comparing fig. 3 to fig. 2. (N.B: Fig. 2 corresponds to one day's operation, while three day's operation is shown in fig. 3)

What is the basic reason for this improvement when computer control is installed? Because a computer can check continuously and carefully what is happening in all parts of the mill and, basing its calculations on the actual situation, plan for future events. This is, of course, much too complex and hence impossible for an operator to comprehend. - The computer keeps a continuous check on all parts of the plant in an intelligent manner and attracts the attention of the operator, i.e., the shift foreman, only when necessary. In addition to this, the operator receives in the usual manner a shift-log of the plant performance from the computer. - A few of the control functions are, for instance:

- the alarm limits of the level in the buffer tanks are variable and depend upon whether the level varies slowly or rapidly.

- the computer keeps continuous track of which grinders are available, shut down for repairs, etc.

- it makes reports of paper breakes in the machines

Even if extended operation, without starts and stops, of the wood grinders has most influence on the quality of the pulp, the actual operation of the grinders is of importance as well. The computer, therefore, continuously calculates the specific energy consumption of the wood grinders and in this manner provides information on when it is time to sharpen the stones, when the logs are unevenly filled, etc.

Weekly planning schedule

It has been a comparatively simple matter to extend computer calculations to include the planning for a whole week's operation of the mill. Twice a week a one week's schedule for mill operation at Hallsta Paper Mill, as well as for all the other factories in the Holmens Group at various sites in Sweden, is fed into the computer. This schedule contains information about wire changes, repairs which alter the capacity of the units, etc. From this information and from the actual situation in the mill the computer calculates and prints out the operation

of the wood grinders, the consumption of wood and sulphite pulp, the production of paper at the machines for every period during the following week, as well as the total consumption and production.

The computer plans and checks the utilization of electrical energy in the whole Group

The weekly planning calculation also includes the power situation of two paper mills, one board mill, textile factories, the hydro-electric power stations in Southern as well as in Northern Sweden, all of which belong to the Holmens Group. With knowledge of the equation for the power consumption and generation in the mills, the computer calculates the utilization of the various kinds of energy, such that

- the low-cost energy available is always used first
- the power from the steam generators at all the mills is utilized
- the limitations for the power from the hydro-electric stations is considered (these limitations vary throughout the week)
- the purchased power is utilized in such a manner that the lowest possible cost per kWh is maintained.

Since such an optimum utilization of the electric power is based on the week's planning schedule for the Group, all changes in this schedule must be reported to the computer as soon as they are known. For this purpose a simple semi-on-line transmission is used, based on the ordinary telex communication system. Orders from the computer to the other mills and the power stations are transmitted in the same manner.

The computer also continuously checks that these calculated power limits are not violated or will not become violated within the nearest hour or so. There are important disturbances in the power balance which must be taken into account as soon as they appear, e.g. paper breaks. The various types of power that must be checked and compared with their limits cannot be measured directly but must be calculated from measurements at a number of points and from the information stored in the computer.

The Computer

As may be seen from a description of the computer hardware, the amount of programming for this project has been rather limited. Compressed coding to minimize the requirements of memory space or packing of information into the same words has been avoided to facilitate future work with the programme and to make documentation clear and straightforward. On the other hand, much effort has been made to simplify the strategies as much as possible without affecting the performance of the computer programme. Furthermore, the amount and types of typewriter reports have been screened carefully to include only such information as is necessary for the specified task.

The computer has a memory cycle time of 5 /usec. and a word length of 24 bits plus one parity bit. It is a serial machine, with multiply, divide, double precision and floating operations in the form of quasi instructions, i.e., software implemented. For this project is is equipped with 8 K core and 16 K drum memory. The software package and the central computer programme is well developed. This, in combination with the 24 bit word length, has facilitated the programming work. -The process communication is accomplished in the usual manner by means of analogue and digital inputs and outputs and via 24 automatic priority interrupt levels. The latter are also used for pulse counting.

Communication with the operator

One alarm and one logging typewriter, a paper tape reader and punch are connected to the computer. There is also a special type of paper tape conversion unit and a tape editing set. Even if programmes and data are usually fed into the computer via the tape editing set with a paper tape reader, the operator can feed in constants and programme changes from the operator's console (fig. 4). On one set of thumb wheels the operator chooses the correct address and on a second set he introduces the new data. On a nixie-display he may check the values of variables, the content in a certain memory location or the new data before introduction into the correct memory location. By means of pushbuttons and indicating lamps he can operate any of the peripheral units from the operator's console.

The operator's panel is installed in an instrument room adjacent to the computer room. There is a glass partition between the two rocms. This permits full use of the operator's panel in connection with check-out of new programmes, service of the computer, etc., but has the advantage of not causing the instrument room to be blocked by the service crew and their

apparatus during maintenance visits, etc. Furthermore, with this arrangement the air ventilation may be selected from the most technically advantageous point of view rather than primarily taking into account the comfort of the operator.

Programme debugging, connecting the process, start-up

All function programmes, the central computer programme and the coordination of these have been tested on a computer of the same type before any programmes were loaded into the Hallstavik computer. During the start-up at Hallstavik all the programmes, therefore, were loaded from paper tape with a set of the programmes which was,as far as possible, correct. In fact, there were very few corrections to be made at site, only two or three minor faults.

The process connections are galvanically separated from the process in a marshalling cubicle. With this arrangement it was possible to connect all cables to and from the process into the computer room and have all the signals checked and calibrated before the computer was connected to the process. Also, in checking out the computer programme it was possible to introduce artificial signals to the computer connection side of the marshalling cubicle. This step method of linking the process and computer has facilitated the entire start-up procedure. In the final stage it was merely a matter of connecting strip after strip for each process signal and taking the corresponding parts of the programme into operation.

At the time when this paper is being written, the system has been in operation for too short a period to allow any final judgement regarding operating experience. A statement of that nature must therefore be postponed until the time of the congress.

Economy

An installation of the nature described influences the total production, consumption and losses of a large mill. Hence only small improvements are needed to pay off the computer investment within a fixed time. In addition to this, a computer installation of this nature may be rather simple, both hardware-wise and, perhaps most important, software-wise. This brings down the actual costs which have to be covered.

The most important benefits of this computer installation are:

1. **The pulp quality will be improved, resulting in increased throughput and better paper quality.**

2. There will be less fresh water intake, lower and more even flow of water, leading to reduced loss of fibres and calories.

3. Electrical energy costs will be decreased, not only for the Hallsta Paper Mill but for the whole Holmens Group.

4. There will be improved information to the operators, such that they can, at the correct moment, adopt correct measures and such that a clearer picture of the consequences of these measures may be obtained.

Acknowledgements

The author greatfully acknowledges the kind permission of Holmens Bruks & Fabriks AB and ASEA to publish this paper, and, also, expresses his gratitude for the encouraging cooperation of the members of the project group for the Hallsta computer installation.

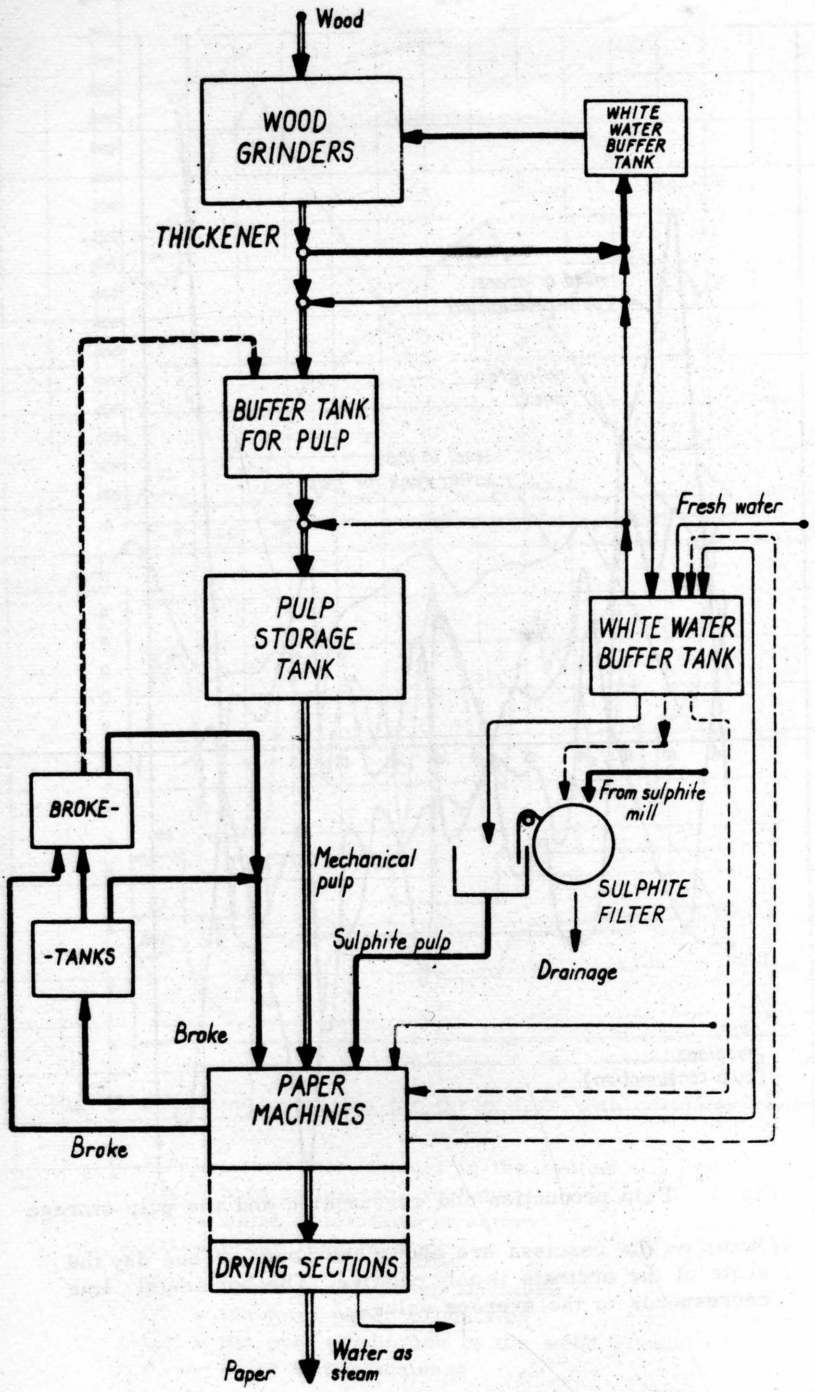

Fig. 1 Flow sheet of Hallsta Paper Mill

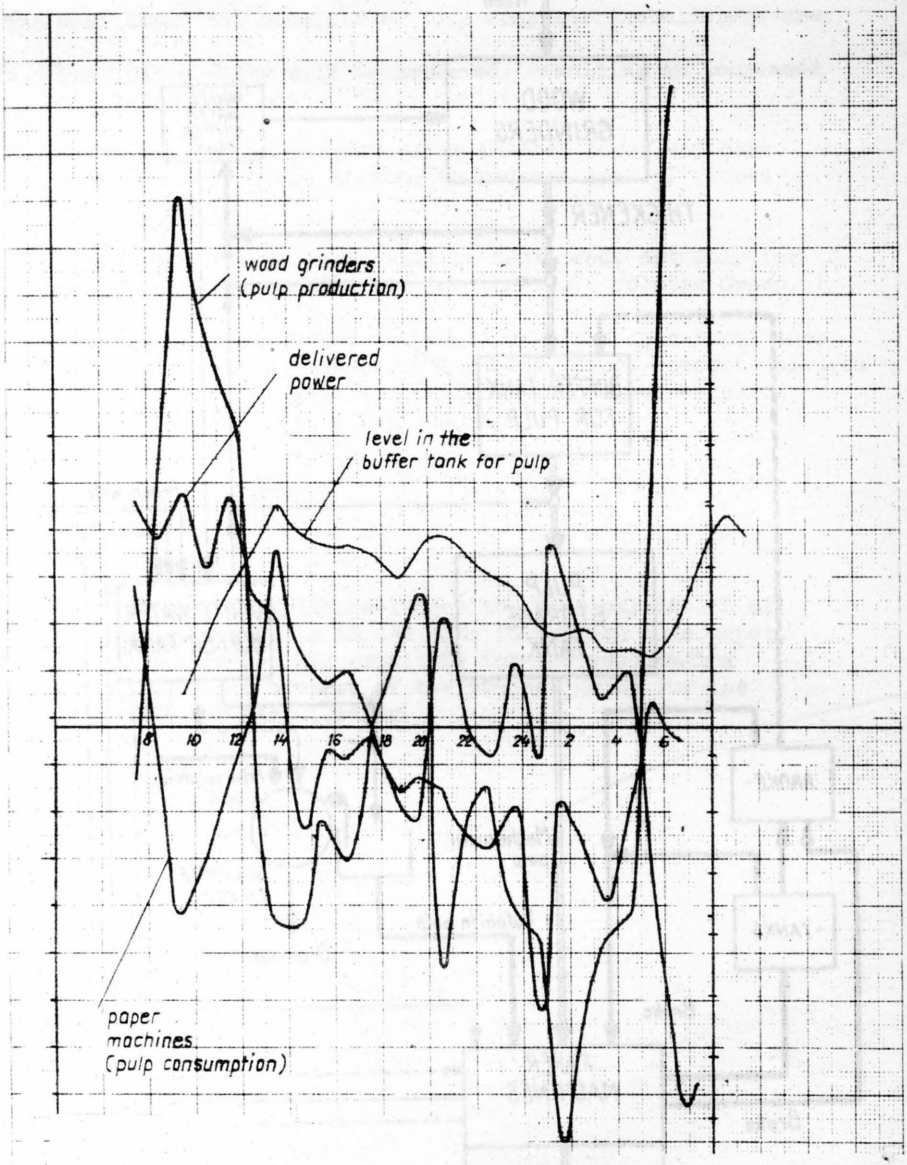

Fig. 2 Pulp production and consumption and the pulp storage

/Note: on the obscissa are shown the hours of one day the scale of the ordinate is only relative. The horizental line corresponds to the average values./

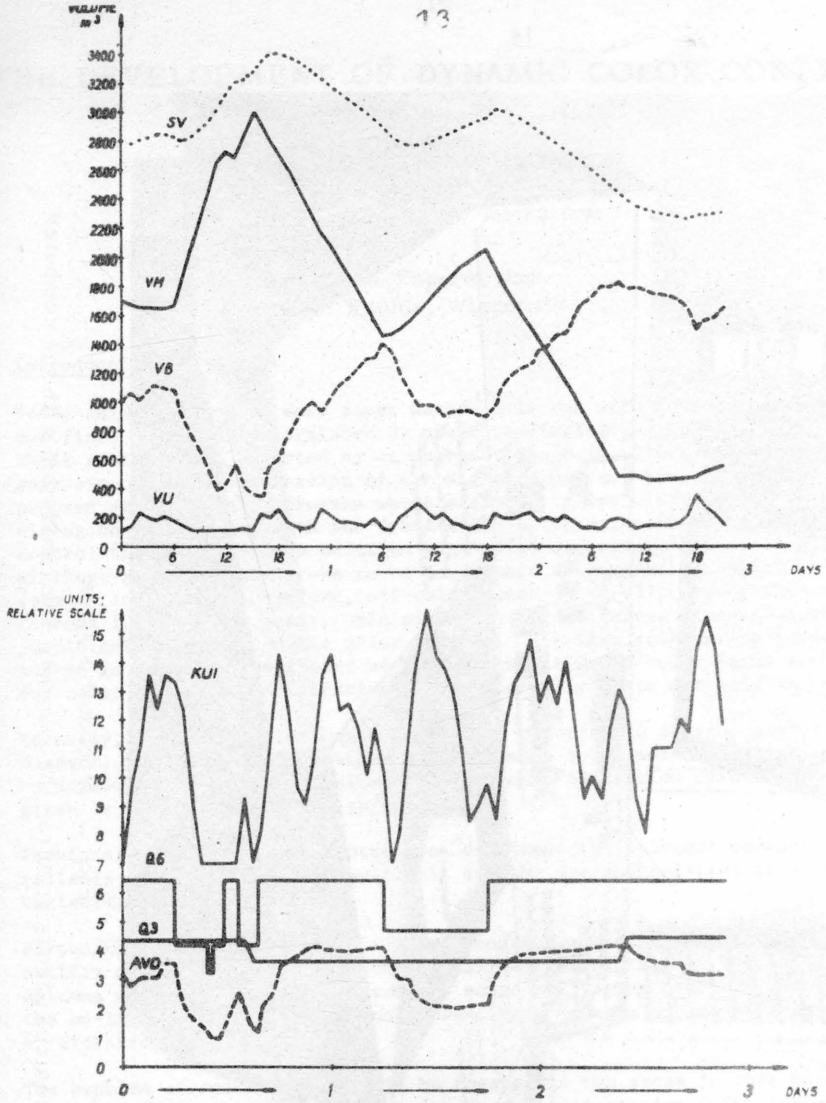

Fig. 3 Simulated operation for three days with computer control

SV = total water content in the system
VM = pulp buffer tank inventory
VB = white water tank inventory
VU = broke tank inventory

KU1 = broke to the paper machines
Q6 = the total paper production
Q3 = the pulp production of the wood grinders
AVD= white water drainage

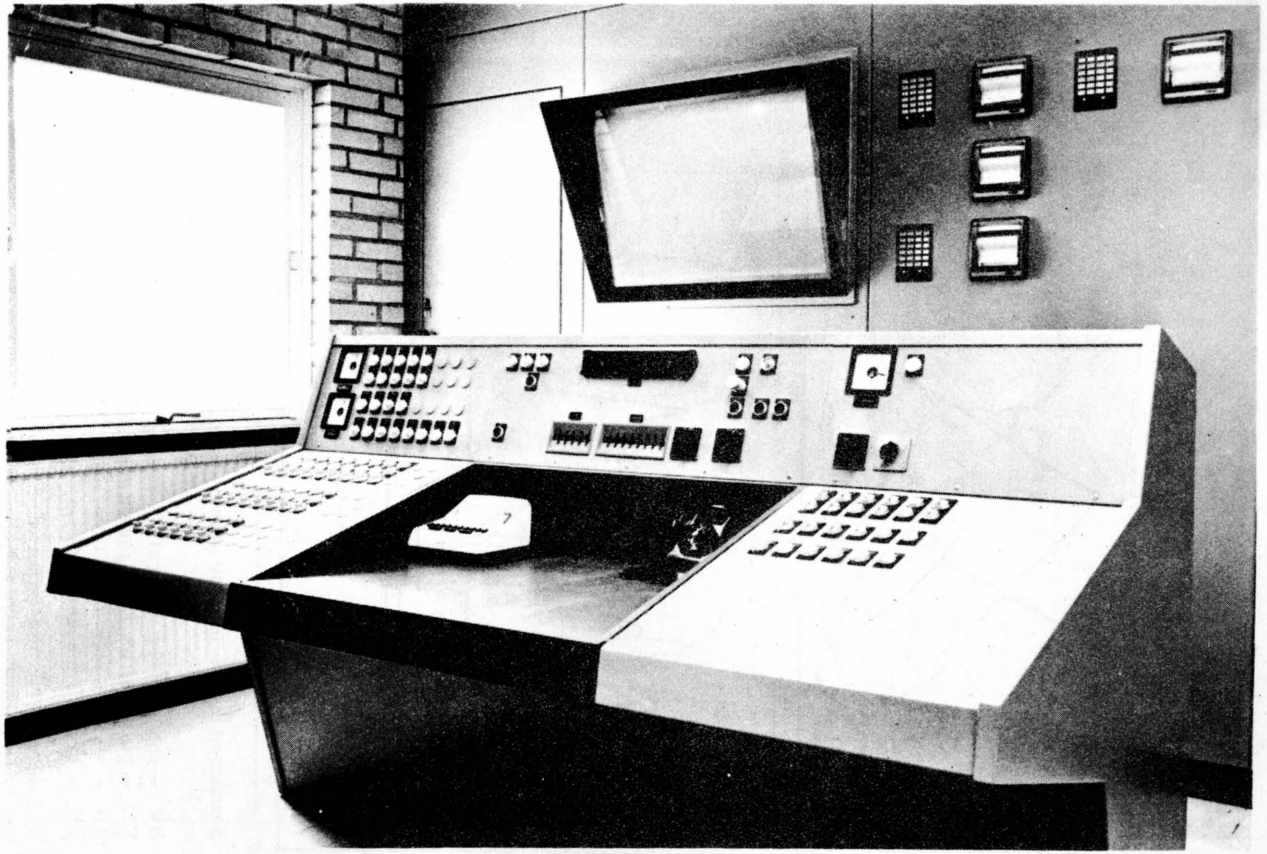

Fig. 4 Operator's panel

Only the central part is used for the two-way communication with the computer

THE DEVELOPMENT OF DYNAMIC COLOR CONTROL ON A PAPER MACHINE

By

Henry Chao And Warren Wickstrom

Consolidated Papers, Inc.
Wisconsin Rapids, Wisconsin

Introduction

Today color control on most paper machines is run with open-loop control. Dye flows are usually regulated by positive displacement pumps, while their settings are adjusted by an operator based on either laboratory analysis or plain observation of the finished paper. Some machines even prepare stock in batch process where different pulps are mixed in a huge mixing chest together with the dyestuffs. An experienced operator will control the amount of dye addition on a trial-and error basis. Either of these practices may prove to be inadequate as demands for color uniformity increase. Therefore, off-color paper is usually one of the major reasons for rejected paper. Minimizing the grade change time is another justification for automatic color control. The time lost during grade change is generally dominated by the response time of color (time required for color to reach specification), which normally lasts for half an hour.

Recently, automatic color control has been reported in several papers. However, these papers are either on batch mode color matching[1,2,3,4] or developed on a theoretical basis where only simulation results were given as a proof of the design validity.

Previously, on-line color control was difficult to implement because a reliable instrument was not available and the dye manipulation is a multivariable system.

Fortunately, the development of modern control theories and the availability of real-time process computer allow the solution of the latter dilemma while new on-line instruments solve the former problem. One of the on-line instruments, the Hunter D44, has been evaluated and reported by Wickstrom[5].

The problem of color control will be treated in two steps in this paper, i.e., steady state compensation and dynamic consideration. The former is an algorithm for varying the dye concentration to compensate the difference between color measurement and specification at a steady state basis. In other words, it is assumed that the process response to change in manipulating variables is instantaneous. The latter is the design that takes the process dynamics into consideration.

Before discussing the control aspects, color measurement will be briefly discussed. For the reader who wishes to study color measurement theory in detail, the text[6,7] is recommended.

Color Measurement

There are many ways of interpreting color depending upon whether one is a physicist, a psychologist, or a chemist. In reviewing color measure-

ment here, the physicist's interpretation will be used. The physicist thinks of color in terms of how each individual wavelength is reflected or transmitted from the sample.

Basically, three things are required to produce what the physicist calls color: (1) a source light, (2) a sample illuminated by the same source light, (3) a sensor receiving the reflected or transmitted light from the sample.

The eye acts as if the incoming light were divided into three beams (each of which passes through a different optical band-pass filter). This trichromatic property of the eye allows a physicist to use only three primary colors. The band-pass characteristics of the filters used to represent the eye are shown by the three functions $\bar{x}$, $\bar{y}$, and $\bar{z}$ in Figure 1.

Defining quantitatively how the eye reacts to the reflection from the sample is the most difficult part of color measurement. In 1931 the International Commission on Illumination, known as the CIE[6], standardized the numerical measurement of color by selecting three sets of primary lights, a standard source of illumination, and a set of color match characteristics defined as the standard observer. The CIE defined the $\bar{x}$, $\bar{y}$, and $\bar{z}$ by determining a hypothetical standard observer, taking test data from many different persons with normal vision.

As mentioned above, color is a function of the light source, the sample, and the reflected light interacting with the eye. Then the three primary CIE tristimulus values are defined by:

$$X = \int_{400}^{700} E_d(\alpha) \cdot R_f(\alpha) \cdot \bar{x}(\alpha)\, d\alpha \qquad (1)$$

$$Y = \int_{400}^{700} E_d(\alpha) \cdot R_f(\alpha) \cdot \bar{y}(\alpha)\, d\alpha \qquad (2)$$

$$Z = \int_{400}^{700} E_d(\alpha) \cdot R_f(\alpha) \cdot \bar{z}(\alpha)\, d\alpha \qquad (3)$$

With the visible spectrum from 400 to 700 millimicrons, the symbols above are defined as:

$E_d(\alpha)$ = energy distribution by wavelength of the source light.

$R_f(\alpha)$ = reflectivity of sample.

α = wavelength of visible spectrum.

As shown in Figure 1, the function $\bar{x}$ peaks in the orange-red region of the spectrum and has a secondary peak in the blue. The function $\bar{y}$ peaks in the green and the $\bar{z}$ peaks in the blue region. However, they are not measurements of primary color such as blueness, redness, and yellowness. Some mathematical transformations can be used to convert the tristimulus values to pigment or dye-related colors. One of such transformations, Hunter units, will be discussed later in this paper.

Steady State Compensation

Using the total differential and neglecting higher order terms, the effect of dye concentration change, Δc, on tristimulus values at steady state, can be expressed as:

$$\Delta X = \frac{\partial X}{\partial c}\ \Delta c_1 + \frac{\partial X}{\partial c}\ \Delta c_2 + \frac{\partial X}{\partial c_3}\ \Delta c_3$$

$$\Delta Y = \frac{\partial Y}{\partial c_1}\ \Delta c_1 + \frac{\partial Y}{\partial c}\ \Delta c_2 + \frac{\partial Y}{\partial c_3}\ \Delta c_3 \qquad (4)$$

$$\Delta Z = \frac{\partial Z}{\partial c_1}\ \Delta c_1 + \frac{\partial Z}{\partial c_2}\ \Delta c_2 + \frac{\partial Z}{\partial c_3}\ \Delta c_3$$

The partial differentials can be evaluated by running an identification on the process, changing one dye at a time, and measuring the change of tristimulus values from one steady state condition to the other. Our experience has shown that for the same grade and dye, the value of the partial derivatives will not change.

The systems of equation (4) can be expressed in matrix form:

$$[\Delta T] = [A]\ [\Delta C] \qquad (5)$$

where:
$$[\Delta T] = \begin{bmatrix} \Delta X \\ \Delta Y \\ \Delta Z \end{bmatrix} \quad ; \quad [\Delta C] = \begin{bmatrix} \Delta c_1 \\ \Delta c_2 \\ \Delta c_3 \end{bmatrix}$$

and:
$$[A] = \begin{bmatrix} \frac{\partial X}{\partial c_1} & \frac{\partial X}{\partial c_2} & \frac{\partial X}{\partial c_3} \\ \frac{\partial Y}{\partial c_1} & \frac{\partial Y}{\partial c_2} & \frac{\partial Y}{\partial c_3} \\ \frac{\partial Z}{\partial c_1} & \frac{\partial Z}{\partial c_2} & \frac{\partial Z}{\partial c_3} \end{bmatrix}$$

For a set of deviations in tristimulus values, the dye concentration change is:

$$[\Delta C] = [A]^{-1}[\Delta T] \qquad (6)$$

Dye Selection

Our initial combination of red, blue, and green dyes seemed to be a good selection. The A matrix was found to be:

$$\begin{bmatrix} -3{,}720 & -32{,}400 & -17{,}900 \\ -11{,}400 & -28{,}300 & -17{,}680 \\ -9{,}000 & -9{,}700 & -9{,}030 \end{bmatrix}$$

The solution of equation (6) exists because the value of $|A|$ determinate is 438,000 (non-zero) so that the matrix A is non-singular. To illustrate the problems encountered with this dye combination, let's take an example

of changing each tristimulus value by +1.0. By equation (6) the change in dye concentration is given by:

$$[\Delta C] = \begin{bmatrix} 0.000072 \\ 0.000152 \\ -0.000352 \end{bmatrix}$$

It is interesting to look graphically at the path taken by the above change in dye concentrations. Figure 2 is a plot of both Y versus X and Y versus Z as the result of dye concentration changes.

The change in green dye concentration ($\Delta c_3 = -.000352$) by itself will move $|\Delta T|$ from the origin to the point A. The coordinates of latter point are calculated as follows:

$$\begin{bmatrix} \Delta X \\ \Delta Y \\ \Delta Z \end{bmatrix} = \begin{bmatrix} -3{,}720 & -32{,}400 & -17{,}900 \\ -11{,}400 & -28{,}300 & -17{,}680 \\ -9{,}000 & -9{,}700 & -9{,}030 \end{bmatrix} \begin{bmatrix} 0 \\ 0 \\ -0.000352 \end{bmatrix} = \begin{bmatrix} 6.30 \\ 6.22 \\ 3.18 \end{bmatrix}$$

Similarly, the movement caused by green and blue dye concentration changes is:

$$\begin{bmatrix} \Delta X \\ \Delta Y \\ \Delta Z \end{bmatrix} = \begin{bmatrix} -3{,}720 & -32{,}400 & -17{,}900 \\ -11{,}400 & -28{,}300 & -17{,}680 \\ -9{,}000 & -9{,}700 & -9{,}030 \end{bmatrix} \begin{bmatrix} 0 \\ 0.000152 \\ -0.000352 \end{bmatrix} = \begin{bmatrix} 1.32 \\ 1.90 \\ 1.70 \end{bmatrix}$$

which is indicated as point B in Figure 2.

To manipulate all three dye concentrations by specific amount, the tristimulus values will move to (1,1,1).

The paths in Figure 3 are at least ten times longer than the shortest path, i.e., from (0,0,0) to (1,1,1). A small change in reference value or a deviation from set point due to a disturbance will cause a large change in dye flow. The large amount of change might cause a serious error. For instance, in the example just shown, if the blue dye concentration was changed by -0.000317 instead of -0.000352 (10% less) either due to a pump movement error or due to the inaccuracy of A matrix, then the variation of the tristimulus value would be (0.4, 0.4, 0.7) instead of (1,1,1), an error of more than 50%.

Also, if the changes in dye flow are too large, either the control valve or the pump will run out of range, or possibly a negative flow may be requested. Another problem with large changes in dye concentration is that the model linearity assumptions may be violated because the identification of matrix A is based on small perturbations.

The problems with red, blue, and green dyes suggested another dye combination was needed. Therefore, a red, blue, and yellow dye combination was tried. The A matrix of this combination is:

$$\begin{bmatrix} -12{,}013 & -114{,}096 & -9{,}490 \\ -79{,}843 & -107{,}643 & -8{,}127 \\ -22{,}519 & -15{,}188 & -25{,}513 \end{bmatrix}$$

The plot of tristimulus value changes with the latter dye combination and

the unit tristimulus deviation vector is given in Figure 3. The paths in Figure 3 for the same change in reference value are shorter than the paths in Figure 2 (note the scale difference between Figures 2 and 3).

The above examples suggested the need for a criteria in dye selection. Belanger[3] said the singularity or near-singularity of A matrix indicates a poor choice of dye combination. As stated in any linear algebra text, the singularity of matrix A (the condition that the inverse matrix, i.e., the solution of equation (6) does not exist) occurs if and only if its determinant is zero. Bristol[8] and Mesarovic[9] suggested some ways to measure the interaction between multivariable system. In this particular case, the interaction can be decoupled as shown later in this paper so that the interaction does not concern us so much as the similarity of the dyes.

The authors proposed that the degree of orthogonality of A matrix, called dye efficiency, be defined by the triple product of the normalized dye vectors, $\bar{V}_1$, $\bar{V}_2$, and $\bar{V}_3$, That is:

$$E = \bar{V}_1 \times \bar{V}_2 \cdot \bar{V}_3 \qquad (7)$$

where:

$$V_i = \frac{\begin{bmatrix} a_{1i} \\ a_{2i} \\ a_{3i} \end{bmatrix}}{\left(\sum_{j=1}^{3} a_{ji}^2 \right)^{\frac{1}{2}}} \qquad \text{for } i = 1, 2, \text{ and } 3$$

or it can be written as (8)

$$E = \frac{\det [A] \times 100}{\left(\prod_{i=1}^{n} \sum_{j=1}^{n} a_{ji}^2 \right)^{\frac{1}{2}}} \quad \%$$

where: a_{ji} is the element of A matrix and n = 3

By this definition, the efficiency will be 100% if the dye vectors are orthogonal, and zero if the matrix is singular. Efficiency values between 0-100% represent the degree between the two extremes.

The efficiency of the red, blue, and green dye combination is thus 2.6% and that of the red, blue, and yellow dye combination is 51.5%.

The efficiency of the tristimulus system is limited by the nature of how the color space is defined, that is, the efficiency is a function of both dyes and how the dyes interact with a particular definition of color space. A transformation of the basic XYZ system to another system of color measurement by itself can improve the efficiency.

A practical problem with the tristimulus system is that the measurements are sensitive to instrument drift from such sources as voltage variation to the light source power supply, dust accumulation on the light source lenses, etc. Another practical problem is that the tristimulus values are difficult to interpret in terms of what the eye visually perceives.

Because of these problems, the Hunter units[10] were chosen as the color measurement units. They are defined as:

$$R_d = Y$$

$$a = 175\ f_y\ (1.02\ X - Y) \qquad (9)$$

$$b = 70\ f_y\ (Y - .847Z)$$

$$\text{where } f_y = \frac{.51\ (21 + 20Y)}{(1 + 20Y)}$$

The Hunter color space is shown in Figure 4. Redness and greenness are defined by "+a" and "-a," while yellowness and blueness are defined by "+b" and "-b." In addition, lightness varies 0 to 100 where 0 is black and 100 is white. Because "a" and "b" are functions of tristimulus differences, they are less sensitive to instrument drift. With near-white papers, the eye has a greater tolerance for changes in lightness (R_d) than either "a" or "b", that is, the eye is more sensitive to the saturation and hue of the material.

In the case to be considered, the level of lightness achieved was such that close control of this color element was not required. This allowed the control problem to be reduced to controlling the Hunter "a" and "b" elements using only two dyes. Where lightness must be controlled more closely, titanium dioxide is frequently used as a third dye component.

The steady state process relation in Hunter units, neglecting the lightness scale is given by:

$$\underset{2x1}{[\Delta H]} = \underset{2x2}{[A]}\ \underset{2x1}{[\Delta C]} \qquad (10)$$

$$\text{where: } [\Delta H] = \begin{bmatrix} \Delta a \\ \Delta b \end{bmatrix}$$

where equation (10) is derived similar to equation (5).

Since the mill had been using red and blue dyes for many years to control color on a laboratory test basis, it is easy to use these dyes for closed loop control. Generally, a yellow dye should be avoided because it lowers paper brightness, a standard by which printing paper is sold. For red and blue dyes, the A matrix is:

$$[A] = \begin{bmatrix} 1.211 & 0.128 \\ 0.454 & 0.593 \end{bmatrix}$$

The dye efficiency for this system is defined similar to equation (8) where n is 2 instead of 3. In this case, the efficiency is 84.9%.

Process Dynamics

As shown in Figure 5, dye is added to the paper machine on the inlet side of the fan pump. Together with the recycle white water and stock flow, the mixture passes through the Centri-cleaners, pressure screens, and headbox. Approximately 80% to 90% of the dyes are retained on the wire as part of the paper web leaving the couch roll. The dye and fiber passing through

the wire is collected in the white water silo and recycled to the fan pump. It is theorized that the dye passing through the wire is attached to the fine fibrous material that filters through the fourdrinier wire.

The process between the dye addition point and the headbox can be considered as a mixing system with a transport delay. The mixing effect, represented by a first order lag, is caused not only by cleaners and headbox but also by the turbulent flow in the pipeline. The dynamics for the web passing from the wire to the end of the paper machine (where the color meter is installed) is a pure transport delay.

Figure 6 shows a block diagram of the paper machine system and its open-loop configuration as suggested by Sullivan[4] or Beecher[11]. C_i is the dye concentration in pounds of dye per pound of fiber entering the system and C is the dye concentration passing the color meter. R is the dye-fiber retention factor.

Figure 7 shows the system response with different dye retentions. Even though the response of 80% dye retention is a little different from 100% retention, it can still be approximated by a first order system with time delay as shown in Figure 8. Therefore, the Laplace transport function of open loop dye system between dye addition point and color meter can be represented as:

$$\frac{[C(s)]}{[C_i(s)]} = \frac{e^{-sD}}{\tau s+1} \tag{11}$$

where D means dead time and τ stands for time constant.

Then equation (11) can be combined with equation (10) to give:

$$[H(s)] = \frac{e^{-sD}}{\tau s+1}[A][C_i(s)] \tag{12}$$

The dead time, time constants, as well as the elements of the matrix can be evaluated by process identification[12].

Figure 9 is a typical open loop response where dead time was found to be 85 seconds with a time constant of approximately 35 seconds. Figure 9 shows that the actual data compares closely with theoretical up to about 270 seconds. After 270 seconds, the silo effect causes the response to continue to drift. Because the drift is slow, it can be compensated with closed loop control.

Decoupling of Interaction

The multivariable control system of equation (12) can be represented by Figure 10. For this system to be non-interacting, the system represented by Figure 10 should be reduced to Figure 11, which is a system of two independent loops. To decouple the interaction, the following equations must be satisfied:

$$[G(s)][A] = [F(s)] \tag{13}$$

where $[F(s)]$ must be a diagonal matrix.

This results in:

$$g_{12}(s) = \frac{-a_{12}}{a_{11}} g_{22}(s) \tag{14}$$

$$g_{21}(s) = \frac{-a_{21}}{a_{22}} g_{11}(s) \tag{15}$$

and:

$$\frac{a_{11}a_{22} - a_{12}a_{21}}{a_{22}} g_{11}(s) = f_{11}(s) \tag{16}$$

$$\frac{a_{11}a_{22} - a_{12}a_{21}}{a_{11}} g_{22}(s) = f_{22}(s) \tag{17}$$

where $f_{11}(s)$ and $f_{22}(s)$ are diagonal elements of $[F(s)]$. Thus, by specifying $f_{11}(s)$ and $f_{22}(s)$, $[G(s)]$ may be determined.

Design of a Digital Controller

It was found that the elements of matrix A do not change significantly for the same grades of paper but will only depend on the type furnish. Therefore, the gain of controllers should be varied by grade to achieve the decoupling criteria. However, automatic gain adjustment is difficult with analog controllers. Because an IBM 1800 was available, the entire control scheme has been run on a digital computer. It is possible to use the PI control in the digital sense, that is, the PI controller can be set in difference equation form. However, the stability of such a system will depend on the sampling period. Because of the versatility of the digital computer, it is not necessary to restrict control algorithm to proportional, integral, and derivative action. By using modern control philosophy, we can design a control algorithm by specifying the overall closed loop response[13].

To obtain a realistic and stable design, the closed loop transfer functions were specified as a first order response with dead time such as:

$$\frac{a_m}{a_r} = \frac{\lambda e^{-sD}}{s+\lambda} \tag{18a}$$

$$\frac{b_m}{b_r} = \frac{\lambda e^{-sD}}{s+\lambda} \tag{18b}$$

where λ is the reciprocal of time constants and D is the same process dead time.

From Figure 11, we can obtain the closed loop transfer functions in terms of f_{11} and f_{22}:

$$\frac{a_m}{a_r} = \frac{f_{11}e^{-sD}}{\tau s+1+f_{11}e^{-sD}} \quad ; \quad \frac{b_m}{b_r} = \frac{f_{22}e^{-sD}}{\tau s+1+f_{22}e^{-sD}} \tag{19}$$

By comparing equations (18) and (19) f_{11} and f_{22} can be solved by:

$$f_{11}(s) = f_{22}(s) = \frac{\lambda(\tau s+1)}{s+\lambda - \lambda e^{-sD}} \tag{20}$$

By equations (14) to (17), the controliers are solved as:

$$\begin{vmatrix} g_{11}(s) & g_{12}(s) \\ g_{21}(s) & g_{22}(s) \end{vmatrix} = \frac{(\tau s+1)\lambda}{s+\lambda-\lambda e^{-sD}} \cdot \begin{vmatrix} \frac{a_{22}}{a_{11}a_{22} - a_{12}a_{21}} & \frac{-a_{12}}{a_{11}a_{22} - a_{12}a_{21}} \\ \frac{-a_{21}}{a_{11}a_{22} - a_{12}a_{21}} & \frac{a_{11}}{a_{11}a_{22} - a_{12}a_{21}} \end{vmatrix} \tag{21}$$

Using the definition of $g_{11}(s)$ as shown in Figure 10, $g_{11}(s)$ can be expressed as:

$$g_{11}(s) = \frac{c_{i11}}{\Delta a} \tag{22}$$

The recursion formula is:

$$c^m_{i11} = \frac{a_{22}}{a_{11}a_{22} - a_{12}a_{21}} \{ \lambda\tau\Delta a^m + \lambda (T-\tau) \Delta a^{m-1} \} +$$

$$+ (1 - \lambda T) c^{m-1}_{i11} + \lambda T c^{m-\Gamma-1}_{i11}$$

where: T = sampling period

Γ = nearest integer of D/T

m = present reading; m-1 = previous reading, etc.

c_{i12}, c_{i21}, and c_{i22} can be expressed like equation (23).

Then:
$$c^m_{i1} = c^m_{i11} + c^m_{i12} \tag{24}$$

$$c^m_{12} = c^m_{i21} + c^m_{i22} \tag{25}$$

To test the validity of the controller design and its assumption, set point changes of approximately 0.35 unit on "b" were stepped into the color controller with different values of λ . Figure 12 gives plots of actual and theoretical response with sampling period of 60 seconds and a closed loop time constant of 58 seconds, 115 seconds, and 287 seconds (which are equivalent to a λ of 10, 5, and 2 cycles per hour).

All the responses deviated slightly from theoretical. Surprisingly, the actual response with 287-second time constant deviated the most and overshot more than the others. Theoretically, the system with larger time constant should be more sluggish.

The difference is probably due to the fact of forcing the process transfer function into a first order lag. With the recycled dye from the silo, the

transfer function is not actually first order. Therefore, a controller with a smaller overall time constant is able to keep up with the difference. In all cases, the "a" color unit was not significantly affected, which means the decoupling has produced excellent results.

These results prove the validity of the overall design (provided that the parameters are properly chosen). As a matter of fact, the color control has been successfully run on Consolidated Papers' near-white grades since January, 1968.

Summary and Conclusion

It has been demonstrated that closed loop color control is feasible when using red and blue dyes to control the Hunter "a" and "b" color units. Hunter units are used primarily because the mill uses these units for its laboratory paper specifications and the operators are familiar with them.

There is no theoretical reason why the tristimulus values cannot be controlled with a three-dye manipulating system. Dye selection is aided by calculating the dye efficiency. High dye efficiency implies better controllability.

Because color control is an interacting multi-loop system, the decoupling and predefined closed-loop response features reduce the controller design into the following procedure:

1. Identifying the process time constant and dead time as well as the B matrix.

2. Specify the proper closed loop time constant and sampling period.

3. The controller algorithms are given in equations (23), (24), and (25).

BIBLIOGRAPHY

(1) H.R. Davidson and H. Hemmendingr, "Industrial Use Of Instrumentation And Computations For Color Matching And Control," Color Engineering, 4, May-June (1966)

(2) C. Presten and David Tough, "Automated Shade Matching," Color Engineering, 3, May-June (1965)

(3) P.R. Bélanger, "An Application Of Optimal Control Theory To The Control Of Color On The Paper Machine," 1967 IEEE International Convention, March 21, 1967

(4) P.R. Sullivan, "Paper Machine Color Simulation And Control," IBM Confidential Report, August 10, 1967

(5) W.A. Wickstrom, "The Evaluation Of An On-line Colorimeter, " 1968 TAPPI Testing Conference, June 25-27, 1968

(6) D.B. Judd, "Color In Business, Science, And Industry," John Wiley and Sons, Inc., New York, New York, 1963.

(7) Carroll, C.W., "Color: Industrial Color Measurement, Laboratory Color Matching And Production Color Control," IBM Midwestern Region, June 26, 1963.

(8) Bristol, E.H., "On A New Measure Of Interaction For Multivariable Process Control," IEEE Transactions on Automatic Control, January (1966).

(9) Mesarovic, M.D. "The Control Of Multivariable Systems," Technology Press, MIT and Wiley Publishing; N.Y., 1960.

(10) Richard S. Hunter, "Photoelectric Tristimulus Colorimetry With Three Filters," J. Opt. Soc. Am., 32, 509-538 (1942)

(11) Beecher, A.E., "Dynamic Modeling Techniques In The Paper Industry," Tappi, 46, 117-120, February, 1963.

(12) Dahlin, E.B., "On-line Identification Of Process Dynamics," IBM Journal, July, 1967.

(13) E.B. Dahlin, "Designing & Tuning Digital Controllers," Instruments And Control Systems, June, 1968

TABLE OF NOMENCLATURE

$[A]$	matrix of coefficient of tristimulus value change due to dye concentration change.
a_{ij}	the element of ith row and jth column of $[A]$ matrix.
a_m, a_r, Δa	measured value, set point and the difference of Hunter's unit a.
b_m, b_r, Δb	measured value, set point and the difference of Hunter's unit b.
$[\Delta C]$	column matrix of dye concentration change.
c_1, c_2, c_3	dye concentrations. lb. of dye per lb. of fiber.
$[C_i]$	column matrix of dye concentrations at inlet.
Δc_{i11}	contribution of first (red) dye concentration change due to Δa.
Δc_{i12}	contribution of first (red) dye concentration change due to Δa.
Δc_{i21}	contribution of second (blue) dye concentration change due to Δa.
Δc_{i22}	contribution of second (blue) dye concentration change due to Δb.
c_{i1}	first (red) dye concentration at inlet, $c_{i1} = c_{i11} + c_{i12}$.
ci2	second (blue) dye concentration at inlet $c_{i2} = c_{i21} + c_{i22}$.

D	dead time of process
det	determinant of matrix
E	dye efficiency, defined in equation (7) or (8).
E_d	energy distribution by wavelength of source light.
$[F]$	the product of $[G]$ and $[A]$ matrices as defined in equation (12).
$f_{ij}(s)$	the element of $[F]$ matrix. f_{11} and f_{12} are given in equations (15) and (16). Others are zero for decoupling.
$[G]$	the matrix of controller transfer function.
$g_{ij}(s)$	controller transfer function in s domain.
$[\Delta H]$	column matrix with Hunter "a" and "b" as its elements.
m	time index of recursion formula.
R_f	reflectivity of sample.
s	Laplace operator.
T	sampling period.
$[\Delta T]$	column matrix of tristimulus value change.
$\bar{V}_1$, $\bar{V}_2$, and $\bar{V}_3$	vectors defined in equation (7).
X, Y, and Z	tristimulus values.
$\bar{x}$, $\bar{y}$, and $\bar{z}$	tristimulus function.
α	wavelength of spectrum
c	time constant of process
Γ	the nearest integer of D/T
λ	the reciprocal of overall closed loop time constant.

FIGURE 1

DEFINITION OF TRISTIMULUS CURVES

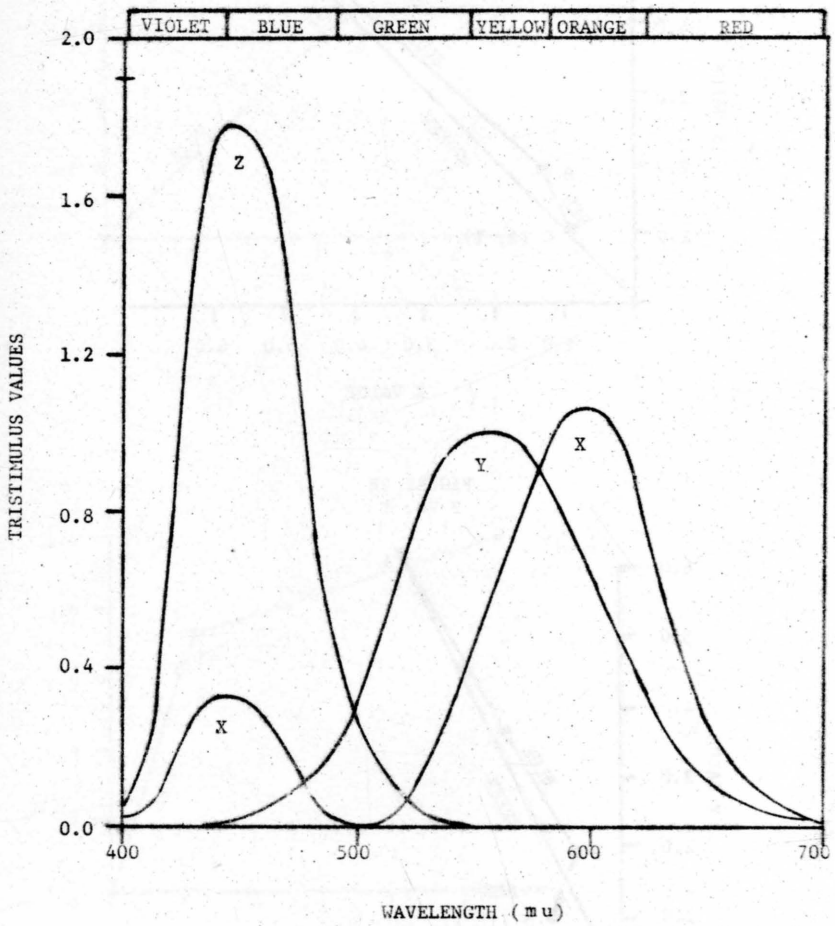

FIGURE 2A
X VS. Y

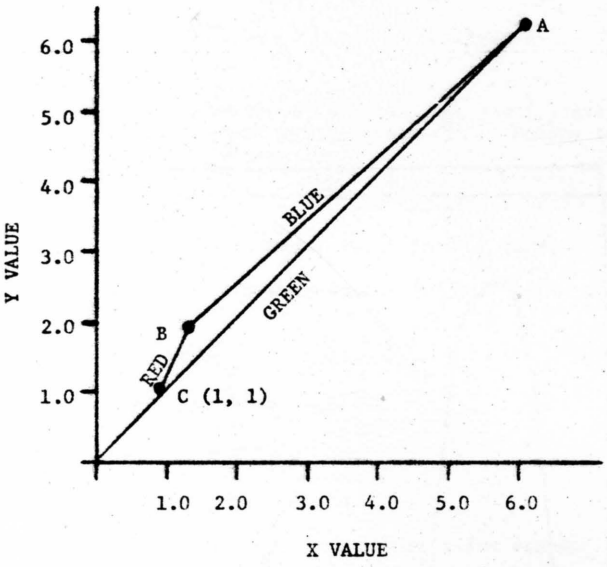

FIGURE 2B
Z VS. Y

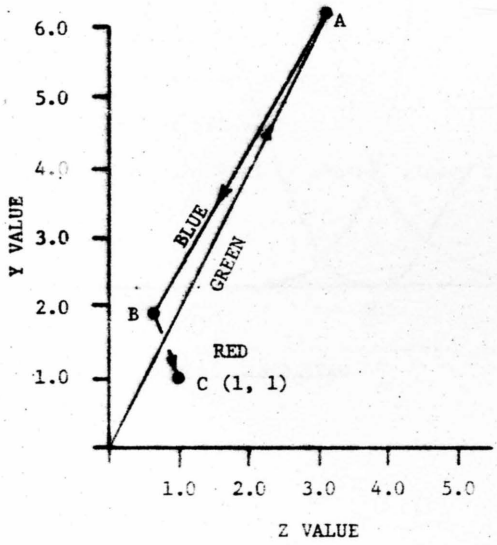

FIGURE 3A
Y VS. X

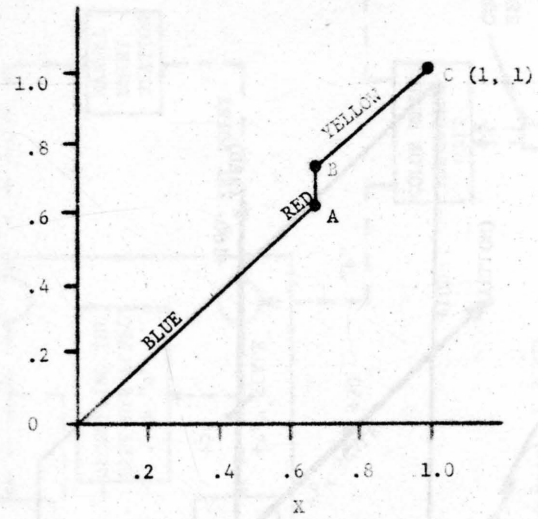

FIGURE 3B
Y VS. Z

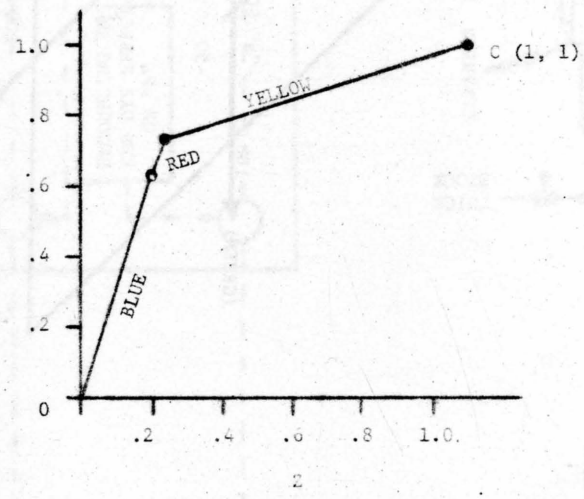

FIGURE 4

HUNTER COLOR SCALES

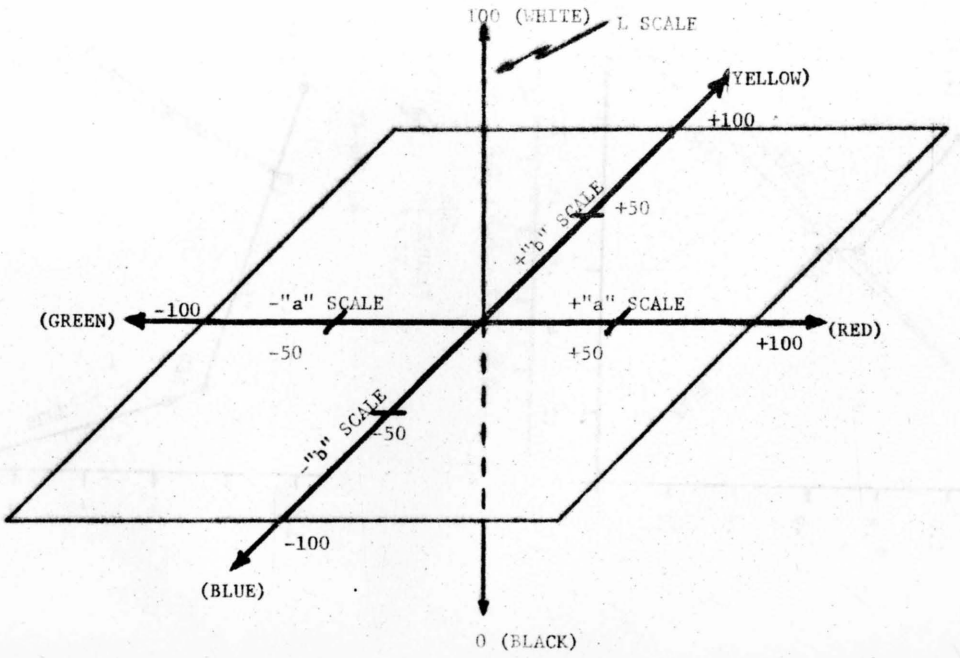

FIGURE 5

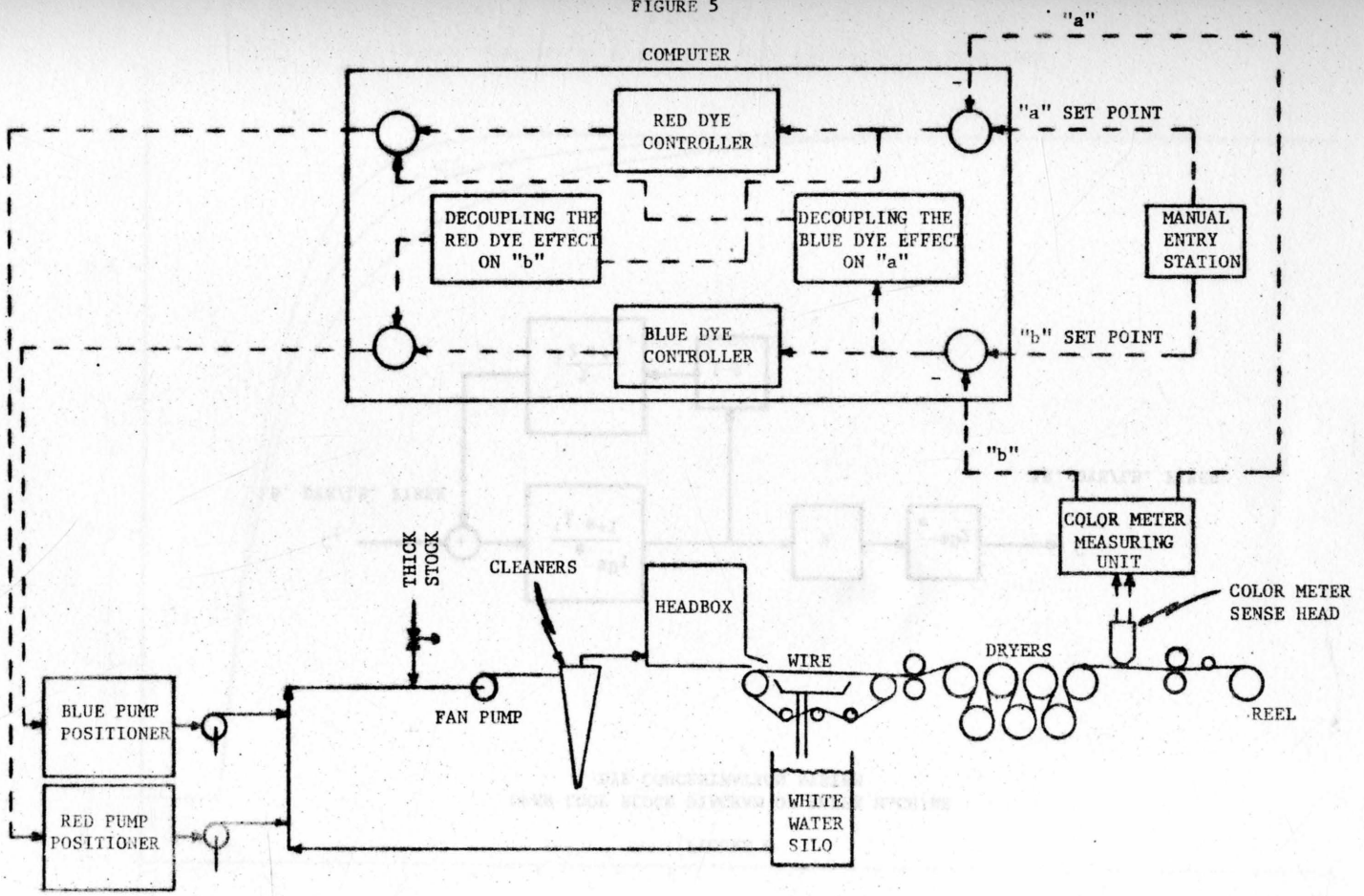
"a"
COMPUTER
RED DYE CONTROLLER
"a" SET POINT
DECOUPLING THE RED DYE EFFECT ON "b"
DECOUPLING THE BLUE DYE EFFECT ON "a"
MANUAL ENTRY STATION
BLUE DYE CONTROLLER
"b" SET POINT
"b"
COLOR METER MEASURING UNIT
COLOR METER SENSE HEAD
THICK STOCK
CLEANERS
HEADBOX
WIRE
DRYERS
REEL
FAN PUMP
BLUE PUMP POSITIONER
RED PUMP POSITIONER
WHITE WATER SILO

FIGURE 6

OPEN LOOP BLOCK DIAGRAM OF PAPER MACHINE
DYE CONCENTRATION SYSTEM

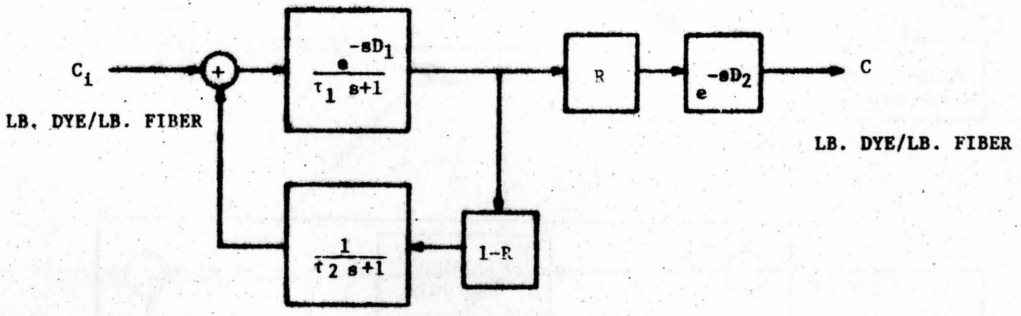

FIGURE 7

THE PROCESS RESPONSE TO A UNIT STEP WITH DIFFERENT DYE RETENTION

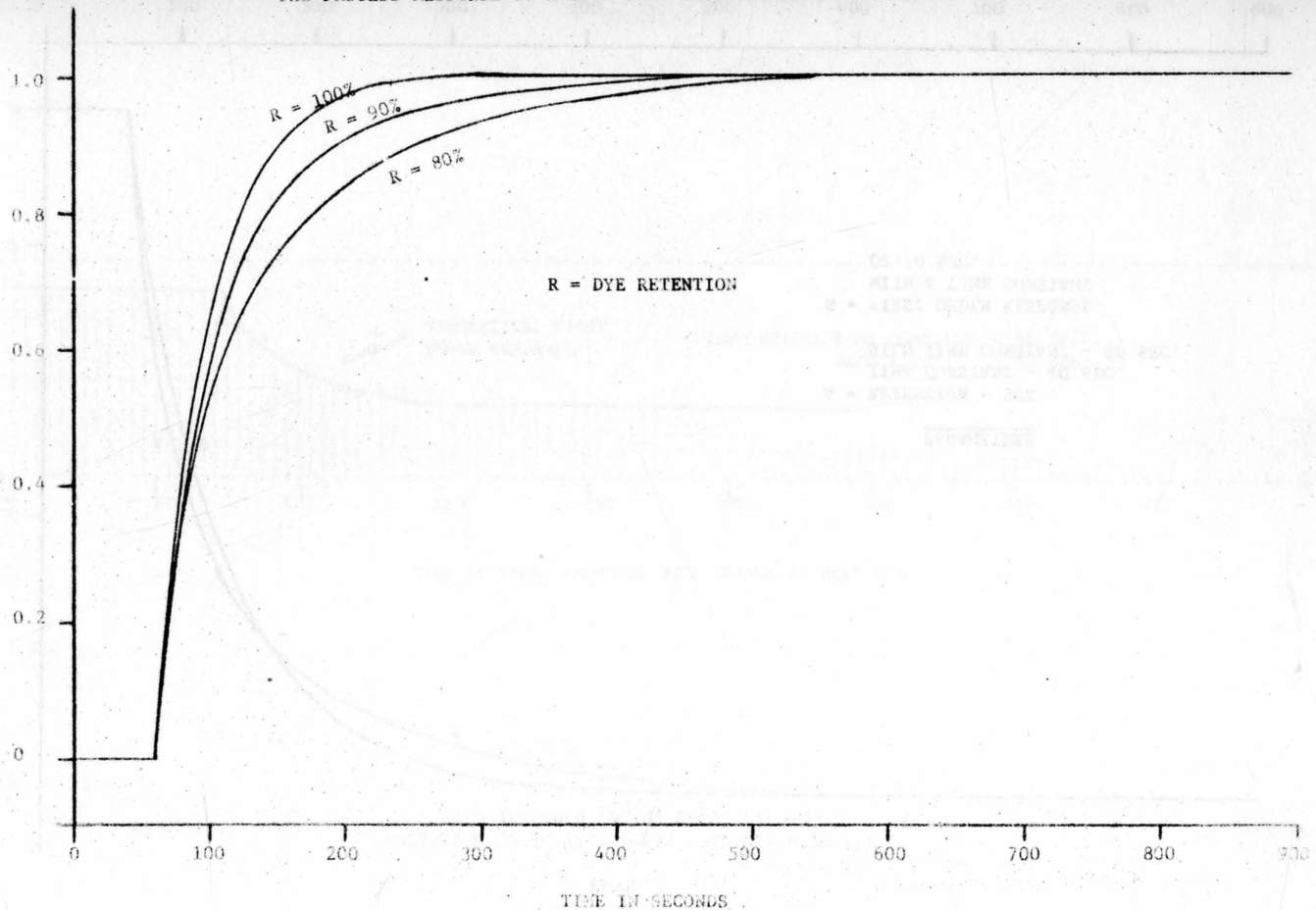

FIGURE 8

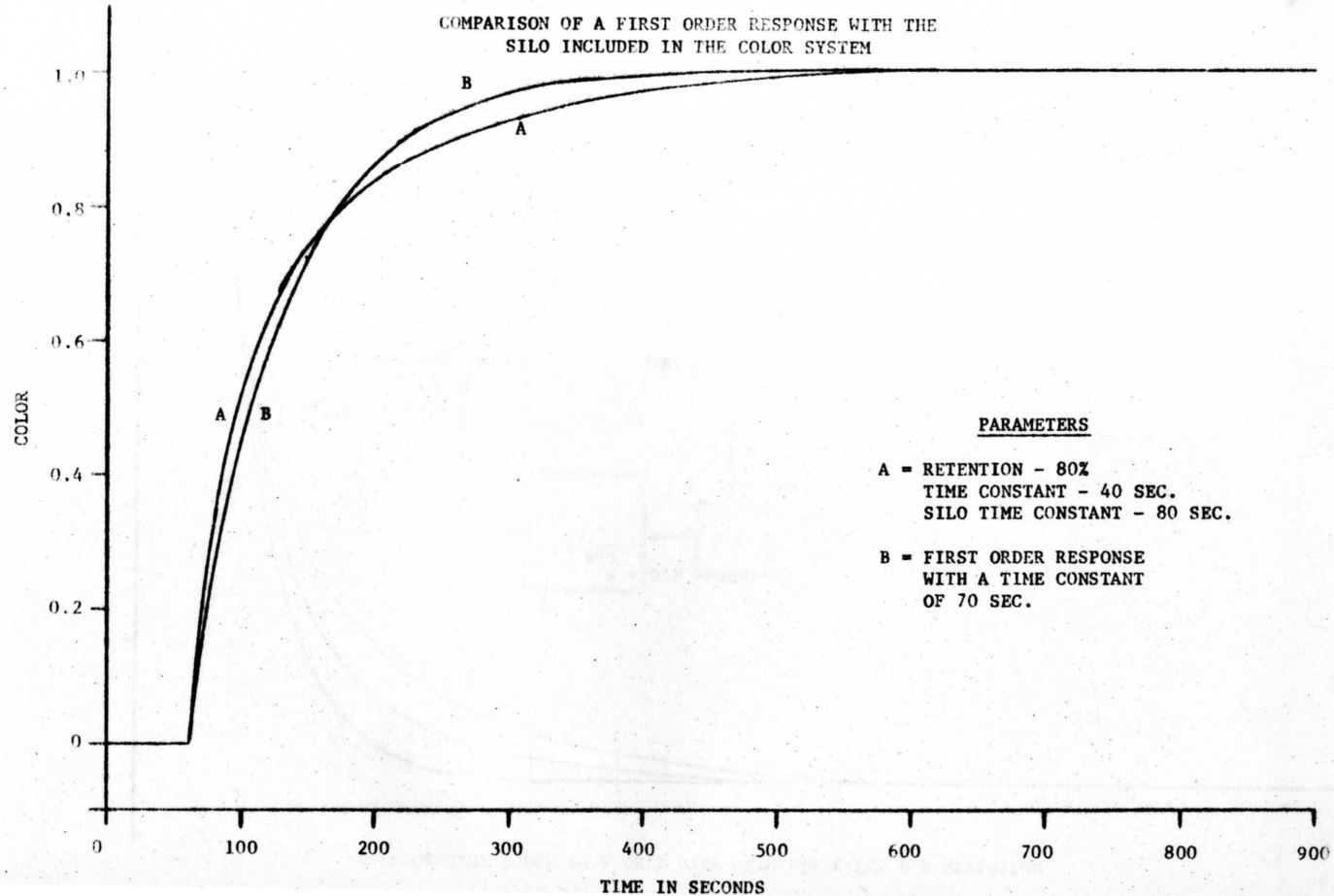
COMPARISON OF A FIRST ORDER RESPONSE WITH THE
SILO INCLUDED IN THE COLOR SYSTEM
COLOR
1.0
0.8
0.6
0.4
0.2
0
A
B
B
A
A
B
PARAMETERS
A = RETENTION - 80%
TIME CONSTANT - 40 SEC.
SILO TIME CONSTANT - 80 SEC.
B = FIRST ORDER RESPONSE
WITH A TIME CONSTANT
OF 70 SEC.
0
100
200
300
400
500
600
700
800
900
TIME IN SECONDS

FIGURE 9

THE EFFECT OF A BLUE DYE STEP CHANGE ON "b" COLOR

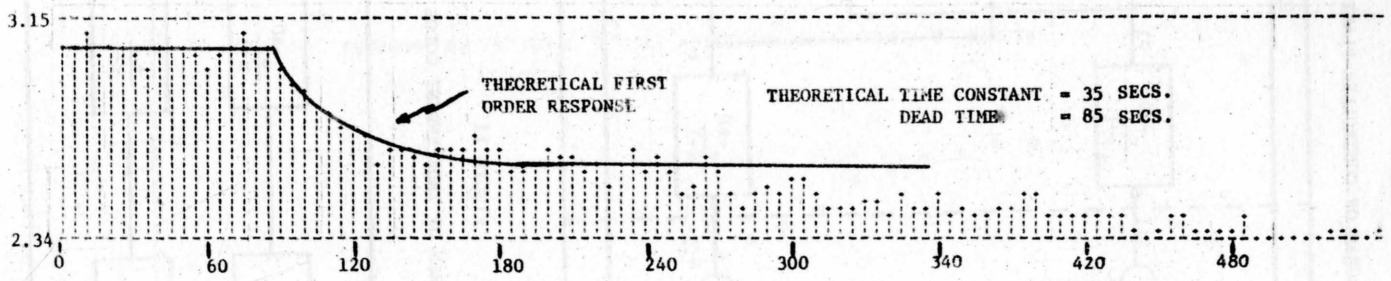

TIME IN SECS. FROM THE STEP CHANGE IN BLUE DYE

FIGURE 10

BLOCK DIAGRAM OF CONTROLLER-PLANT SYSTEM

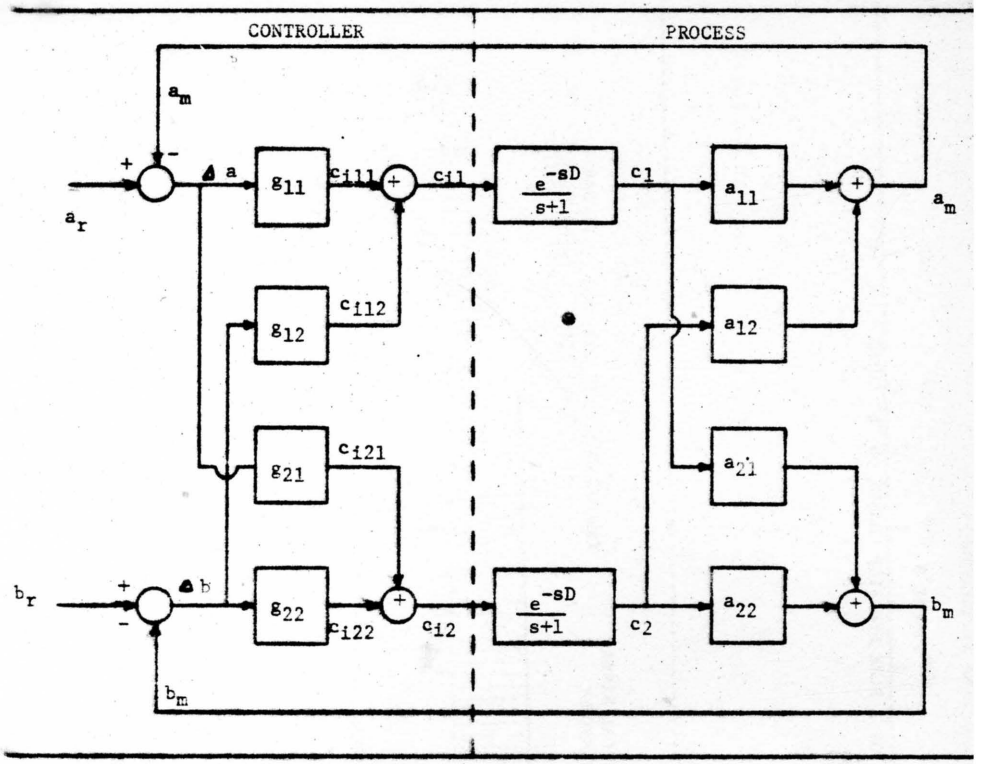

FIGURE 11

BLOCK DIAGRAM OF INDEPENDENT COLOR LOOPS

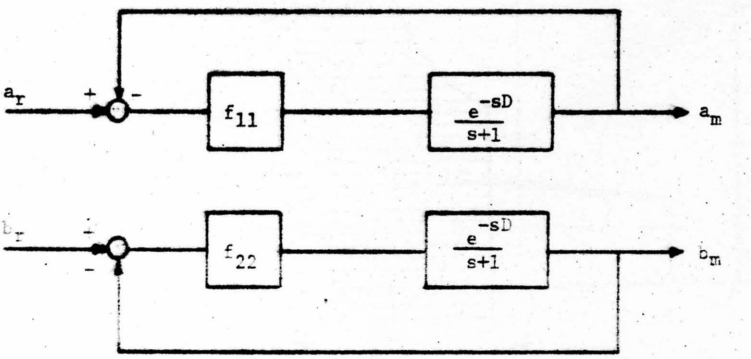

FIGURE 12A

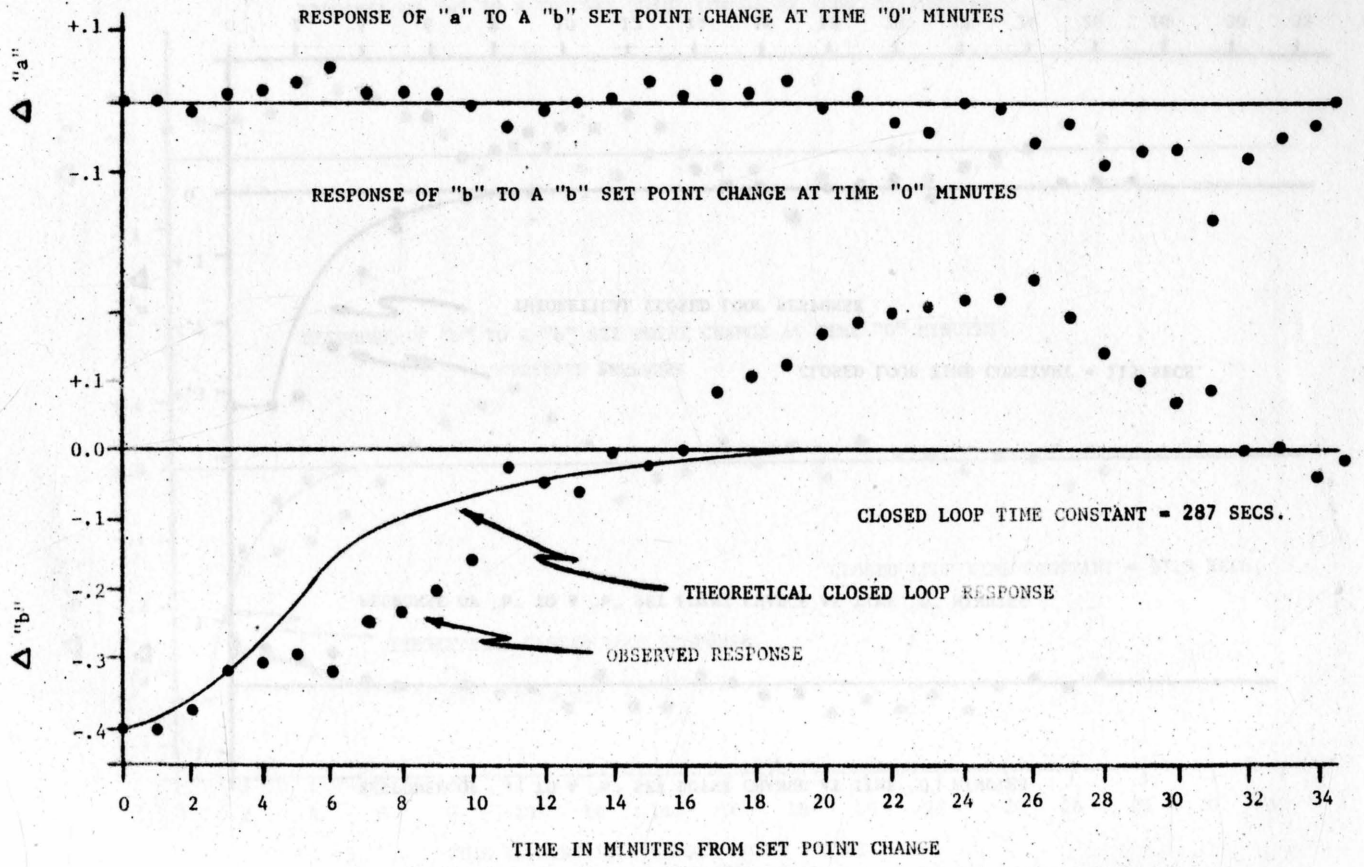
RESPONSE OF "a" TO A "b" SET POINT CHANGE AT TIME "0" MINUTES
Δ "a"
+.1
-.1
RESPONSE OF "b" TO A "b" SET POINT CHANGE AT TIME "0" MINUTES
+.1
0.0
-.1
-.2
-.3
-.4
Δ "b"
CLOSED LOOP TIME CONSTANT = 287 SECS.
THEORETICAL CLOSED LOOP RESPONSE
OBSERVED RESPONSE
0
2
4
6
8
10
12
14
16
18
20
22
24
26
28
30
32
34
TIME IN MINUTES FROM SET POINT CHANGE

X = THEORETICAL

FIGURE 12B

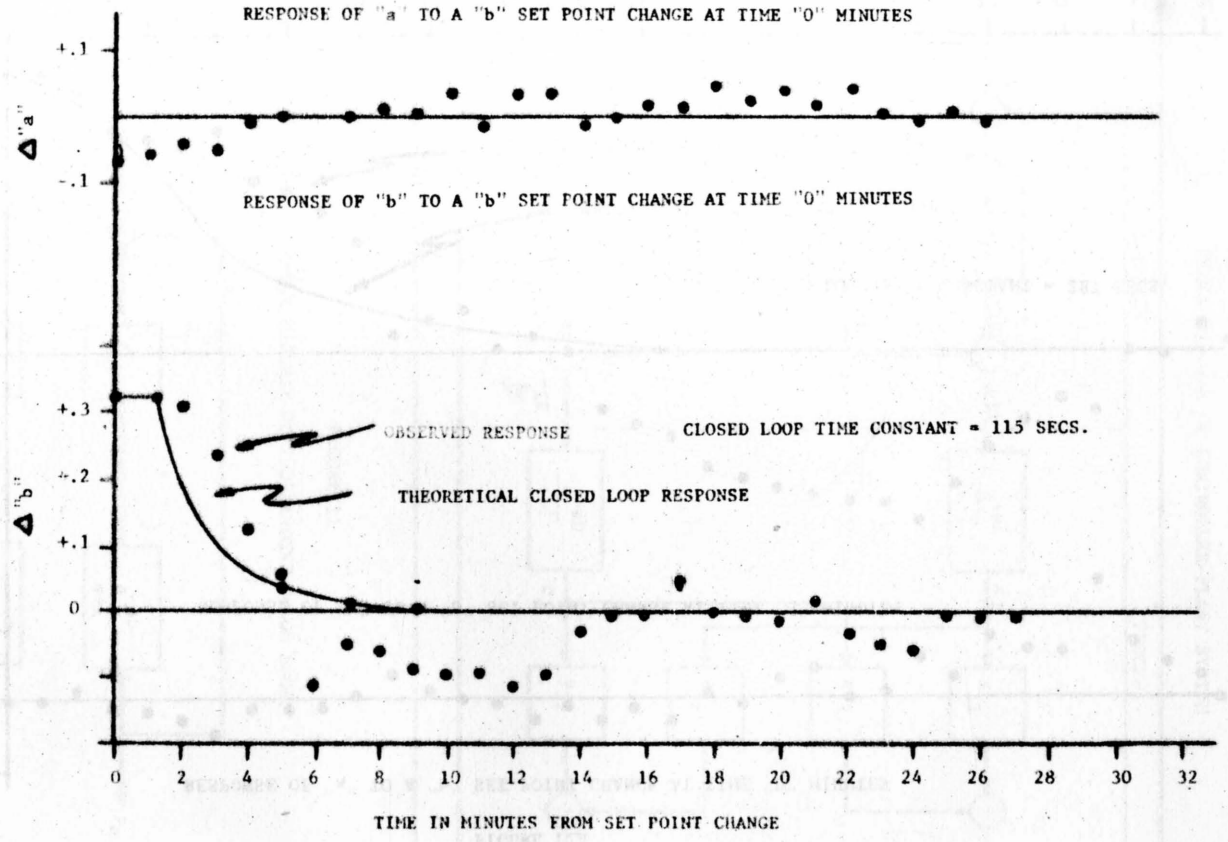

FIGURE 12C

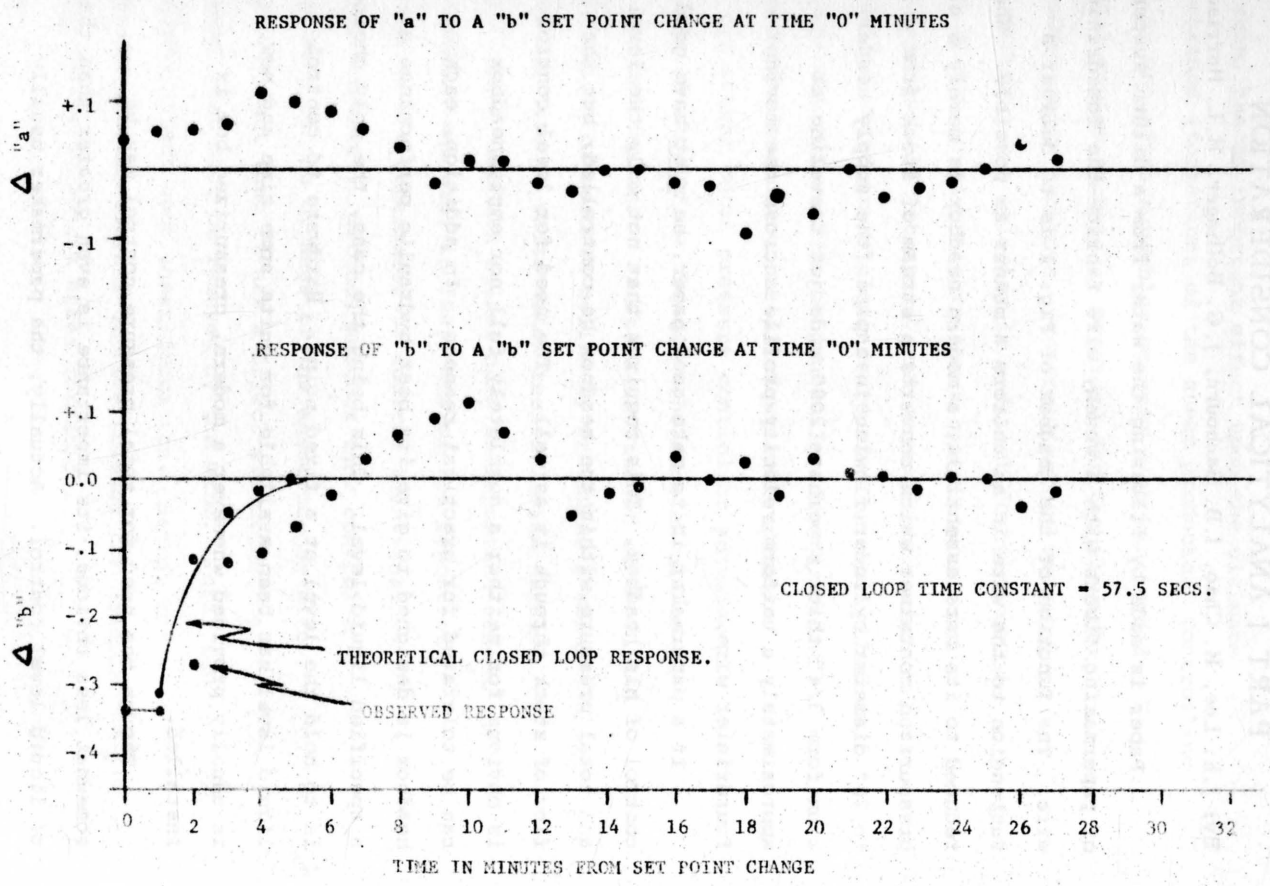
RESPONSE OF "a" TO A "b" SET POINT CHANGE AT TIME "0" MINUTES
Δ "a"
+.1
-.1
RESPONSE OF "b" TO A "b" SET POINT CHANGE AT TIME "0" MINUTES
Δ "b"
+.1
0.0
-.1
-.2
-.3
-.4
CLOSED LOOP TIME CONSTANT = 57.5 SECS.
THEORETICAL CLOSED LOOP RESPONSE.
OBSERVED RESPONSE
0
2
4
6
8
10
12
14
16
18
20
22
24
26
28
30
32
TIME IN MINUTES FROM SET POINT CHANGE

THE DESIGN OF A HEADBOX CONTROL SYSTEM PART I ANALYTICAL CONSIDERATION

By: J.K. Lee, H. Chao, I.B. Sanbourn, J.G. Bollinger, H.L. Harrison

Paper is made by filtering the water from a dilute suspension of papermaking fibers with a woven, wire fabric--the fourdrinier wire. The function of the headbox of Fig. 1 is to deliver a suspension to the wire in as uniform a manner as possible. When reduced to its bare essentials, a modern headbox is merely a closed, pressurized container which converts a stream of stock from a 14" to 20" diameter cylinder flowing in a pipe (the supply header) to a uniform 3/4" thick × perhaps 200" wide jet traveling at approximately a uniform velocity profile accross the moving fourdrinier wire.

If a papermaker is to make good paper, he must have good control of his headbox. This requires that not only the level and total pressure within the headbox be controlled, but the flow of stock through it as well. The need for level control is obvious for neither a completely full nor empty headbox can be tolerated for practical reasons. In addition, each headbox is designed to give its best hydraulic performance at a specified liquid level. This being the case, the only choice is to hold the level at a fixed point. Hardware to control liquid level has been available for quite some time and now is usually provided whenever a modern, pressurized box is installed.

Though the need for total pressure control may be somewhat less obvious, its importance is even greater than that of liquid level control. Actually, the papermaker usually wishes to hold a constant difference between the velocities

of his wire and stock jet. The drag created has an important bearing on how the sheet forms and drains on the fourdrinier which, in turn, has an important effect upon the ultimate visual appearance (formation) of the sheet produced. Controlling wire speed is not often a problem because a sophisticated speed control system is usually provided for the electric drive of modern paper machines. Controlling jet velocity is another matter. Jet velocity is a direct function of the square root of the total pressure for a given slice opening within the headbox. If jet speed, and consequently drag, is to be controlled, headbox total pressure must be controlled. This fact does not yet seem to be generally recognized and many new headboxes are being installed without adequate provisions for either total pressure control or adjustment.

The rate of stock flow through a headbox should be controlled for two reasons. First, a control of stock flow allows manipulation of headbox solids by providing a means of adjusting the rate of white water recirculation through the wet end system. Headbox solids have an important effect on sheet formation and are, in fact, one of the important variables used by the papermaker to control the visual appearance of his sheet. Second, headbox flow control allows adjustment of the dryness of the sheet on the wire by virtue of the fact that it has a direct effect on the amount of water that must be removed by the wire. This, too, has an important effect upon sheet formation. Hence, the prime reason for needing control of flow through the headbox is to make it easier to adjust sheet formation.

To summarize, careful analysis of the papermaker's needs indicates that it would be beneficial for him to be able to specify the liquid level, drag, and headbox flow at which he wished to operate; and then have an automatic control system maintain these factors at the levels specified. To meet such criteria the liquid level, total pressure, and flow through the headbox must be controlled independently. Methods for achieving this aim using water valve position, air valve positions (both inlet and blowing), and slice opening as the manipulated variables have been developed, but for the present the analysis will consider only means for controlling liquid level and total head via manipulation of water valve and air valve positions.

Literature Review

Much work has already been done to develop better controls for the headbox. Beecher[1] in 1963 outlined the general nature of the problem. In 1966, Mardon et al[2] demonstrated how a headbox could be modeled on an analog computer. The equations describing the system were set forth and experimental verification was included. Mehaffey et al[3] also modeled the headbox and other components intimately associated with it on an analog computer. Various control schemes were investigated on the analog model and subsequently tested on an actual system. Sullivan and Schoeffler[4] demonstrated how the entire wet end of a paper machine could be dynamically modeled on a digital computer. Simple subroutines were written for basic components and a

main program called for them in proper order. This type of model is very versatile and can be used for both experimental purposes and to improve control of the actual process.

Model Development

Figure 1 is a schematic of the headbox system. Mardon et al[2] have already shown that the equations characterizing such a system can be derived analytically from the application of the physical principles of the device and a knowledge of important headbox parameters. In this particular instance, a 138-inch wide, Valley, air-loaded, multiplex headbox was studied. The seven equations describing this system are presented in Column (a), Eqs. 1a-7a, of Table 1 from which it can be seen that some are decidedly nonlinear. In order to deal with these expressions conveniently they may be linearized about a specific operating point. The equations that result are found in Column (b), Eqs. 1b-7b. For convenience the notation may then be changed such that $h \sim \Delta h$, $H \sim \Delta H$, etc. The Laplace transformed equations are in Column (c), Eqs. 1c-7c where the simplified notation has been adopted. Study of these equations shows that ten constants are required to quantize the behavior of the entire system.

The block diagram in Fig. 2 was developed from Eqs. 1c-7c of Table 1 and shows how the various parameters of the mathematical model of the headbox interrelate. Such a diagram is quite useful for it can serve as the starting point for the synthesis of the headbox control system. Before proceeding with the synthesis, however, the overall control concept may be outlined.

First, the controlled variables in the headbox system will be total head (H) and liquid level (h). Second, the manipulated variables will be flow into the headbox (q_{il}), inlet air valve position (X_{ia}), and outlet air valve position (X_{oa}). Third, the process disturbances will be considered as changes in slice position (Y_{ol}) and flow changes (q_{il}). Set point adjustments in H or h will be considered commands.

Control Strategy

The first step toward developing an adequate controller design is to condense the block diagram of Fig. 2 by means of the techniques of block diagram algebra. The results of such a condensation are presented in Fig. 3. With this diagram available and the knowledge that an adequate headbox controller must 1) hold both liquid level and total head at their set points despite process disturbances and 2) follow desired changes in the set points, it is possible to proceed with the syntehsis of the necessary controllers.

Mardon et al[2] have already shown that the headbox control problem can be approached in either of two ways, depending upon how the controllers are connected to the headbox. Total head H may be controlled via manipulation of the air valves as shown in Fig. 4. This arrangement is referred to here as the straight configuration. At this point one should note the introduction of two new symbols $H_r(s)$ and $H_\varepsilon(s)$. Here H_r is the command variation from the true head reference level and H_ε is the difference between H(s) and $H_r(s)$. If H is controlled by adjustment of the water (or stream flow) valve as shown in Fig. 5, then it is referred to here as the reversed configuration.

Mardon's work claimed the two arrangements showed essentially the same performance when used on a real headbox. Consequently, it was decided to concentrate attention on the reversed configuration in this investigation because it is easy to transfer from control of liquid level by conventional means (see Fig. 6) to the reversed configuration (see Fig. 5). Only the closing of the total head control loop with an appropriate gain in it is required since the liquid level loop is already extant. Upsets to the headbox system are minimized, if not entirely eliminated, when it is necessary to go on or off total head control as a result.

Steady State Response

With a control strategy decided upon, the designer is faced with a decision as to what type of control action to provide in each loop. Here it should be recalled that systems specifications are such that total head and liquid level set point must be maintained regardless of upsets to flow due to slice adjustments and set point changes. To accomplish this the block diagram in Fig. 5 was first reduced to the more condensed form shown in Fig. 7. Then, the steady state response of both total head and liquid level to changes in set points and flow upsets were estimated by deriving the appropriate transfer functions from Fig. 7 and applying the final value theorem.

For example, if only proportional action is considered for each loop and a step change in total head set point variation is considered we obtain the following.

For change in total head:

$$H_{ess} = \lim_{t\to\infty} \left[H(t) - H_r(t)\right] = \lim_{s\to 0} s\left[H(s) - H_r(s)\right]$$

$$= \lim_{s\to 0} s\left[\frac{(as + b + K_{p2}c)\,K_{p1}}{As(ds + b) + (K_{p1} + K_1)(as + b + K_{p2}c)} - 1\right]\frac{1}{s} \qquad (1)$$

$$H_{ess} = \frac{-K_1}{K_1 + K_{p1}} \qquad (2)$$

For changes in liquid level:

$$h_{ss} = \lim_{t\to\infty} h(t) = \lim_{s\to 0} s\,h(s)$$

$$= \lim_{s\to 0} s\left[\frac{K_{p1}\,(ds + b)}{As(ds + b) + (as + b + K_{p2}c)(K_1 + K_{p1})}\right]\frac{1}{s} \qquad (3)$$

$$h_{ss} = \frac{K_{p2}b}{(b + K_{p2}c)(K_1 + K_{p1})} \qquad (4)$$

Note that the most desirable result is to have both the limits in Eqs. (2) and (4) go to zero. Similar analyses were carried out for all possible combinations of proportional and proportional plus integral action, and the results are presented in Table 2.

From Table 2 it can be seen that overall system specifications can only be met if both proportional and integral action are present in each loop. Hence, the reversed configuration with PI action in each loop was the design finally decided upon for the system.

Transient Response

With the system configuration and controller actions specified, the remaining task is to determine the gains required in each loop of the controller for desirable response. A variety of methods are available for such studies leading to gain settings; however, considerable difficulty may be encountered when a multi-loop system is involved. One effective approach is the root contour method, as described by Kuo[5] which may be applied to multi-loops design problems of the type at hand if modified appropriately.

The root contour method involves first writing the characteristic equation for the system. This is readily derivable from the block diagram shown in Fig. 7 and is of the form:

$$\frac{1}{As}\left[\frac{as^2 + bs + K_{p2}cs + K_{p2}c/T_{i2}}{s(ds + b)}\right]\left(K_{p1} + K_1 + K_{p1}/sT_{i1}\right) + 1 = 0 \tag{5}$$

Unfortunately, such an expression is not in a form capable of direct treatment via the root contour method. Additional manipulation is required to put Eq. 5 in a form such that the root contour for K_{p1} (gain in the total head loop) can be developed while holding K_{p2} (gain in the liquid level loop T_{i1} and T_{i2} (integral terms) constant. The required expression is of the form

$$\frac{K_{p1}\left[as^3 + \left(b+K_{p2}c+\frac{a}{T_{i1}}\right)s^2 + \left(\frac{K_{p2}c}{T_{i2}} + \frac{b}{T_{i1}} + \frac{K_{p2}c}{T_{i2}}\right)s + \frac{K_{p2}c}{T_{i1}T_{i2}}\right]}{Ads^4 + (Ab + K_{1a})s^3 + (K_{1b} + K_1K_{p2}c)s^2 + \left(\frac{K_1K_{p2}c}{T_{i2}}\right)s} + 1 = 0 \tag{6}$$

Figure 8 is a typical root contour[6] of K_{p1} for $K_{p2} = 2$ and T_{i1} and $T_{i2} = 20$. The gain of the liquid level loop was held constant at 2, and the integral action in each loop was held at 5% (reciprocal of T times 100) of the gain while the gain of the total head loop was varied from zero to infinity. From the figure, it may be seen that there are two short loci on the real axis close to the origin. These loci have little effect on the overall stability of the system. The loci of interest are those beginning at the complex poles located at $-0.198 \pm 0.968j$ and proceeding to the two real axis zeros located at -2.41 and minus infinity. The shape of these two loci implies that stability increases without bound as K_{p1} increases without bound. The response times of the water and air valves being actuated by the headbox controllers were neglected. In actual fact, the dynamics of the control valves are not negligible as compared to that of the headbox. In fact increasing gain along an altered shape would lead to instability.

If the dynamics of both the air and water valves are introduced into the problem, the system's characteristic equation is changed from fourth to sixth order. This makes a mathematically difficult problem all the more complex. Analysis as well as simulation results (to be discussed later) indicate that most practical design problems engendered by considering control valve dynamics are encountered even if only the water valve time constant is considered. Elimination of the air valve time constant greatly simplifies the mathematics involved, therefore all of the root contour work presented herein ignores air valve dynamics.

Figure 9 contains a root contour plot for K_{p1} where K_{p2} is again 2.0 and T_{i1} and T_{i2} are held at 20, but a time constant of 5 seconds is assumed for the water valve. As is readily apparent, the root loci are substantially different. In this instance, there are three loci located along the negative real axis, but again these have little effect on overall stability. It is the two loci issuing from the complex poles (-0.198 ± 0.968j) and crossing the imaginary axis at about ±1.1j that dominate. This type of contour implies that the system will be quite oscillatory for even low values of K_{p1} and become unstable if K_{p1} exceeds 600. Hence, it is apparent that the design problem in this instance is to devise a strategy for picking controller gains that yield a reasonably non-oscillatory headbox system despite relatively high values for K_{p1}. Various root contour studies have shown that reductio in K_{p2} are the most effective means for achieving this end.

The effect of lowering K_{p2} is best illustrated by comparing Figs. 9 and 10. In Fig. 10, K_{p2} has been reduced to 0.2 whereas T_{i1}, T_{i2}, and T_v were held constant. This plot is much the same as the one in Fig. 9 except that the two complex poles have been moved closer to the real axis (-0.190 ± 0.200j) and the loci issuing from them have been bent to the left so that they never do cross the imaginary axis. This being the case, it would appear that the best strategy to use in tuning the headbox control system is to decrease K_{p2} to the point that K_{p1} can be increased sufficiently to give good total head control without undue system oscillatiom.

Discussion of Results

With a strategy for tuning the headbox system decided upon, the only item that deserves further discussion is the technique by which specific controller settings were chosen. One of the more popular methods of controller gain selection used in conjunction with root locus plots is to assume that a system's transient response is closely approximated by that of an underdamped second-order system. This being the case, it can be shown that lines emanating from the origin are lines of constant damping ratio; lines parallel to the real axis are loci of constant damped natural frequency; and lines parallel to the imaginary axis are lines of constant time constant. This approach is adequately described in a number of standard texts such as the one by Harrison and Bollinger[6] Suffice it to say here that such an approach was taken in this case with lines of constant damping ratio being the primary tool used for gain selection.

Choice of Controller Parameters

Figure 11 contains an enlarged root contour plot for K_{p1} with $K_{p2} = 0.2$, $T_{i1} = T_{i2} = 20$ (5% integral action), and $T_v = 5$. Lines of constant damping ratio have been superimposed on the plot from which it can be seen that K_{p1} varies all the way from 130 for a zeta of 0.5 to 550 for a zeta of 0.30. The time constant of the system did not change greatly but the damped natural frequency increased from about 0.32 to 0.55 radians per second. This would indicate that though the system becomes appreciably more oscillatory as the damping

ratio is decreased, its speed of response to upsets does not improve substantially.

The validity of such generalizations is dependent upon the exactness of the analogy drawn between the behavior of the closed loop response of this multi-loop system and a simple second-order system. Even at first glance, it appears that the analogy may be weak and as a result, the headbox system was modeled via an IBM digital simulation program [CSMP (8) described in IBM Manual H20-0282-0]. The simulation diagram of the headbox system is shown in Fig. 12.

Two sets of curves from the simulation are presented in Fig. 13. Controller parameters were held at $K_{p1} = 200$, $K_{p2} = 0.2$, $T_{i1} = T_{i2} = 20$ and T_v was set at 5.0 seconds. In the first set of curves, the response of system liquid level to a one-inch set point change in total head ~~variation~~ and a 1% upset in flow through the headbox is shown. The disturbance in liquid level was both small and quickly corrected in each case indicating that the liquid level upsets can probably be ignored as a design consideration in this particular case. The other set of curves shows the response of total head to the same disturbances.

From these curves, it appears that the analogy between the system at hand and an underdamped second order system is rather weak. Total head response is slightly oscillatory but shows none of the overshoot to be expected of a system with a damping ratio of only 0.45. In this instance, it appears that the proportional part of the controllers have completed their action in a mere 20-30 seconds but an additional 50 seconds is required for the integral portions to drive the total head

to set point. This suggests that the system might perform better with even a lower damping ratio.

Figure 14 shows a comparison of the system's response to a one-inch set point change in total head variation for damping ratios of 0.45 and 0.35. The lower damping ratio brings the system to within 5% of set point in only 29 seconds versus 57 seconds for the higher zeta. The tendency for the system to oscillate increases, but again overshoot is minimal and no serious control problems seem to result. Hence, in this instance it would seem best to use a zeta somewhat lower than usual for design purposes despite the conclusions originally reached from an inspection of root contour plot in Fig. 11.

One factor that has been ignored in the above is that the time constants of the air valves being actuated by the liquid level controller were neglected in developing all of the plots presented in Figs. 11, 13, and 14. It has already been mentioned that ignoring air valve dynamics is not as serious as neglecting the response time of the water valve, but the lags introduced by these valves do have an appreciable effect on system stability as will be illustrated.

Figure 15 contains plots of the response of the system to a total head set point change with and without air valve dynamics being considered. In curve a, the time constant of the air valves was taken as zero whereas in b, it was assumed to be 5 seconds. In both cases, controller parameters were held constant at $K_{p1} = 200$, $K_{p2} = 0.2$, and $T_{i1} = T_{i2} = 20$. From these curves, it is obvious that introducing a time constant into the dynamics of the air valves has not only made the system more oscillatory, but slower to respond as well.

(62 versus 38 seconds to reduce system error to 5% of the set point change). No overshoot is experienced but still it would seem wise to be somewhat conservative and use a damping ratio of 0.45 in choosing K_{p1}. This being the case, it would seem that adequate, if not optimal, performance by the system would be achieved if controller parameters were set at the following values: $K_{p1} = 200$, $K_{p2} = 0.2$, $T_{i1} = T_{i2} = 20$.

One question remains to be answered before these values can be finally decided upon, however, and that concerns the effect that variations in T_{i1} and T_{i2} have on system performance. Thus far, it has been assumed that 5% of integral action would be adequate. The effect of varying the amount of integral action is best illustrated by studying Fig. 16 and comparing its root contours with those in Fig. 11.

From such a comparison, it can be seen that increasing the amount of integral action (by decreasing the values of T_{i1} and T_{i2}) tends to move the two loci dominating system stability to the right toward the imaginary axis while at the same time increasing the value of the imaginary part of the poles. Both effects tend to make the system more oscillatory and less stable. In addition, another disturbing change takes place. Two of the three contours that formerly lay on the negative real axis are now seen to leave it and terminate at two complex poles located at $-0.128 \pm 0.189j$. These tendencies continue if the amount of integral action is increased beyond 10% and the net effect is to introduce serious stability problems. With this in mind, it would then seem best to leave the amount of integral action low, at about 5%, and to achieve increased speed of response by raising K_{p1} if possible.

This being the case, it would appear that the values of the controller parameters stated above are, in fact, close to optimal.

Limitations Imposed by Linearization

It has already been mentioned, and is well known, that considerable accuracy with respect to the servo problem must be sacrificed for the mathematical convenience achieved when a system is linearized. Most of the work reported herein was carried out with a total head in the 42-43 inch of water range. Figure 17 contains a root locus plot of the system when total head is in the 28-29 inch of water range. Comparison of this plot with the one in Fig. 11 shows that though the shapes of the curve have not changed significantly, their positions on the S plane have been shifted. Fortunately, the shift has been such that stability has been increased rather than decreased. This means that if a headbox controller is tuned for close to optimal operation at a high total head, it will not be operating at its best at lower total head set points. An ability to adjust controller parameters dynamically during operation would be of considerable benefit. This point will be discussed at quite some length in Parts II and III of the paper. For the present, suffice it to say that if one designs a controller to give semi-optimal performance at the highest total head envisioned for the headbox system, it will give adequate performance at all lesser set points.

On-Line Performance

Before closing this paper, the performance of a headbox using the control strategy and parameters developed herein should be presented to verify the validity of the approach. The headbox chosen was one with the very same engineering parameters as used in our simulation work. Initially

K_{p2} was set at 0.2, T_{i1} and T_{i2} at 20 and K_{p1} at 130. The result was rather sluggish performance and K_{p2} was increased in a step-wise fashion as our simulation work indicated it should be. The speed of response was not "satisfactory" until K_{p2} reached 365 at which time the headbox behaved as shown in Figures 18 and 19.

Comparison of the data in these figures with that in Figures 13 and 14 shows the analytical model to be a remarkably good approximation of true headbox performance. Three controller parameters (K_{p2}, T_{i1}, and T_{i2}) give near-optimal performance at exactly the value predicted by the model whereas the model would have set K_{p1} at an excessively conservative value (K_{p1} = 130 - 150 vs. K_{p1} = 350 - 375). Such performance on the part of a model is exactly what an engineer desires for it allows him to place controller parameters in a good range and then reach optimality by fine tuning in the manner prescribed as best by simulation work. In summary, the headbox in question is now operating with K_{p1} = 365, K_{p2} = 0.2, and $T_{i1} = T_{i2}$ = 20 levels that are remarkably close to the values predicted as being nearly optimal by simulation (K_{p1} = 130, K_{p2} = 0.2, $T_{i1} = T_{i2}$ = 20). In addition, the discrepancy that does exist may very well be explained by the choice of an unfortunately large water valve time constant (T_v).

Conclusion

From the above, it may be concluded that it is possible to attack the multi-loop headbox system from an analytical standpoint, develop a linearized model for the system, determine the action required of the controllers in the system on a rigorous basis, and then finally tune the controllers in such a way that near-optimal performance is achieved. Controller action is best determined by means of the study of system by means of the root contours approach. All indications are that in the headbox system, the gain in the liquid level loop should be kept relatively low so that the gain in the total head loop can be kept as high as possible.

In addition, about 5% integral action in each loop seems useful. Finally, it appears that the dynamics of the air valves in the system can be ignored to simplify the problem but that doing this also requires that the designer not go much lower than 0.5 for a value of zeta when picking a value for K_{p1} to be used in the total head controller.

NOMENCLATURE

A	cross section of headbox, sq. in.
a	defined in Table of Headbox Constants.
A_s	opening area of slice, sq. in.
b	defined in Table of Headbox Constants.
c	defined in Table of Headbox Constants
C_d	discharge coefficient of slice, dimensionless.
C_g	outlet air valve coefficient, a function of valve position, dimensionless.
C_g'	inlet air valve coefficient, a function of valve position, dimensionless.
d	defined in Table of Headbox Constants.
g	gravitational constant, in./sec.^{2}
H	total head, inch.
H_r	total head set point, inch.
h	liquid level, inch.
j	square root of -1.
K_1 thru K_8	defined in Table of Headbox Constants.
K_{p1}	the gain of water valve controller; cubic inch per second flow per inch of total head difference.
K_{p2}	the gain of air valve controller, fraction of air valve travel per inch of liquid level difference.
M	mass of air in headbox, lb.
m_{ia}	mass flow of inlet air, lb./sec.
m_{oa}	mass flow of outlet air, lb./sec.

P	air pad pressure, p.s.i.
P_s	pressure of air supply, p.s.i.
q_{il}	liquid flow into headbox, cubic inch per sec.
q_{ol}	liquid flow out of headbox, cubic inch per sec.
R	gas constant $(in.^3)$ (p.s.i.)/(lb.-mole) (R^o)
s	Laplace operator.
T	temperature, R^o.
T_{i1}	the equivalent time constant of integral action in water valve controller, or the reciprocal of ratio of integral to proportional action, second.
T_{i2}	the equivalent time constant of integral action in air valve controller, second.
T_v	time constant of water valve, second.
V	volume of headbox air pad, cubic inch.
X_{ia}	inlet air valve position, %.
X_{oa}	outlet air valve position, %.
Y_{ol}	slice opening, inch.

Greek Letters

ρ_a	density of air, lbm/ft^3.
ρ_w	density of liquid, lb. per cubic inch.
ζ	damping ratio.

HEADBOX CONSTANTS

$A = 4{,}000.$

$q_{il} = 14{,}250.$

$H = 43.$

$Y_{ol} = 0.75$

$V = 119 \times 12^3$

$T = 80 + 460$

$\rho_w = 62.4/12^3$

$\rho_a = 28.97$

$R = 10.731 \times 12^3$

$P_s = 16.7$

$K_1 = q_{il}/2H = 165.7$

$K_1' = q_{il}/Y_{ol} = 19{,}000.$

$K_2 = 1/\rho_w = 27.7$

$K_3 = \frac{RT}{\rho_a V} = 1.68$

$K_4 = \frac{PA}{V} = 0.316$

$$K_5 = \frac{P\rho_a}{RT} \cdot \frac{975.6 \times 12^3}{3{,}6000} P \left[\frac{2.32 \times (P - 14.7)}{P}\right]^{0.4425}$$

$$= 0.184$$

$$K_6 = \frac{P\rho_a}{RT} \cdot \frac{210 \times 12^3}{3{,}600} \left[0.4425 \left(\frac{P}{P - 14.7}\right)^{0.5575} + 0.5575 \left(\frac{P - 14.7}{P}\right)^{0.4425}\right]$$

$$= 0.0087$$

$$K_7 = \frac{P\rho_a}{RT} \cdot \frac{975.6 \times 12^3}{3{,}600} \cdot P_s^{0.5575} (P_s - P)^{0.4425}$$

$$= 0.0741$$

$$K_8 = - \frac{P\rho_a}{RT} \cdot \frac{210 \quad 12^3}{3{,}600} \cdot \left[0.5575 \left(\frac{P_s - P}{P_s}\right)^{0.4425} + 0.4425 \left(\frac{P_s}{P_s - P}\right)^{0.5575}\right]$$

$$= - 0.0165$$

$$a = \frac{1}{K_2 K_3} + \frac{K_4}{K_3} = 0.210$$

$$b = \frac{K_6 - K_8}{K_2} = 0.00091$$

$$c = K_5 + K_7 = 0.258$$

$$d = \frac{1}{K_2 K_3} = 0.0215$$

TABLE 1

	Original Equations (a)	Linearized Equations (b)	Laplace Equations* (c)
1.	$q_{o1} = C_d A_s \sqrt{2gH}$	$\Delta q_{o1} = K_1 \Delta H + K_1' \Delta Y_{o1}$	$q_{o1}(s) = K_1 H(s) + K_1' Y_{o1}(s)$
2.	$H = h + \frac{P - 14.7}{\rho_w}$	$\Delta H = \Delta h + K_2 \Delta P$	$H(s) = h(s) + K_2 P(s)$
3.	$\frac{dM}{dt} = m_{ia} - m_{oa}$	$\frac{d\Delta M}{dt} = \Delta m_{ia} - \Delta m_{oa}$	$sM(s) = m_{ia}(s) - m_{oa}(s)$
4.	$\frac{dh}{dt} = \frac{1}{A}(q_{i1} - q_{o1})$	$\frac{d\Delta h}{dt} = \frac{1}{A}(\Delta q_{i1} - \Delta q_{o1})$	$sh(s) = \frac{1}{A}[q_{i1}(s) - q_{o1}(s)]$
5.	$P = \frac{M}{\forall} RT$	$\Delta P = K_3 \Delta M + K_4 \Delta h$	$P(s) = K_3 M(s) + K_4 h(s)$
6.**	$m_{oa} = \frac{\rho_s C_d P}{3600}\left[2.32 \frac{(P - 14.7)}{P}\right]^{0.4425}$	$\Delta m_{oa} = K_5 \Delta X_{oa} + K_6 \Delta P$	$m_{oa}(s) = K_5 X_{oa}(s) + K_6 P(s)$
7.**	$m_{ia} = \frac{\rho_s C_d' P_s}{3600}\left[2.32 \frac{(P_s - P)}{P_s}\right]^{0.4425}$	$\Delta m_{ia} = K_7 \Delta X_{ia} + K_8 \Delta P$	$m_{ia}(s) = K_7 X_{ia}(s) + K_8 P(s)$

* Note that the notation has been changed here such that $h \sim \Delta h$, $H \sim \Delta H$, etc.

** Control Valve Handbook, First Edition, Fisher Governor Co., Marshalltown, Iowa.

TABLE 2

Total Head Controller	P + I	P + I	P	P
Liquid Level Controller	P + I	P	P + I	P
Flow Rate Change	$H_{ss} = 0$ $h_{ss} = 0$	$H_{ss} = 0$ $h_{ss} = 0$	$H_{ss} = \frac{1}{K_1 + K_{p1}}$ $h_{ss} = 0$	$H_{ss} = \frac{1}{K_1 + K_{p1}}$ $h_{ss} = \frac{b}{(K_1 + K_{p1})(b + cK_{p2})}$
Total Head Change	$H_{\epsilon ss} = 0$ $h_{ss} = 0$	$H_{\epsilon ss} = 0$ $h_{ss} = \frac{b}{b+cK_{p2}}$	$H_{\epsilon ss} = \frac{-K_1}{K_1 + K_{p1}}$ $h_{ss} = 0$	$H_{\epsilon ss} = \frac{-K_1}{K_1 + K_{p1}}$ $h_{ss} = \frac{bK_{p1}}{(b + cK_{p2})(K_1 + K_{p1})}$

BIBLIOGRAPHY

(1) Beecher, Alfred E., "Dynamic Modeling Techniques in the Paper Industry," TAPPI, Feb., 1963, Vol. 46, No. 2, pp. 117-120.

(2) Mardon, Monahan, Mehaffey, Dahlin, "A Theoretical and Experimental Investigation into the Stability and Control of Paper Machine Headboxes," Part I, No. 1, 1966, Papper och Tra, pp. 3-14; Part II, No.5, 1966, Papper och Tra, pp. 301-310.

(3) Mehaffey, Branscombe, Harman, Monahan, Mardon, "Analog Computer Study of Paper Machine Headbox Control Systems," ISA Transactions, Vol. 5, No. 3, July, 1966, pp. 283-296.

(4) Sullivan, Schoeffler, "Simulation of Stock Preparation and Fourdrinier Dynamics," Vol. 48, No. 10,October, 1965, TAPPI, pp. 552-557.

(5) Kuo, B. C., Automatic Control Systems, Second Edition, Prentice-Hall, Inc.; Englewood Cliffs, N.J., 1967, pp. 280-296.

(6) Root Locus Program adopted from IBM User Program 1620 - 09.4.046.

(7) Harrison, H. L., and Bollinger, J. G.; Introduction to Automatic Controls, First Edition, International Textbook Co., Scranton, Pa., 1966.

(8) 1130 Continuous System Modeling Program, Program Reference Manual, H20-0282-0, Technical Publication Department, IBM, White Plains, N.Y., 1966.

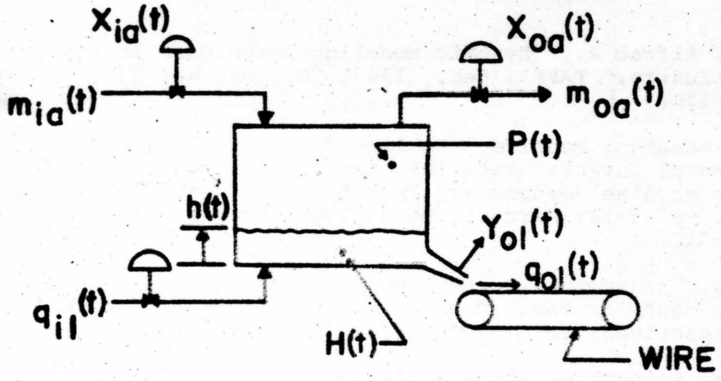

FIGURE 1

Headbox Schematic

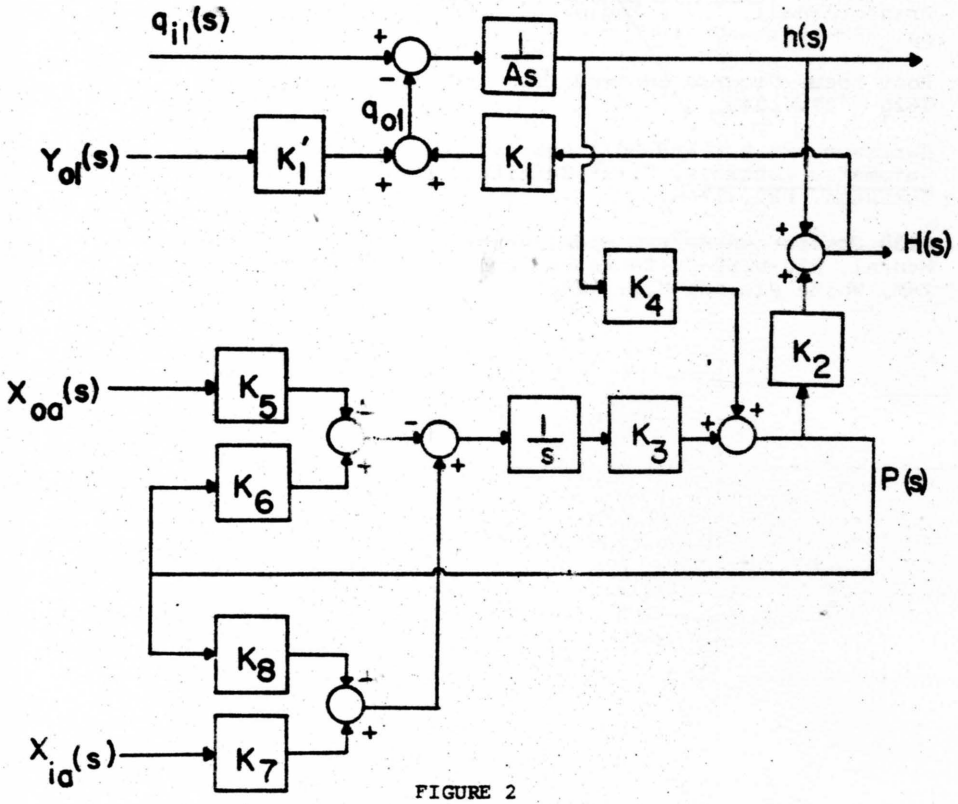

FIGURE 2

Block Diagram of Headbox

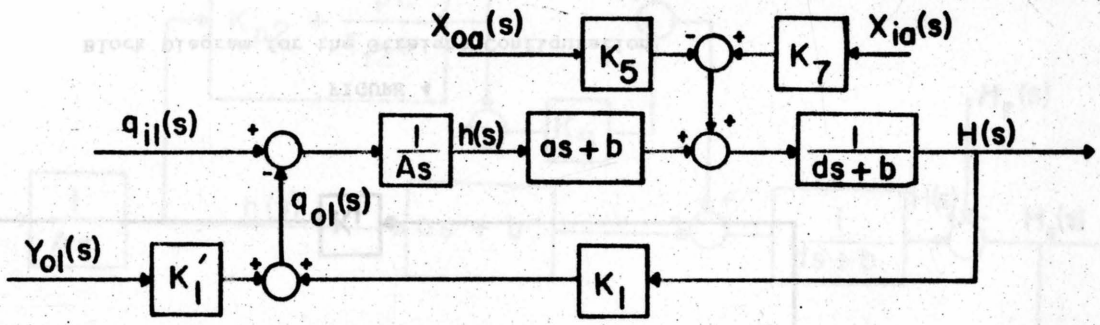

$$a = \frac{1}{K_2K_3} + \frac{K_4}{K_3} \qquad b = \frac{K_6 - K_8}{K_2} \qquad c = K_5 + K_7 \qquad d = \frac{1}{K_2K_3}$$

FIGURE 3

Reduced Block Diagram for Headbox without Controllers

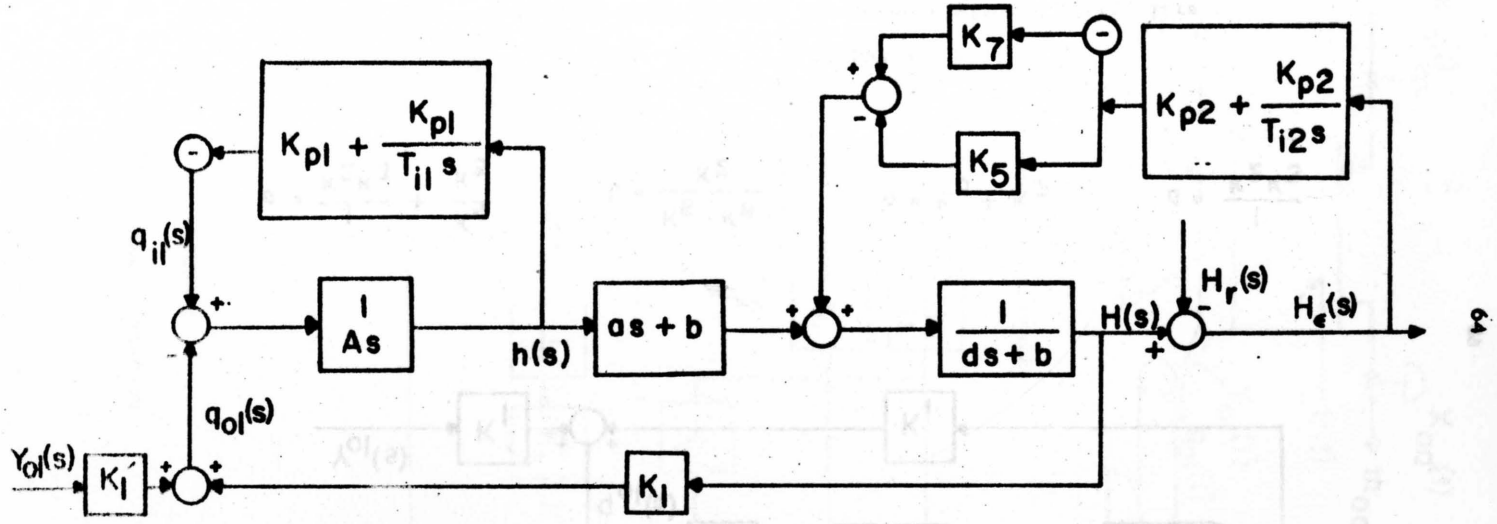

FIGURE 4

Block Diagram for the Straight Configuration

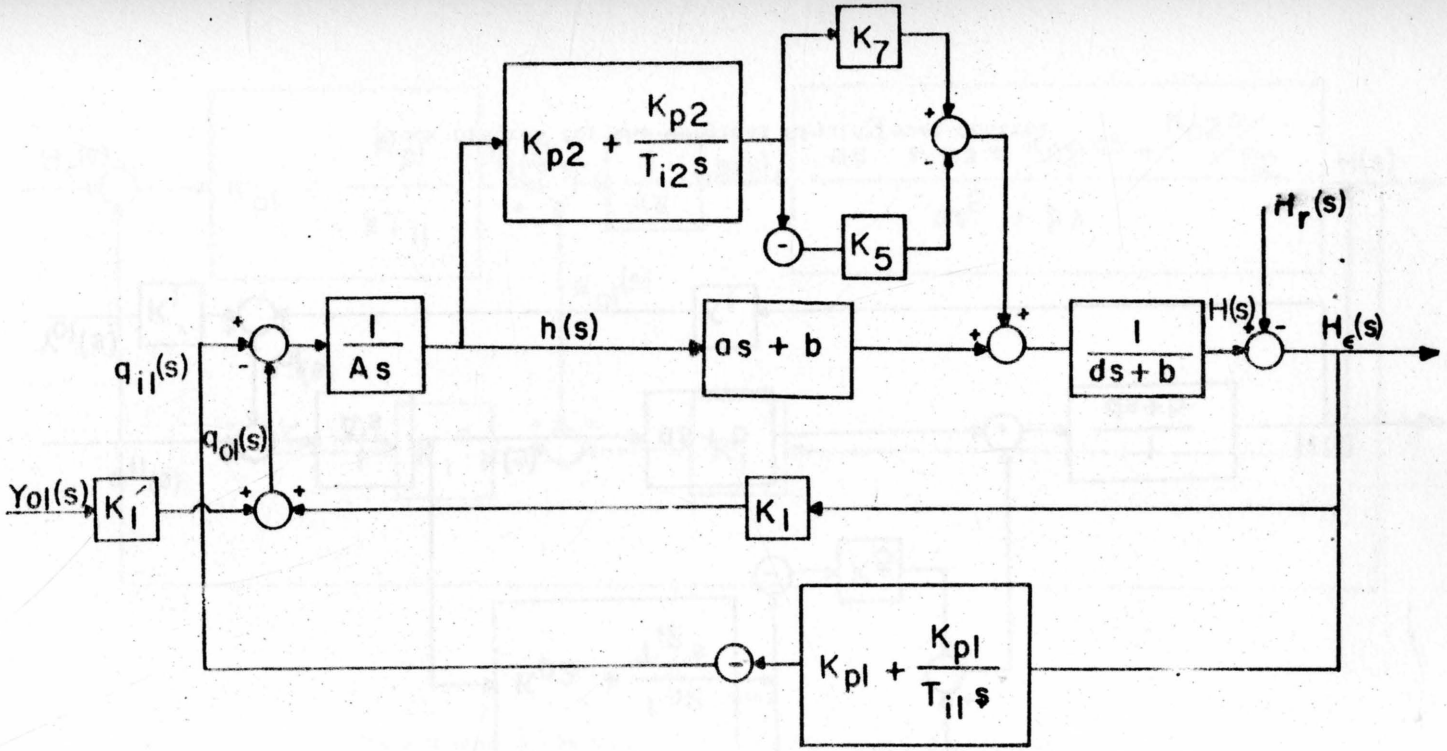

FIGURE 5

Block Diagram for the Reverse Configuration

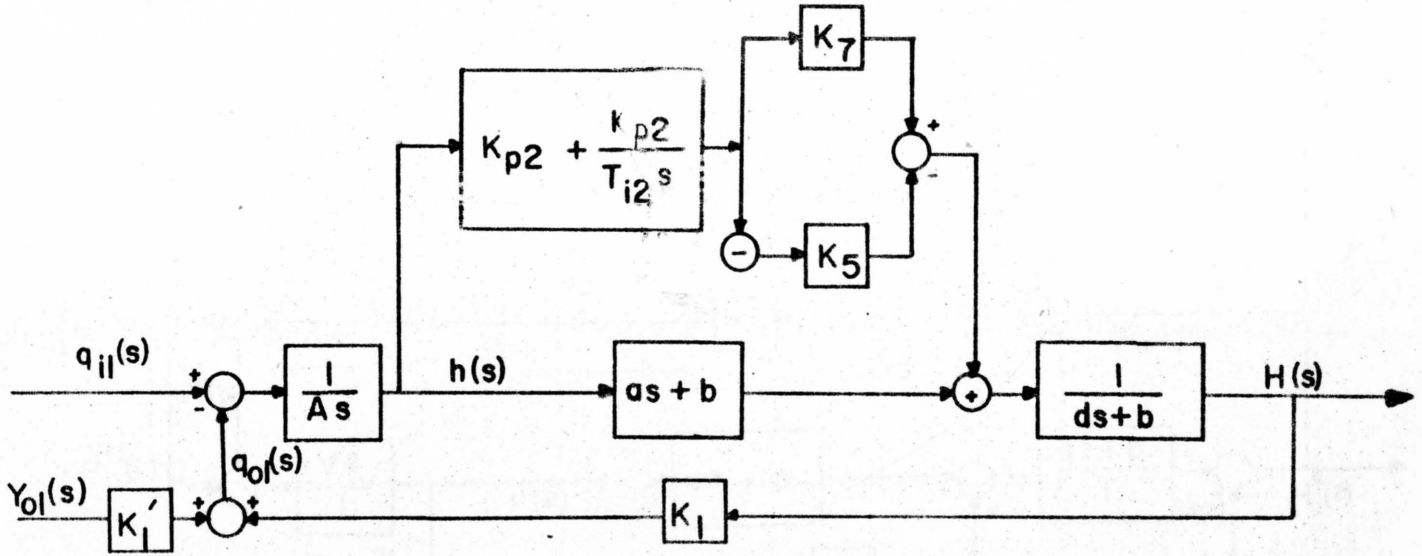

FIGURE 6

Block Diagram for the Original Liquid Level Control

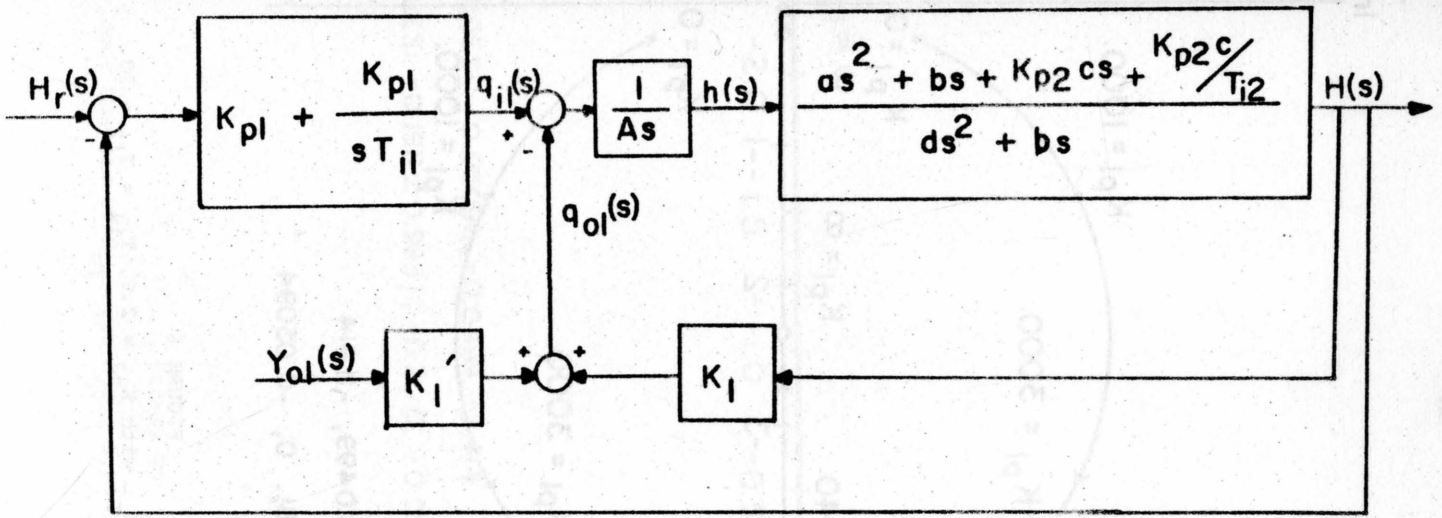

FIGURE 7

Condensed Block Diagram for the Reversed Configuration

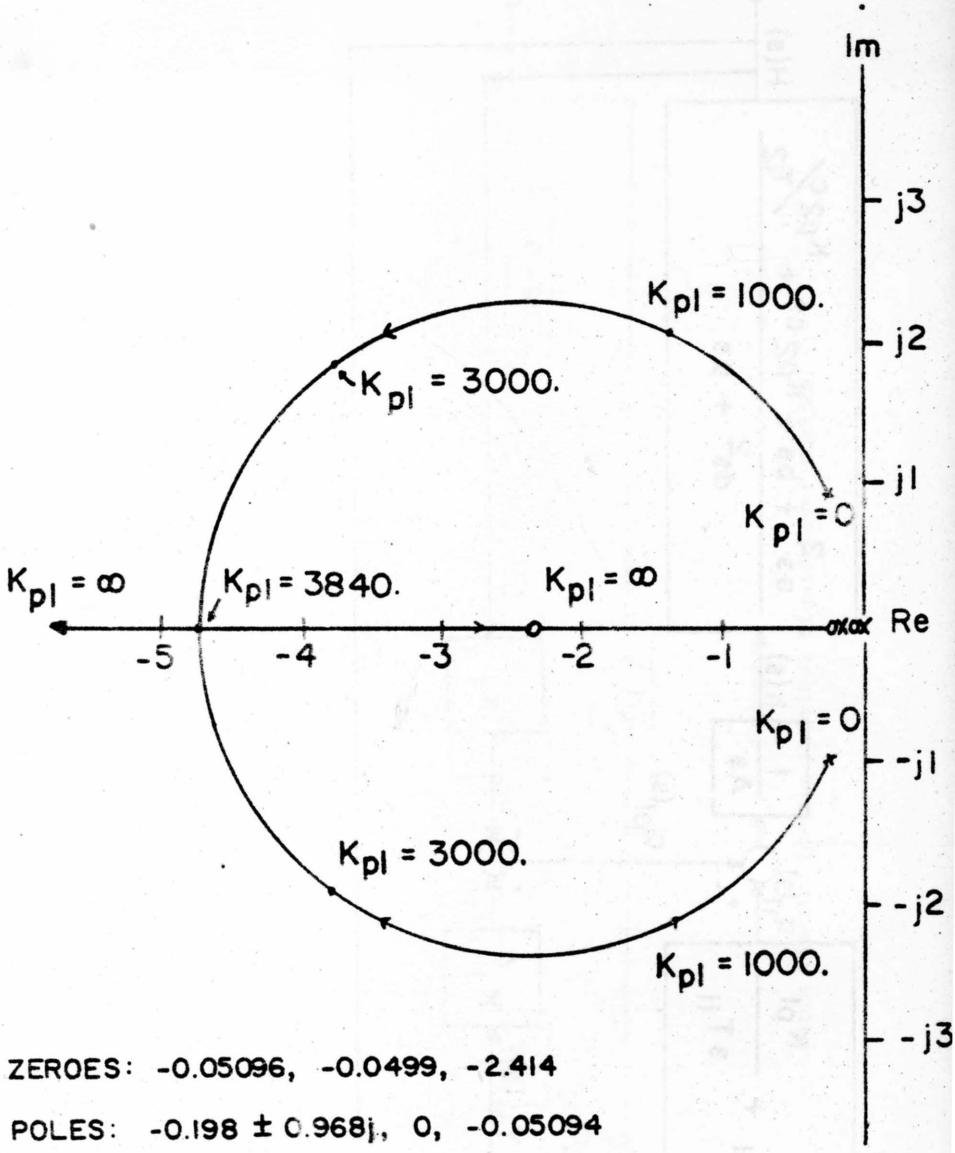

FIGURE 8

Root Contour of K_{p1} with $K_{p2} = 2.0$, $T_{i1} = T_{i2} = 20.$

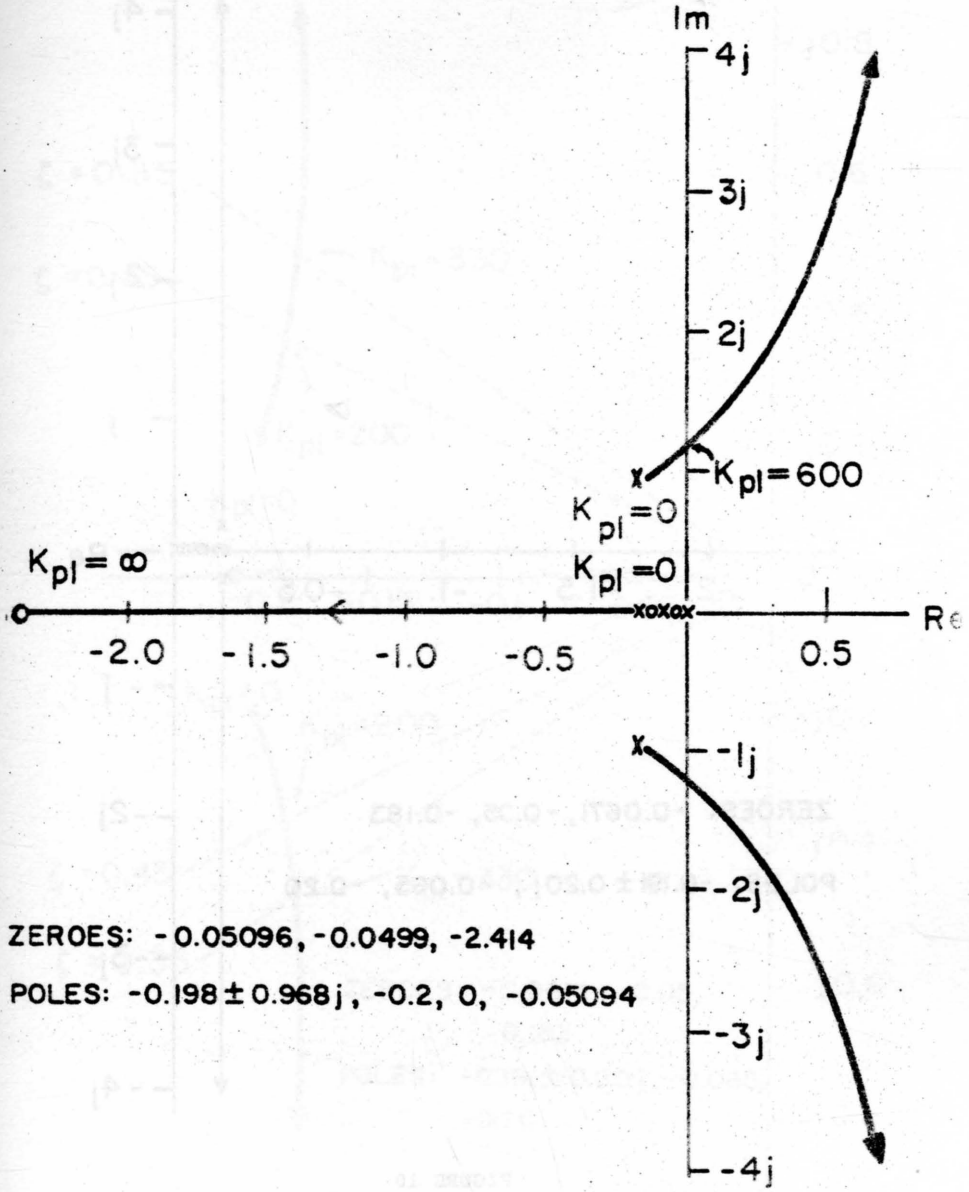

FIGURE 9

Root Contour of K_{p1} with K_{p2} = 2.0, T_{i1} = T_{i2} = 20, T_v = 5.

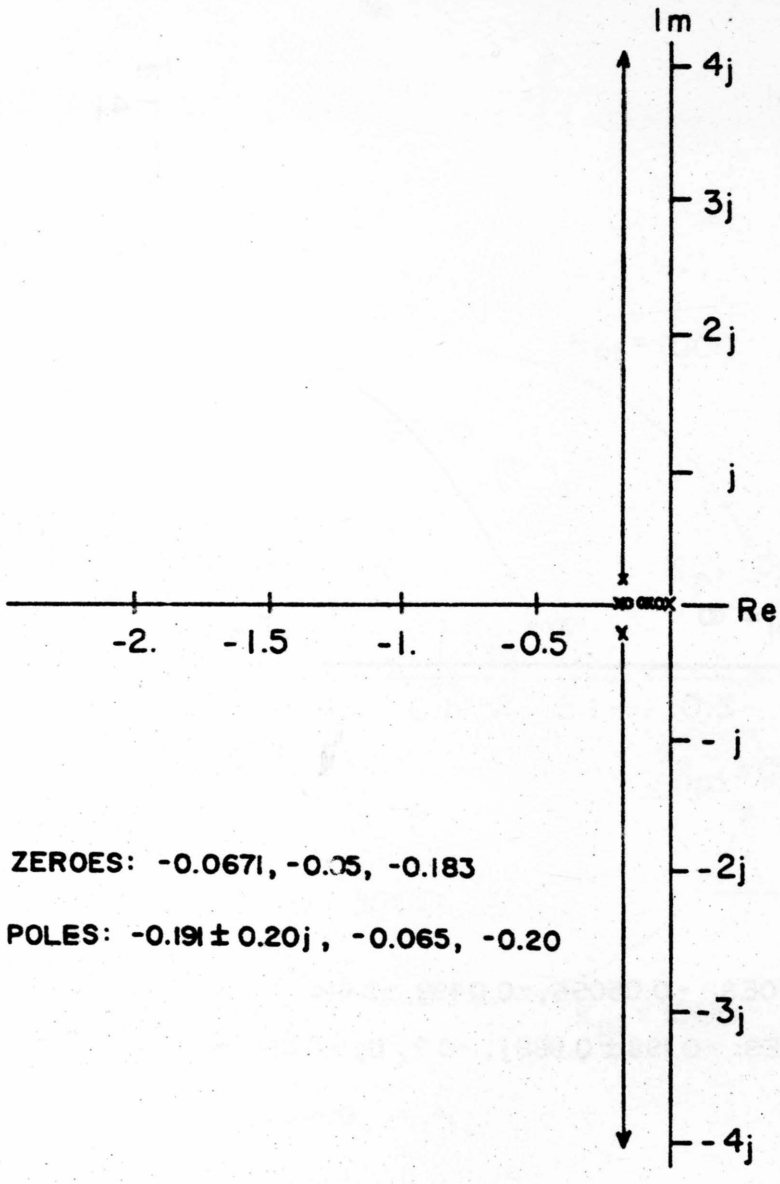

FIGURE 10

Root Contour of K_{p1} with $K_{p2} = 0.2$, $T_{i1} = T_{i2} = 20$, $T_v = 5.0$

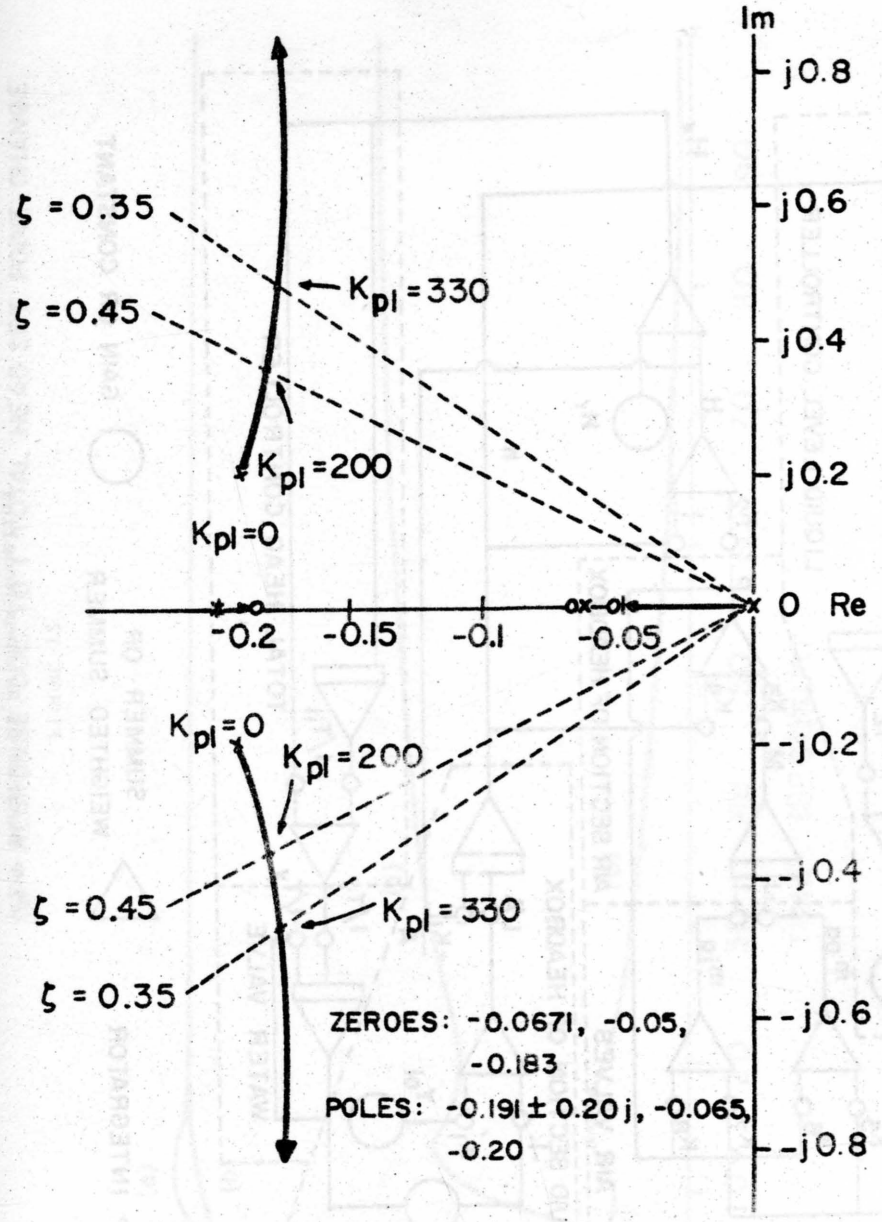

FIGURE 11

Root Contour of K_{p1} with K_{p2} = 0.2, T_{i1} = T_{i2} = 20.0, T_v = 5.

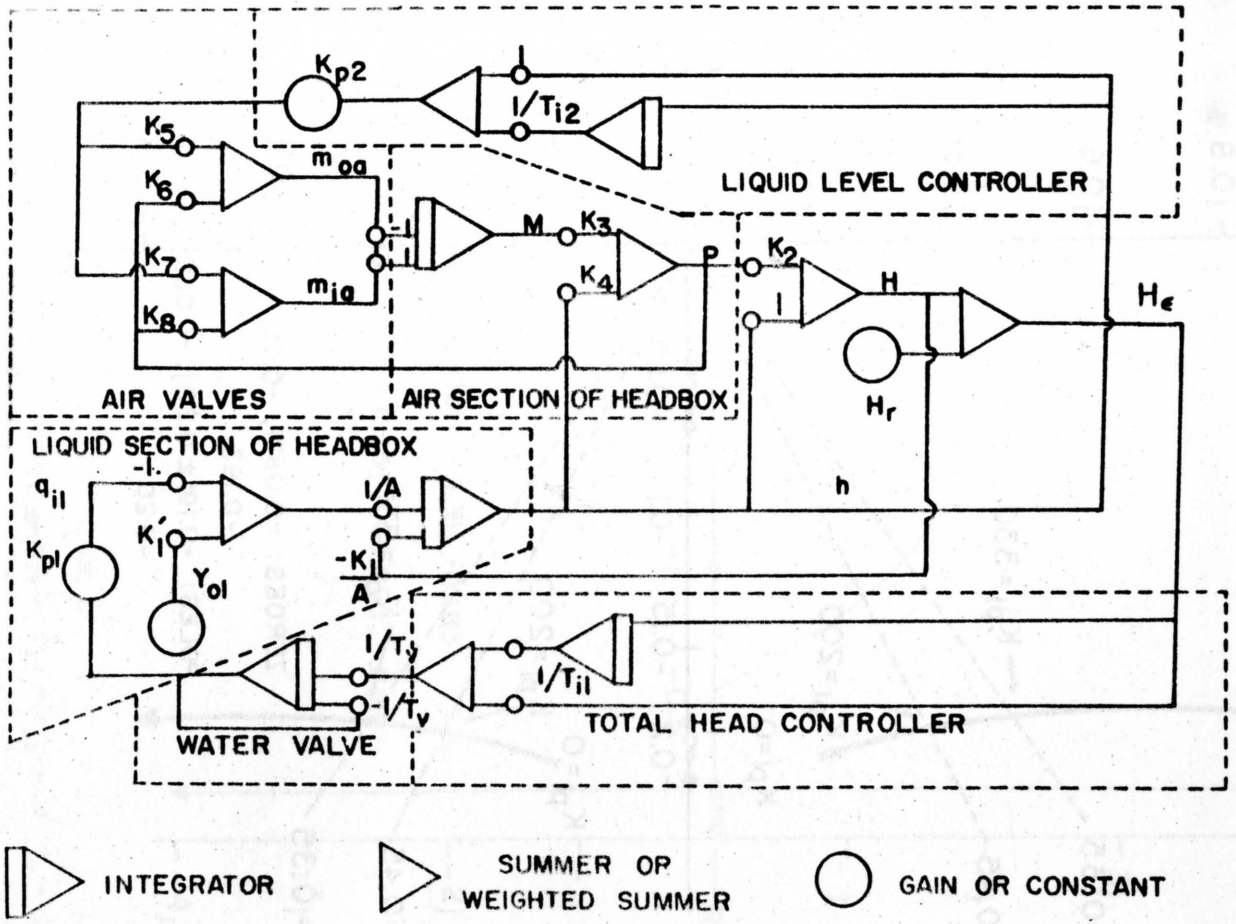

FIGURE 12

CSMP Diagram of Headbox Modeling

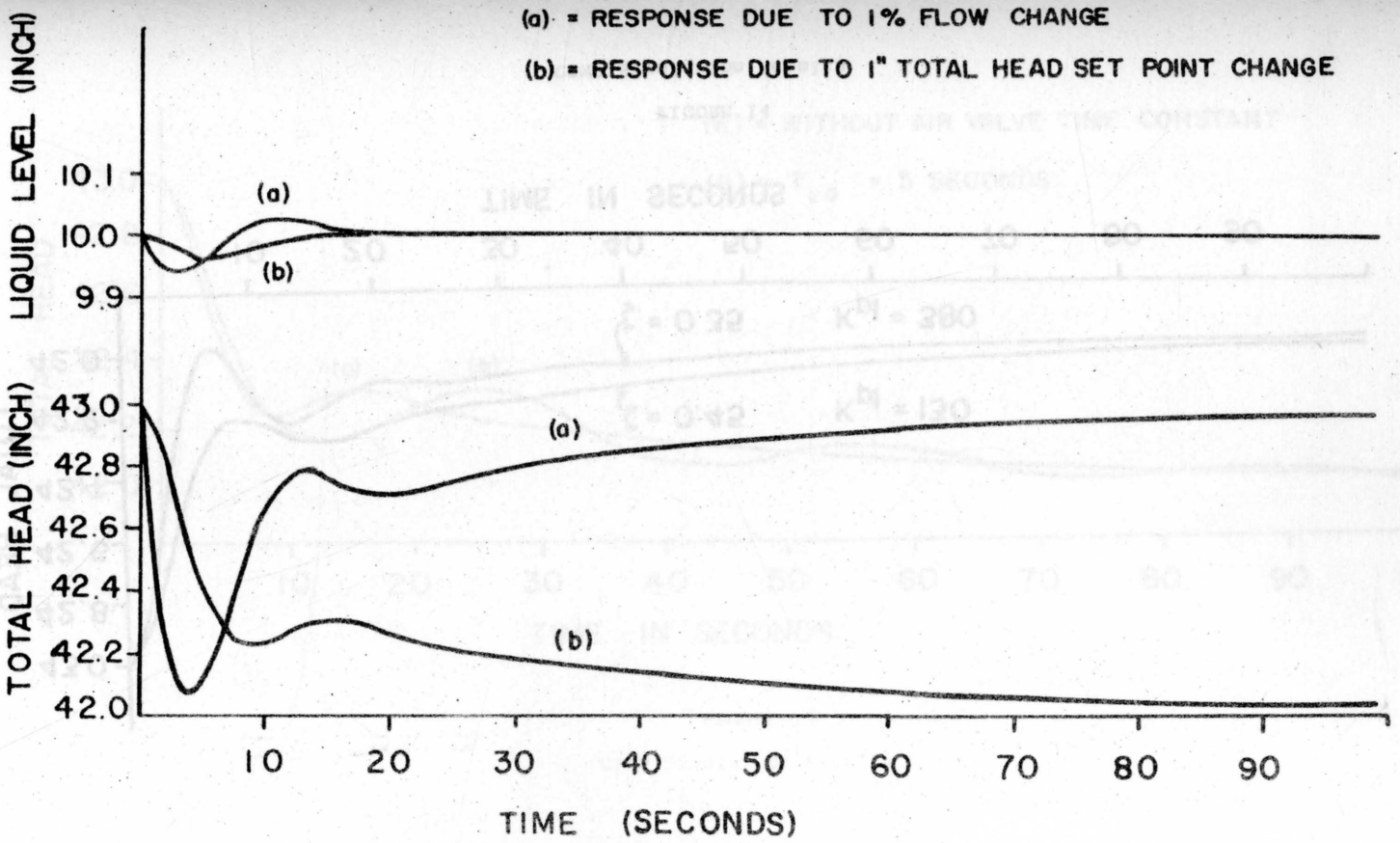

FIGURE 13

CSMP Simulation Results

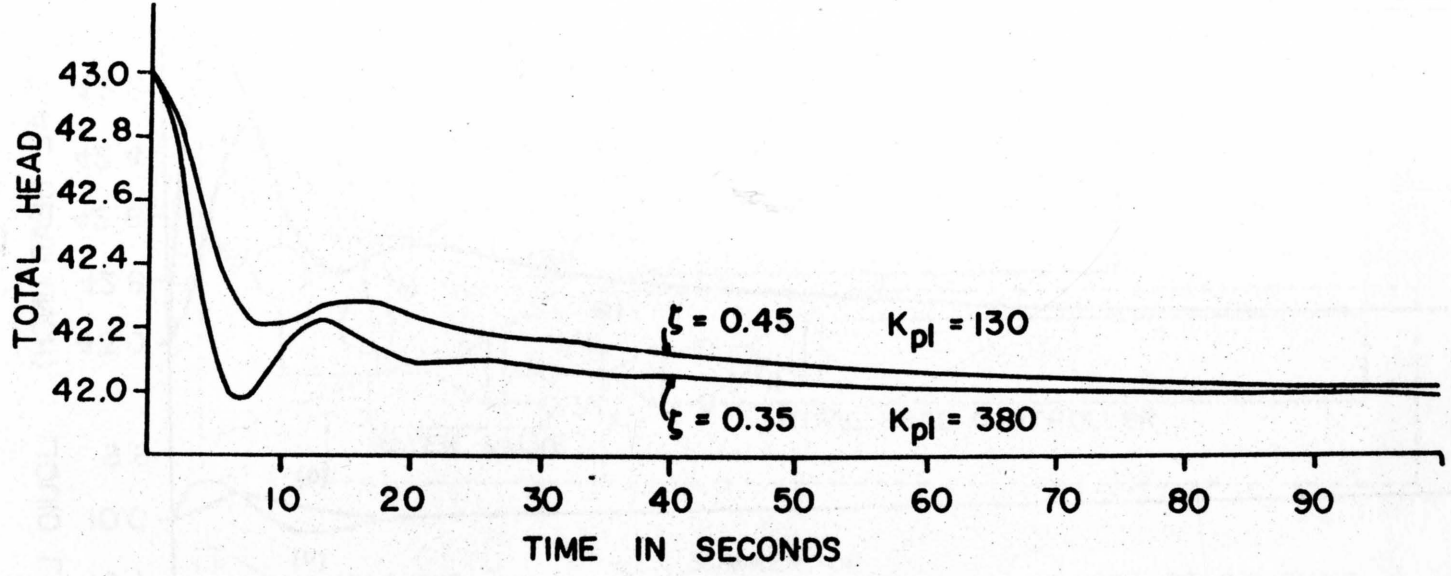

FIGURE 14

CSMP Simulation Results

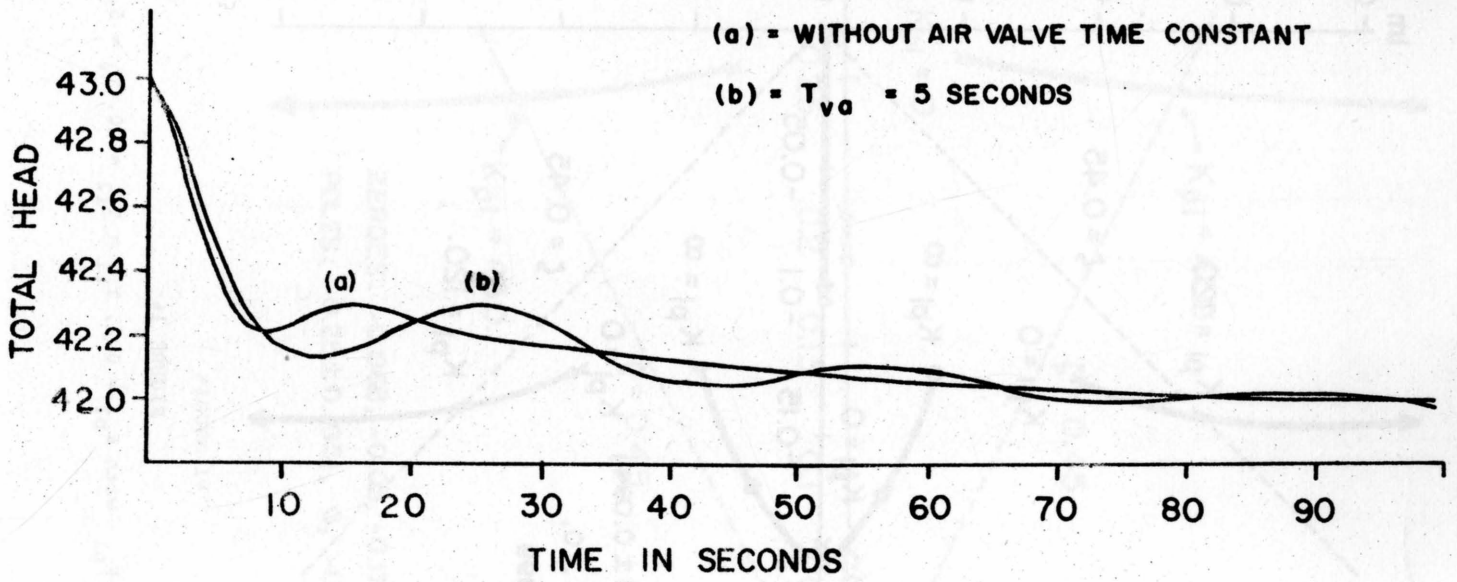

FIGURE 15

CSMP Simulation Results

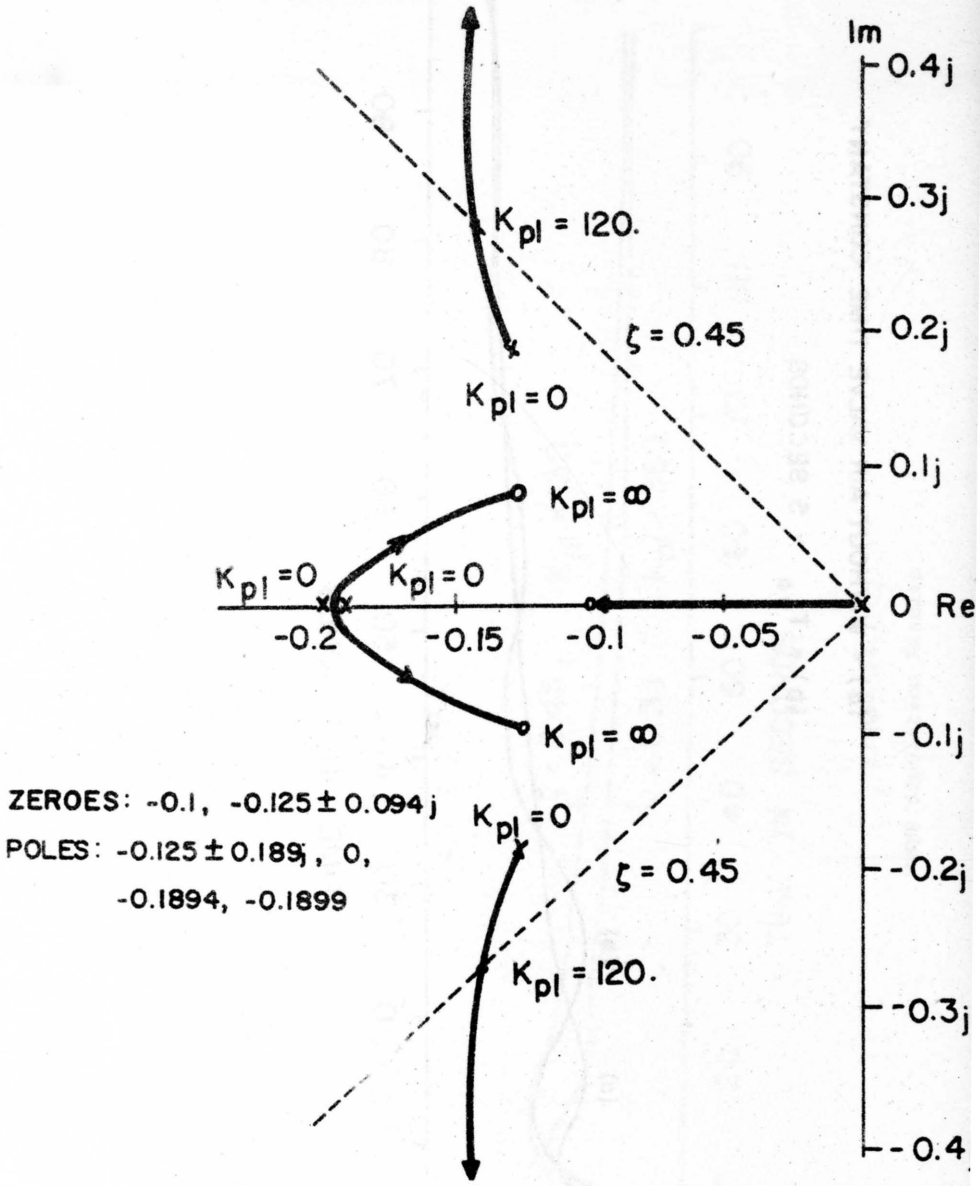

FIGURE 16

Root Contour of K_{p1} with $K_{p2} = 0.2$, $T_{i1} = T_{i2} = 10$, $T_v = 5$.

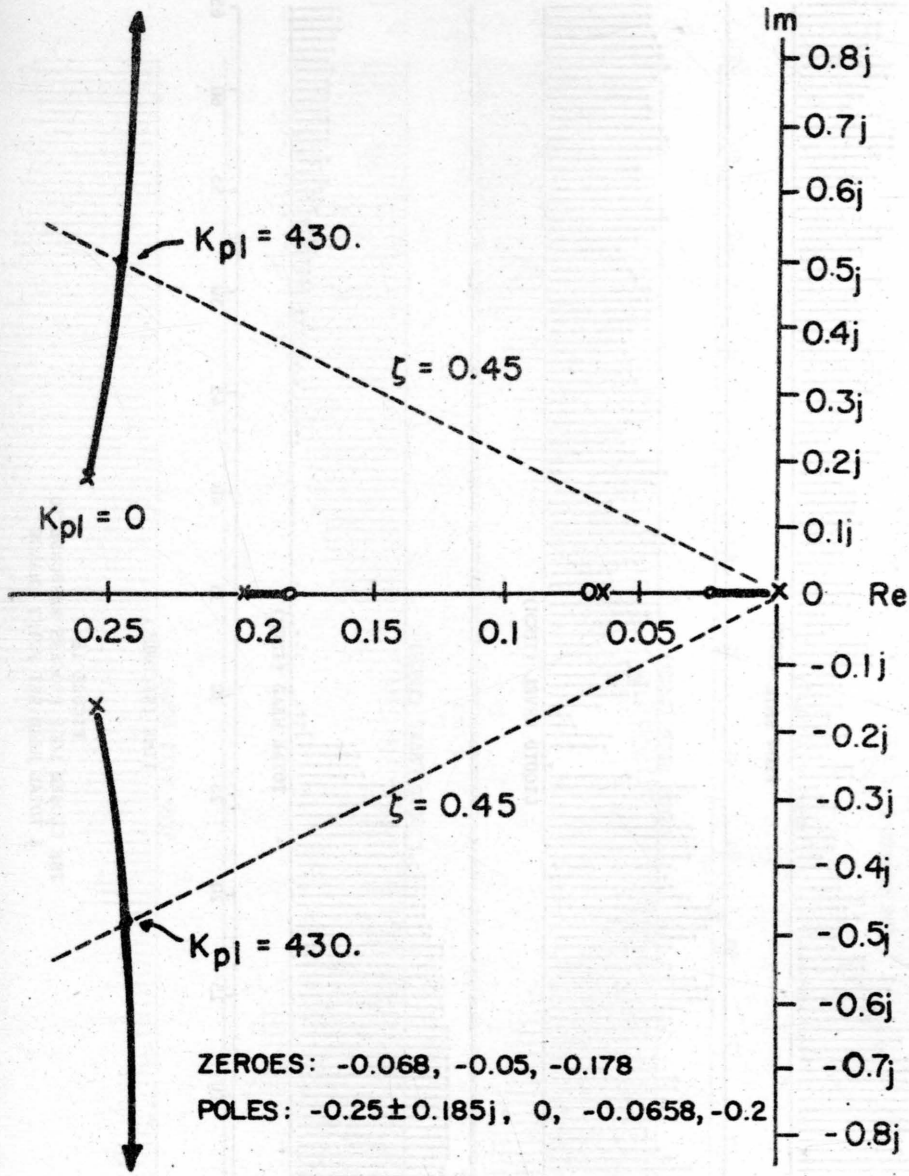
Im
0.8j
0.7j
0.6j
0.5j
0.4j
0.3j
0.2j
0.1j
0 Re
-0.1j
-0.2j
-0.3j
-0.4j
-0.5j
-0.6j
-0.7j
-0.8j
K_{pl} = 430.
ζ = 0.45
K_{pl} = 0
0.25
0.2
0.15
0.1
0.05
ζ = 0.45
K_{pl} = 430.
ZEROES: -0.068, -0.05, -0.178
POLES: -0.25±0.185j, 0, -0.0658, -0.2

FIGURE 17

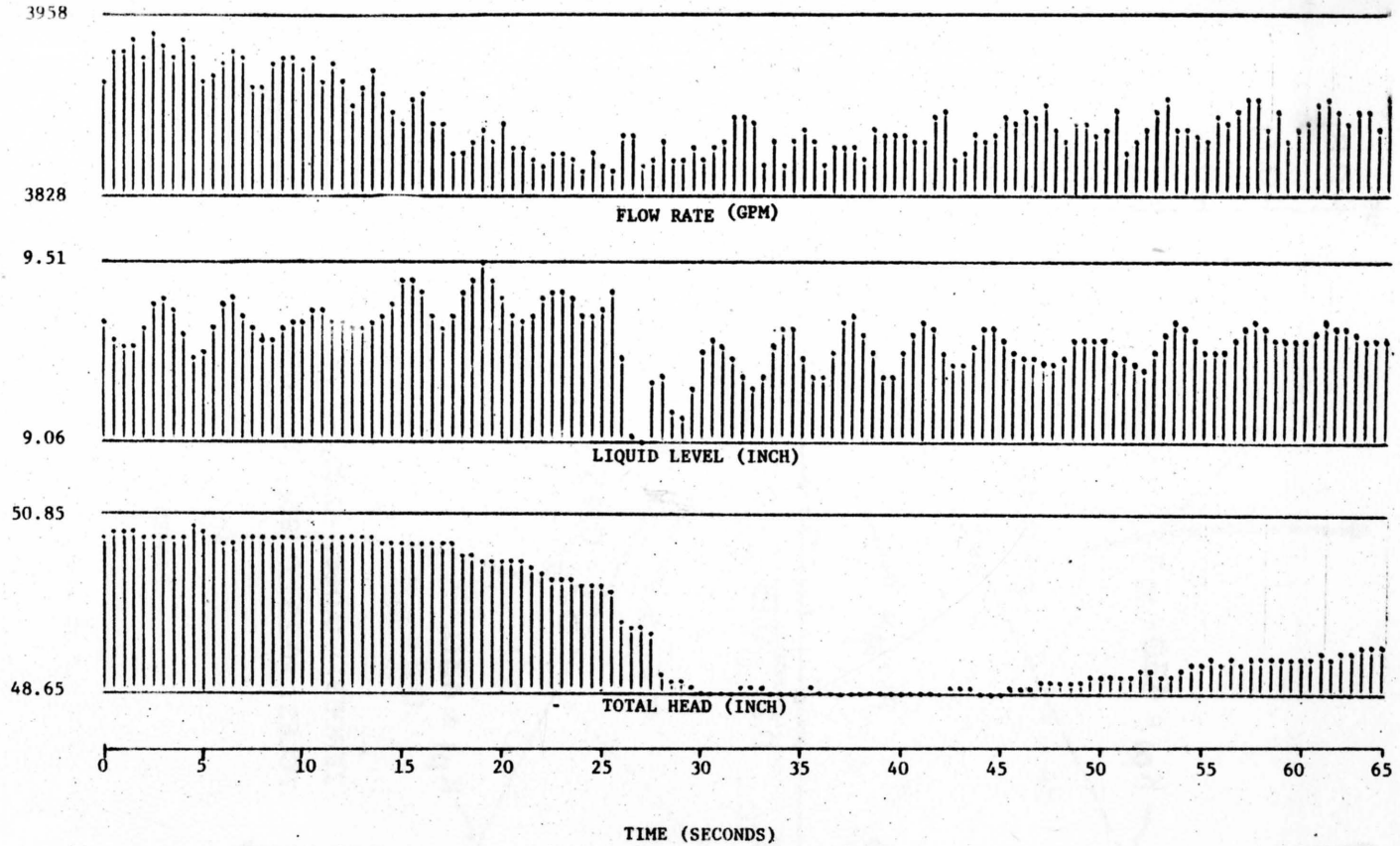

FIGURE 18
THE CLOSED LOOP PROCESS RESPONSE TO
A TOTAL HEAD SET POINT CHANGE

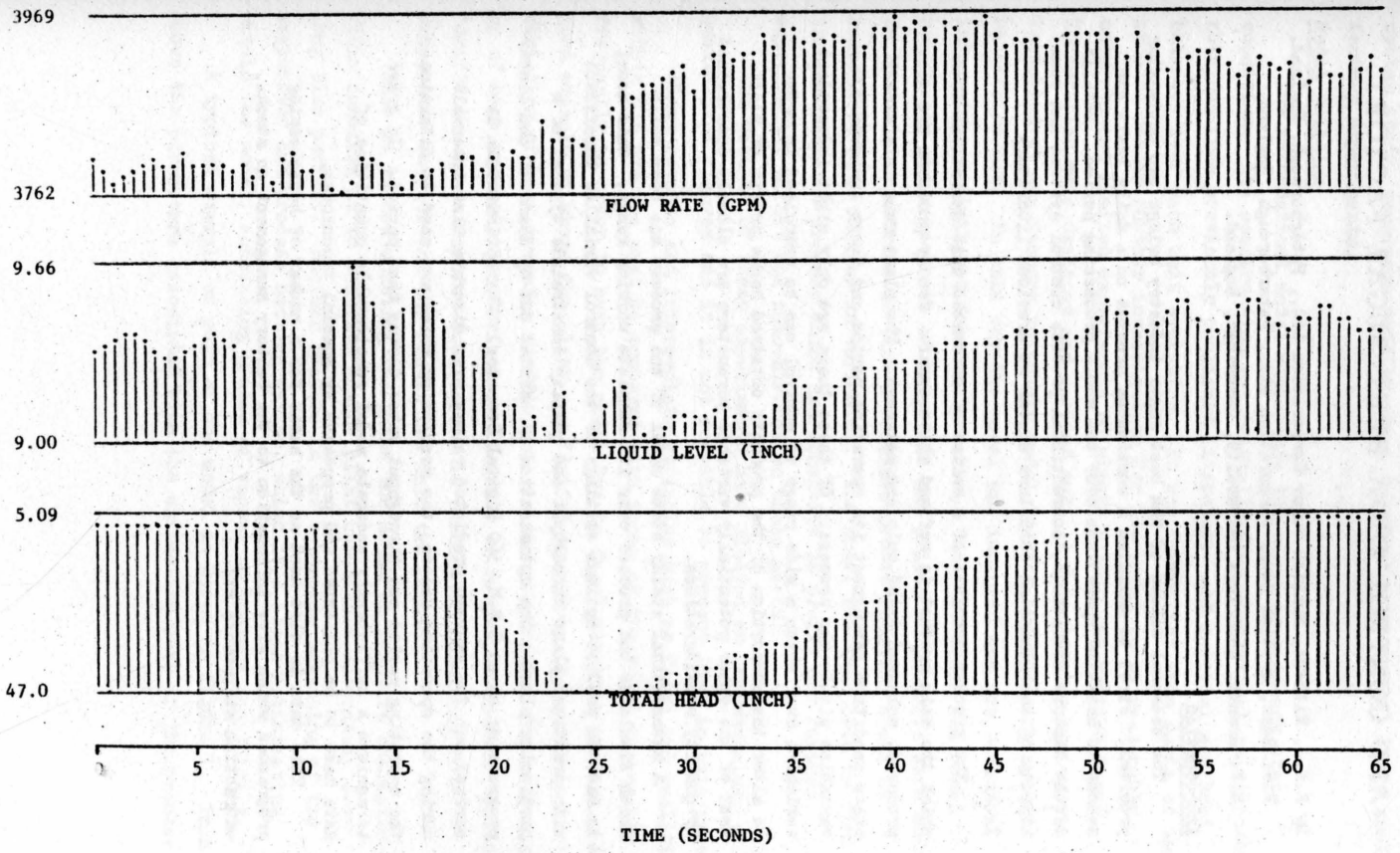

FIGURE 19
THE CLOSED LOOP PROCESS RESPONSE TO
A SLICE MANIPULATION

A MATHEMATICAL MODEL FOR THE OPERATION AND CONTROL OF A BEET SUGAR FACTORY

By R.M.J. Withers, British Sugar Corporation Ltd., Peterborough, England.
R.J. Bass, British Sugar Corporation Ltd., Peterborough, England.
M.F. Branch, Cambridge University, Cambridge, England.

Introduction

The seasonal nature of the beet sugar industry brings two optimising problems. First to maximise a continuous process on a daily basis and second to maximise operations over the whole processing period. Details of the factory operations, conventional process control systems and some aspects of the financial structure appear in previous literature 1, 2, 3.

The process consists of a series of automated unit operations from which the main product is refined white sugar. Two by-products are also produced, molassed dried pulp and molasses. The plant runs in a steady state condition throughout its operating period and there are over 200 variables within the process. Of these there are only eight independent variables over which a wide range of control can be exercised in order to alter the proportion of the products obtained hence profit of plant. Most of the other potentially variable parameters are closely constrained by quality considerations.

A mathematical steady state model of the process has been built which simulates the process over its complete working range. This model is used to predict optimum settings of the control variables consistent with practical plant throughput and quality constraints typical of a particular plant. The optimisation is carried out by means of non linear programming on an I.B.M. 360 Digital Computer. The optimisation is carried out for average predicted values over discrete time intervals during the operating season, the results of which are used to determine the operating period and throughput rates during that period. In order to achieve a sufficiently accurate model considerable quantities of data have to be collected and processed by special techniques.

This data is also used as the basis for a number of housekeeping programmes which give information to the factory management on stocks, extraction statements etc.

Work began in 1963 and has taken approximately six man years of system study, programme writing etc., together with several large scale factory experiments.

Model Building

The mathematical model represents the plant in a steady state condition. Its construction was initially from theoretical relationships obtained from previously published literature[4] and material and heat balances over each unit operation. It was found that some parts of the process needed further investigation for the model to be reasonably accurate and limited experiments on plants within the British Sugar Corporation were designed and carried out. A data logging system was also installed at one factory to enable model testing and updating methods to be carried out. In this way the model was improved and new technical information assimilated from the process. Once the model was found to be reasonably accurate costs of materials and prices of products were added to the model equations so that a relative profit function could be associated with changes in variables. The model was then used to find the parts of the process which are sensitive to profit and further experimental effort was concentrated on these parts.

The results of these experiments have yielded an overwhelming quantity of figures and it is not possible to present them in this paper[5].

Plant outputs and intermediate variables such as flows and qualities within the process must be compared with those of the model reasonably frequently in order to keep the model "up to date" with the process. A good example of where the plant can "drift" away from the model is in the variation of heat transfer coefficients in the evaporators due to fouling up of heat transmission surfaces. In order to keep up with this type of "drift" the heat transfer coefficient is calculated regularly from evaporator outputs and the result fed into the model.

This is termed updating and gives the model an adaptive characteristic enabling it to simulate actual plant conditions accurately over long time periods. Another feature is the automatic balancing of the evaporator and process heating system, which is a local optimisation within the model, scheduling grades of vapour to heaters accordingly.

A typical example of part of the model is given in Figure 1. This shows the parameters associated with the extraction part of the process.

A typical comparison between plant and model is made in the following table. Figure 2. This shows beet end parameters over a wide range of running conditions for steady values averaged over a period of sixteen hours.

Figure 2

PP Actual	PP Predicted	SAJ Actual	SAJ Predicted	SPP Actual	SPP Predicted
35.50	34.50	13.00	13.09	0.76	0.74
37.95	37.70	13.00	13.05	0.56	0.60
38.70	36.40	13.33	13.06	0.72	0.82
40.80	40.10	13.34	13.34	0.82	0.73
45.40	45.80	14.21	13.96	1.25	1.14
34.95	35.22	14.16	14.05	1.04	1.28
35.40	36.70	13.95	13.65	1.12	1.14

The model solution to this part of the process uses the following equations:-

$$DRAFT = (W/BEET + A)/B \quad (1)$$

$$DA = \frac{(DRAFT + 1.0)}{DRAFT} \times DK \times DV \times DZ \quad (2)$$

$$YY = \frac{(DRAFT \times e^{DA} + 1.0)}{(DRAFT + e^{DA})} \quad (3)$$

$$SWP = \frac{(SB - SW)\ (DRAFT - 1.0)}{(DRAFT \times YY \times ND - 1.0)} \quad (4)$$

$$DAJ = DRAFT \times BEET \quad (5)$$

$$SOLPP = AMARC \times BEET + \frac{SWP \times WP \times PK}{1.0 + PK} \times \frac{(1.0 + (1.0 - 0.65)}{0.65} \quad (6)$$

$$PP = \frac{SOLPP}{DRYPP} \quad (7)$$

$$SPP = \frac{SWP \times WP \times \frac{PK}{1.0} + PK}{PP} \quad (8)$$

$$PW = WP - PP \quad (9)$$

$$SPW = \frac{SWP \times WP}{PW \times (1.0 + PK)} \quad (10)$$

$$SW = \frac{SPW \times PW}{W \times BEET} \quad (11)$$

$$AMW = W \times BEET - PW \quad (12)$$

$$SAJ = \frac{BEET \times SB - PP \times SPP}{DAJ} \quad (13)$$

The equations listed above are typical of the many used in the model.

Data

The practical plant model required the collection of a great deal of data from the plant.

There are two reasons for this. First it is important to obtain accurate results, for the model can only be as good as the data fed into it. This is achieved by averaging many readings. Second, the model has to follow small changes in plant characteristics which are difficult to detect with confidence when only a limited amount of data is available.

There are two sources of this information, the plant instruments and the factory laboratory. When it is all collected together it has to be conveyed in some convenient form to the computer 60 miles away at Peterborough.

Where possible the data is collected automatically from the online plant instruments. In many cases the signals from these instruments are used for control purposes (e.g. juice flow signals) which make them readily available for logging. In the remaining cases, (e.g. crystalliser temperatures) the transducer is available but the signal is of a low order and it proved necessary to provide some conversion equipment.

Figure 3 shows a block diagram of the data collection system in use at Bardney Factory. At the heart of the system is an Electronic Associates M.D.P. 200 data logger, the details of which are well documented in the manufacturers literature.

The online signals entering the logger are either in the form of pneumatic air signals (3-15 p.s.i) or electric signals. Each signal has a three figure identification number which is used by the logger to select the required signal. This measurement and the identification number are then printed out on the logger typewriter and punched into paper tape. The identification number is then further used in the data sort programme when it is processed in the computer.

The logger is controlled by a predetermined tape programme. The points to be selected are read into it every ten minutes and the results of each successive point are produced on the typewriter. Several programmes have been developed which vary the signals selected,

depending upon the part of the plant being studied and the frequency with which the information is required.

However, the straight logging of plant information leads to inaccurate results where fast changing signals with a high noise content are concerned, (e.g. flow rates). It was therefore necessary to filter the signals before they were logged. Each air signal has a resistance capacitance network set at 3.3 minute time constant.

All the electric signals come from resistance bulbs measuring temperatures around the plant. In all these cases the process time constant was long enough to eliminate the need for signal filtering. The data logger was designed to accept manually entered information as well as the online input. This was collected in two forms. Information entered once per shift had an individually hand set potentiometer, either on a box situated in the laboratory or on the logger in the factory. These units could be set to an accuracy of better than $\pm \frac{1}{2}$ % and were scanned by the logger at a definite time during the day. Such parameters as juice purity and sugar content are treated in this way. Information entered only once in 24 hours is collected together on a report form and hand keyed into the system on the logger typewriter in the interval between automatic scans.

Each block of data is punched out from the logger in the following form :-

Channel			Sign	Record			FRO
S	1	2	5	+	6	3	5	9	,

The first character isolates the reading from the preceding one and the last character indicates the end of the data. The next three characters identify the record, the value of which is held in characters 6 to 9.

At the end of 24 hours the data collected on the paper tape is removed from the logger and transmitted to the British Sugar Corporation Central Offices at Peterborough, via a data link over the speech network of the General Post Office telephone system working at 800 Bauds a minute.

When the data is received at Peterborough it first goes through a general check and sort routine. This is arranged to eliminate errors due to incorrectly punched paper tape and to gather together all the recordings of the same identification number in their correct chronological order.

At this point the data is still in a raw state. It now enters one of two data editing programmes. These are designed to scale each signal to correct engineering units, to test each record for possible errors and to prepare average values of the good data for model updating programmes which are to follow.

One of the most difficult practical problems in a system of the order described in this paper is that of error detection and correction. Errors can arise at any point along the network shown in Fig. 4. The errors may be "catastrophic" or "non catastrophic". The catastrophic errors are those caused by the malfunctioning of a unit which adversely affects all or a large number of the records. These errors are usually obvious and are often detected very soon after they first begin to occur. The second type may be associated with a small number of signals or perhaps only one record.

Some of the units have a certain amount of error detection and correction built into them. The computer is self checking to a large extent and is also capable of rejecting incorrectly punched paper tape when a parity error occurs. The data link is capable of both detecting and correcting a limited number of errors introduced during transmission due to random noise and interference on the telephone lines. However, the non catastrophic type of errors which occur in the remaining parts of the system have to be detected using data editing programmes on the computer.

The data is divided into two groups when it arrives at the computer for processing. First the vital information, without which the model cannot be updated or the housekeeping programmes continue, is checked for errors and must have any detected errors corrected before the following stages in the programmes are commenced. Second the non vital information is only checked for errors which are simply rejected with no attempt at correction as there is very often ample information from this particular source to justify confidence in the remaining recordings.

As a general rule the vital information is concerned with manually entered data. It is often restricted to only three records of each variable in 24 hours being laboratory measurements and plant read information not scanned automatically. It is subject to errors in measurement entries to the data logger and all the other sources shown in Fig. 4. In the error detection and correction routine each record is checked for parity in every character, and for a fixed number of characters to each record. It is then checked against high and low limits outside of which it is rejected. The limits are set from practical experience of the

range of each variable. The accepted value is written into an array storage within the computer. This type of information is transmitted twice from the plant over the telephone lines to the computer department. The received data is read into the above routine and on the second run any records rejected in the first section due to transmission errors are corrected in the second attempt.

This system does not detect errors in the records which have values very near the true reading, but as most errors are usually serious ones the technique has proved very successful.

The non vital data is considered to be that which is collected automatically by the logger many times in 24 hours. It is edited and given the same parity and complete record tests as used for the vital data and subjected to a high/low limit check. However, this last test is not only to reject errors which are well outside these limits but also to obtain data which only relates to the plant when it is operating at its normal capacity. The data collected at throughput rates below the low limit check can produce updating constants which do not apply to the plant at a higher throughput and which cause the optimising routine to lead to inaccurate results.

The selected data is averaged over the 24 hour period and the number of successful records tested to make sure there were enough of these records to give confidence in the results before they are used in the updating routine.

The analysis of the records commences with a check on three leading parameters. If these parameters show that the plant ran consistantly for the previous 24 hours then the full updating process is allowed to continue.

Optimisation

In order to characterise the plant by means of a model over a period of time parameters are divided into three main types. The inputs to the plant which characterise the raw material, in this case sugar beet. These are sugar content and insoluble non sugars and are dependant on climatic and soil conditions and normally vary over the operating season in a predictable fashion. The second are updated constants which characterise the plant in relation to throughput and efficiency of unit operations. Typical of these is the heat transfer coefficient within the evaporators which usually falls as the heat surface is fouled. These parameters are updated continuously merely by reversing the model algorithms

periodically. The third type of parameter is the costs and prices associated with products and materials. Most of these are reasonably constant but an outstanding exception is world raw sugar price, and this can only ever be a best estimate. Because of the way these three types of parameter varied it was decided that the best strategy would be to find optimum solutions for the plant in discrete time periods of one week over the complete possible operating season. Thus each set of parameters are averaged over the time period of a week. We have then the situation where the input plant conditions are constant for each week. For each of these constant set of conditions an optimum operating strategy can be found that is consistant with plant constraints of both throughput and quality.

Although the process is described by over 200 different variables most of these are constrained closely by product quality and physical plant considerations. We have chosen the variables which are normally varied over quite a wide range by management and affect the product proportions and hence profit rate. These are independently variable and some of them produce a slightly non linear profit variation. This presents a classic hill climbing problem. Because the functions are only slightly non linear it was decided to use a method which had already been developed and used on chemical plants and which came under the heading of non linear programming[6].

The principle behind the method is that of sectionally linearising the profit surface and applying the simplex linear programme technique to each of these linearised sections where the independent plant variables,

$$X_1, X_2 \ldots\ldots X_8 \text{ satisfy the M equations } gi\ (X_1, X_2 \ldots\ldots X_8)$$

$$<, =, > Y\ i$$

$$\text{for } i = 1, \ldots\ldots m,$$

where m is the number of dependant plant variables.

In addition to this the cost function

$$Z = f\ (X_1, X_2 \ldots\ldots X_8) \text{ is maximised.}$$

The dependant plant variables are those which are likely to come up against some quality and capacity constraint e.g. process juice flows, moisture contents of products etc. The number of dependant variables can be changed very easily to bring in constraints where none was previously suspected. The equations of both cost and independant/dependant variable

relationships are all carried implicitly within the model of the process. The optimising programme constructs a linear model about the starting point chosen for the optimisation by calculating the partial derivatives of each dependant variable with respect to each independent variable. The limits of this linearisation are either actual variable constraints or a linearisation criterion which restricts the range so that the error incurred in linearisation is less than a specified value. A linear program simplex solution is carried out on this bounded region and the next iteration begins with the previous optimum as the new starting point. Thus the method adapts itself to the surface with the result that steps are large on the linear portions but smaller over the non linear parts of the surface. The criteria for detecting the optimum are very flexible and can be changed to suit the nature of the model/profit surface near the optimum. The simplest optimum is where all dependant variables reach the stage where they are themselves constrained or the dependant variable constraints limit their movement any further.

The next is where a definite internal optimum is reached and the steps slightly overshoot the peak. In this case the steps are automatically reduced in stages so that the optimum is reached to within a very small distance of the peak. A further strategy defines an optimum solution after a definable number of steps which result in a profit increase less than an increment supplied as data. In this case the optimum could be falsely identified on a very gradual gradient but this can be overcome by adjusting the parameter governing increment mentioned above. The method suffers from the disadvantage of many hill climbing methods in not being able to distinguish between several peaks but the current function is not of this type.

A typical optimisation run is shown in Fig. 5.

This shows a typical optimisation carried out for actual input conditions to one of B.S.C. plants in the 1967-1968 Season. The starting point for the run has been estimated to be reasonably near the optimum. The optimum has been recognised by the fact that all of the independent variables except two are against their limits. These two variables are indirectly constrained by dependant variable limits.

The weekly optimisation figures are then used to calculate a parameter which describes the relative profitability of processing beet in the optimum way during each of these weeks. The type of trajectory obtained if these values are plotted against time is shown in Fig. 6.

The total beet allocated to the plant for that year can then be allocated to the weeks in descending order of profitability. A case where the method can break down is if the plant throughput can be increased by working in a sub-optimal mode because a constraint on a dependant variable has been reached.

In this case the sub-optimal mode of operation can still be assessed in terms of profitability by running the optimiser with the constraint lifted and allowing financially for possible product wastage. A typical example of this is the case where the drying capacity of pulp driers cannot cope with pulp associated with beet slice rate. It is possible to sell this undried pulp at a potentially lower price than if it had been processed normally. This beet would otherwise be processed at the end of the operating season when profitability rate is much lower but when all the pulp could be dried. Thus by calculating the sub-optimal condition profitability it can be considered logically within the framework of the method.

The Overall System and the Results

The final stage in the studies described here is one of comparison between the plant achievements and those of the model. This is done in two ways.

Firstly, the plant performance is computed over a period of seven days from the incoming data. This seven day average can be repeated daily if required. The operating values of the plant independent variables are fed into the mathematical model and it, in turn, produces a predicted plant performance based on maximising the hourly profit rate using current prices. The results of the housekeeping programmes are added to the model results for the same production period. Since the model performance is on the basis of the factory keeping continuously within acceptable limits - the actual performance revealed by the housekeeping programmes must inevitably be the worse. This, in the first instance, allows the validity of the model work to be checked from all aspects and finally allows an accurate estimate to be made of the lost production by the plant due to such factors as mechanical and electrical breakdowns and all mal-operation of the plant.

The model independent variable settings are also optimised weekly using predicted market prices for sugar, molasses and dried pulp and predicted performance and quality criteria. The recommended settings are tabulated against the two previous ones (i.e. actual and idealized).

Again a comparison is made this time between expected overall Campaign profit on the basis of actual performance against that expected from computed recommendations.

In this way a clear picture is built up of the plant achievements under normal operating conditions and the optimised plant production. The information is presented altogether in terms of technical processing factors and in terms of the financial aspects. All operating decisions will of course remain with the local management.

The working routine of the system is illustrated in Fig. 7 where it is broken down into discrete operations. All aspects of this work shown are currently being pursued. In a project of this nature it is difficult if not impossible to finish off one's work! The development work of the model which is described in the top row of the operation in this diagram has received the major parts of the effort involved and will still require some effort in the future as fresh problems arise and the mathematical relationships require improvement.

The lower two rows of the block schematics shown in Fig. 7 describe the routine procedure which is now virtually automatic in its operation after the data is entered at the logger. The amount of effort involved in developing the system has been considerable. A great deal of time has been spent on developing the softwear for the model and the optimiser, but it is considered that this effort has already paid for itself in fresh knowledge gained of the process, quite apart from the computer control project. The restriction on the pace of our progress has been the difficulty in developing an effective system with reliable softwear for it requires not only a thorough knowledge of the process involved but also access to a considerable amount of computing time.

Conclusions

a. A mathematical model has been developed which can be used with confidence to predict production rates.
b. The routine of continually correcting the model for changes in plant characteristics has been proved using updating constants.
c. The use of optimisation techniques on the model are proving that the plant independent variables may be adjusted resulting in significant changes in profitability.
d. The results of the plant experiments have shown that the process has very long time constants. This slow response to command changes

indicates that the optimisation technique need only be attempted at intervals of several days.

e. The collection of the data needs to be accurate and in a form easily handled by the computer.

f. The detection and correction of errors generated in the data network is now an essential and practical part of the system.

g. Once an accurate model is established it can be used for other purposes such as plant design and it can indicate the presence of physical constraints in the system under a wide range of processing conditions.

h. Using the data network established for model studies, certain housekeeping programmes have been developed which aid the general work of plant and model comparison checking.

i. It is considered that the problems mentioned in e and f above will be made easier by the installation of an online computing system and this is to be effected at the reconstructed Wissington factory. It will also enable the housekeeping programmes to be completely in the hands of the local factory staff.

References

1 Campbell-Macdonald & Withers. Automatic & Remote Control, Proc. 1st I.F.A.C. Congress (1960) 252-259.

2 Withers, Automation in the Sugar Industry. Penguin Technology Survey 1967.

3 Withers, Control System in B.S.C. I.E.E. Automation Conference May 1968.

4 McGinnis. Beet Sugar Technology (book) Rheinhold. (1951). 152.

5 Withers, Branch & Bass. Process Optimisation. 19th Technical Conference British Sugar Corporation (1968).

6 Smith, Process Optimisation Program. I.B.M. Research Institute Project No. 14-78. April 1965.

DIFFUSER MODEL

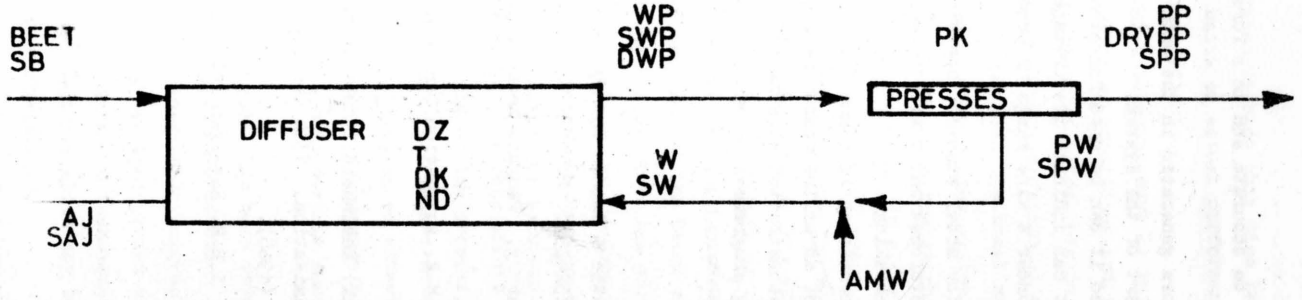

PREDICTED		INPUT		UPDATED	
Sugar in wet pulp	SWP	Beet slice rate	BEET	Diffuser constant	DK
Dry substance wet pulp	DWP	Supply water flow	W	Pressed pulp non sugar solid	AMARC
Sugar in pressed pulp	SPP	Diffuser temp.	T		
Sugar in return water	SPW	Diffuser speed (time for 1 rev.)	DZ	Pressed pulp dry substance	DRYPP
Sugar in supply water	SW				
Sugar in juice	SAJ	Sugar in beet	SB	Press constant	PK
Flow of juice	AJ	No. of cells in diffuser	ND		
Flow of pressed pulp	PP				
Flow of return water	PW	Purity of press water	PPW		
Flow of make-up water	AMW				
Flow of pressed pulp dry matter	SOLPP				

FIG. 1.

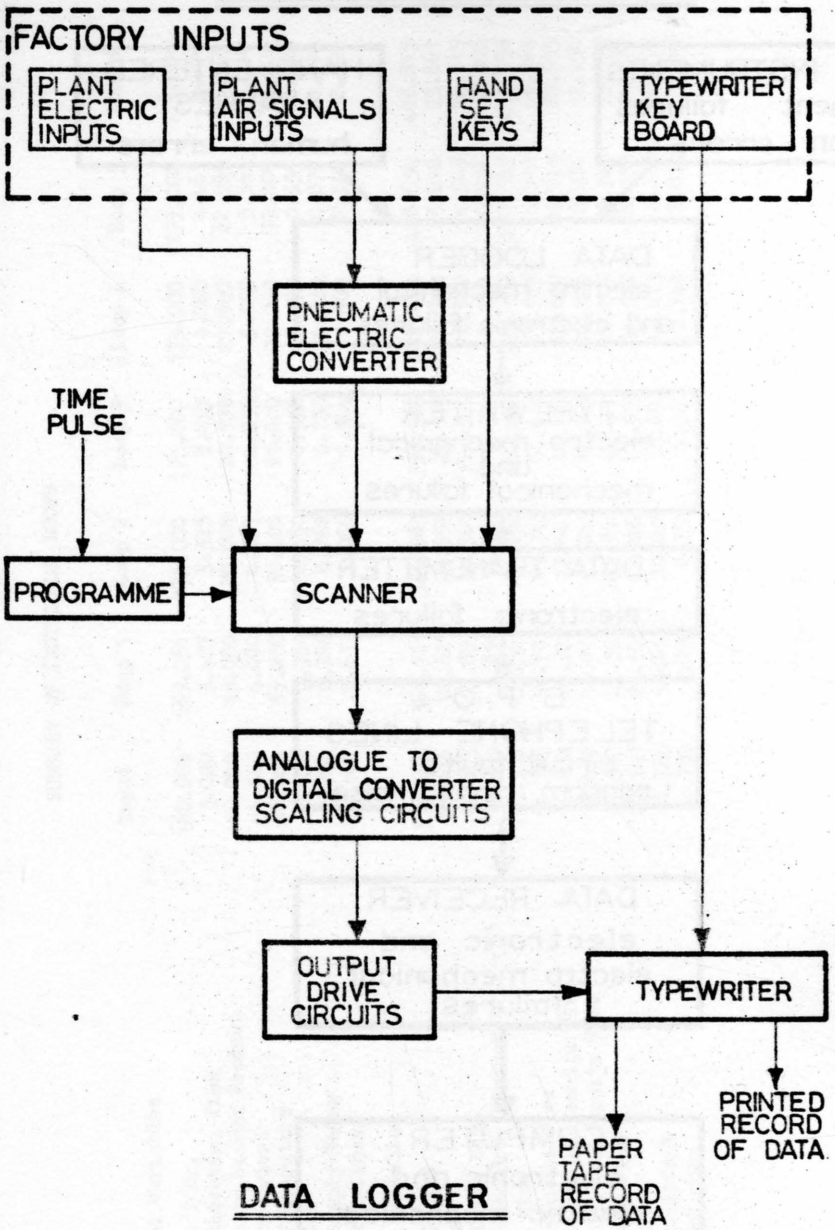
FACTORY INPUTS
PLANT ELECTRIC INPUTS
PLANT AIR SIGNALS INPUTS
HAND SET KEYS
TYPEWRITER KEY BOARD
PNEUMATIC ELECTRIC CONVERTER
TIME PULSE
PROGRAMME
SCANNER
ANALOGUE TO DIGITAL CONVERTER SCALING CIRCUITS
OUTPUT DRIVE CIRCUITS
TYPEWRITER
PRINTED RECORD OF DATA
PAPER TAPE RECORD OF DATA
DATA LOGGER

Fig. 3.

SOURCE OF ERRORS

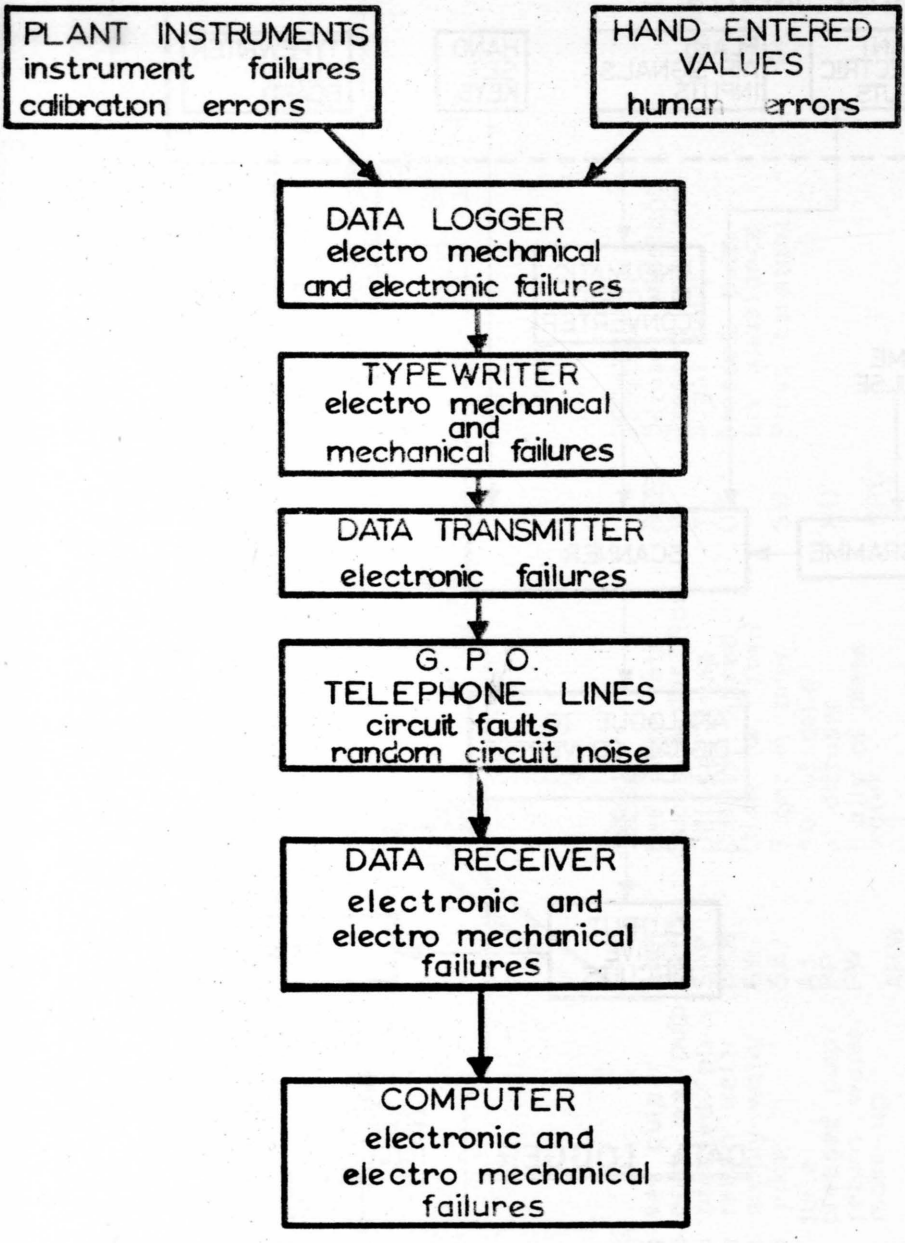

Fig. 4.

SUMMARY OF INDIVIDUAL LOOPS

Independent Variables	Input	Loop 1	Loop 2	Loop 3	Loop 4	Loop 5	Loop 6
Slice Rate T/Hr.	160.000	169.051	175.000	175.000	175.000	175.000	175.000
Diffuser Retention Time	3.000	3.477	3.325	3.493	4.208	4.465	5.000
High Green to Second Product	18.000	19.000	20.000	20.999	21.999	22.999	23.157
Molasses to Driers	4.000	4.400	4.587	4.855	5.255	5.361	5.410
Diffuser Temperature	68.000	69.200	70.400	71.600	72.000	72.000	72.000
Press Factor	0.450	0.350	0.350	0.350	0.350	0.350	0.350
Diffuser Supply Water	0.880	0.780	0.762	0.793	0.828	0.870	0.900
Concurrent Refining	0.100	0.637	1.086	1.944	2.500	2.500	2.500
Dependent Variables							
Relative Profit	338.668	366.361	384.963	397.599	407.478	408.634	408.813
White Sugar	21.276	22.829	23.959	24.975	25.702	25.816	25.861
Molassed Dried Pulp	12.643	13.855	14.566	14.510	14.589	14.549	14.519
High Green to 3rd. Product	3.564	3.596	3.231	2.203	1.191	0.134	0.006
Raw Juice Flow	191.336	183.507	186.456	192.469	199.188	207.369	213.136
White Massecuite Flow	54.975	58.903	61.745	64.215	65.983	66.252	66.364
Second Product Massecuite Flow	15.802	16.722	17.643	18.654	19.639	20.548	20.695
Third Product Massecuite Flow	12.432	13.013	13.249	12.970	12.676	12.288	12.252
Pressed Pulp Flow	37.988	41.559	43.856	42.421	41.006	40.344	39.999
T.S.M. Pulp	22.147	23.505	24.022	23.957	24.255	24.130	24.071
Diffuser Cellfill	8.783	10.215	10.016	10.696	13.123	14.229	16.172
Storage Molasses	2.787	2.730	2.759	2.522	2.142	2.010	1.967

Figure 5.

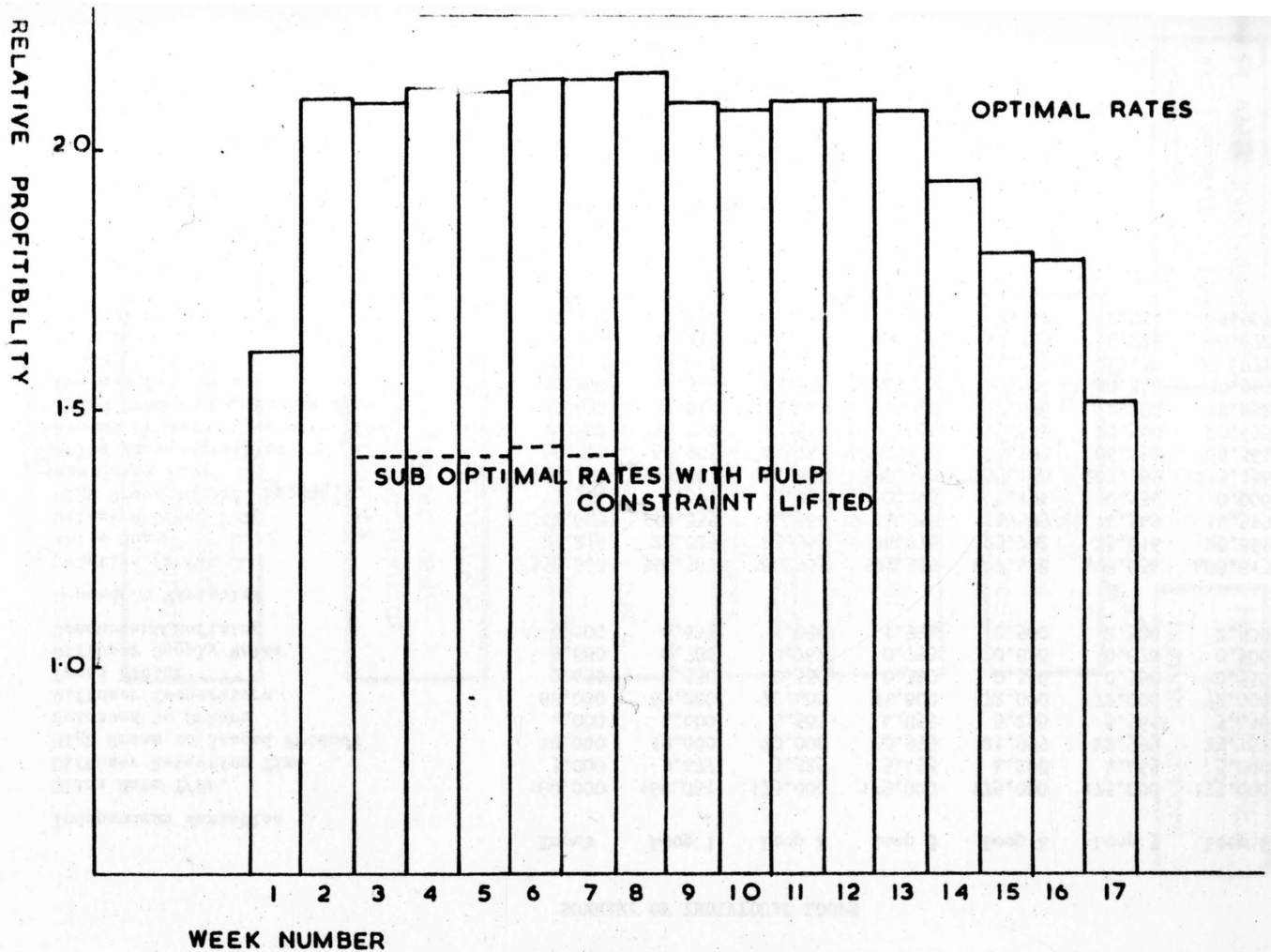
RELATIVE PROFITIBILITY
2·0
1·5
1·0
OPTIMAL RATES
SUB OPTIMAL RATES WITH PULP CONSTRAINT LIFTED
1 2 3 4 5 6 7 8 9 10 11 12 13 14 15 16 17
WEEK NUMBER

FIG. 6.

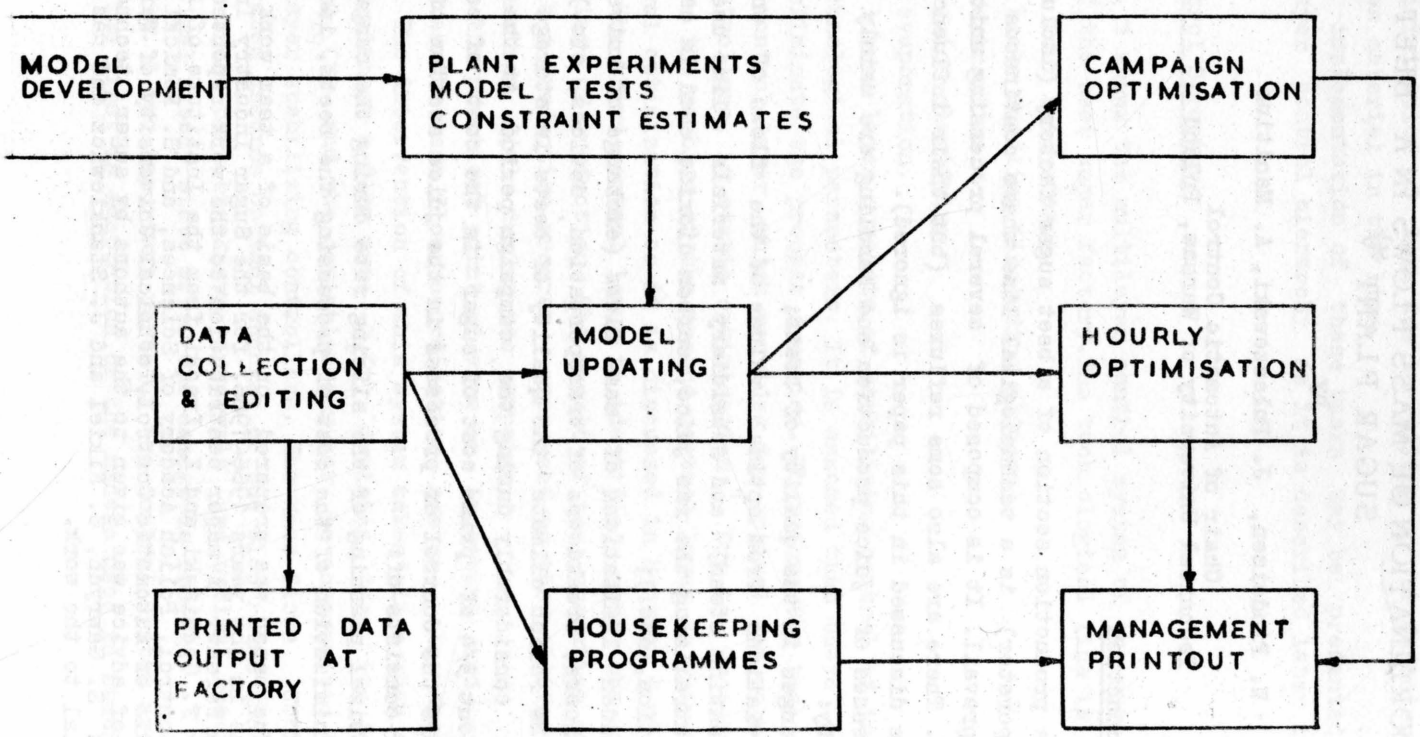
MODEL DEVELOPMENT
PLANT EXPERIMENTS MODEL TESTS CONSTRAINT ESTIMATES
CAMPAIGN OPTIMISATION
DATA COLLECTION & EDITING
MODEL UPDATING
HOURLY OPTIMISATION
PRINTED DATA OUTPUT AT FACTORY
HOUSEKEEPING PROGRAMMES
MANAGEMENT PRINTOUT

FIG. 7.

MULTILEVEL OPTIMIZATION AND DYNAMIC COORDINATION OF MASS FLOWS IN A BEET SUGAR PLANT *)

by

W. Findeisen, J. Pułaczewski, A. Manitius

Chair of Automatic Control
Technical University of Warsaw, Poland

1. Introduction

Juice production section of a beet sugar factory (including the evaporator) is a technological line where continuous processes prevail. It is composed of several processing units in cascade. There are also some refluxes (but their influence on problems discussed in this paper is ignored).

Processes of juice production and handling are mainly affected by:

- changes in the quality of beets;
- deviations from optimal values of the flows of energy (heating steam) and subsidiary materials (lime used in neutralizing the raw juice, carbon dioxide used in carbonation, etc.);
- sudden limitations of mass flows (exchange of knives in slicers, breakdowns of transportation devices, etc.).

In the Polish climate the quality of beets in storage decreases considerably during the campaign period. At the same time about 3/4 of prime cost of sugar is the cost of beets. Therefore the control of processes in the juice section of the factory consists of:

- optimal planning of the slicing rate during the campaign;
- minimization of the cost of processing the beets, includ-

*) The paper was prepared on the basis of a team work that was done in the years 1966-1968, for the Sugar Industry Institute in Warsaw. A major contribution to the work reported was made by F. Gadziński and K. Iracki from the Institute of Automatic Control, Polish Academy of Sciences, and S. Romicki from the Chair of Automatic Control, Technical University of Warsaw. A lot of advice was given to the authors by sugar technology experts S. Gawrych, S. Nikiel and J. Stankiewicz and was most essential to the work.

ing the cost of sugar losses in production;
- minimization of loss due to piling up or deficiency of raw material in the line.

The implementation of these tasks may be presented as a multilayer control hierarchy as it is described later in the paper.

2. Control Structure

Fig. 1 shows the multilayer control system of the juice section of the beet sugar factory. The technological line is divided into four subsystems:

(a) beets handling (including slicers),
(b) extraction,
(c) juice clarifying,
(d) evaporation.

The lowest layer consists of stabilizing control of individual technological parameters. It is assumed that these control loops eliminate the process dynamics. Therefore the task of the second control layer, which provides for optimal set points for the controllers, is static optimization [1]. Due to process complexity, the problem of the second control layer is shaped as a two-level optimization as it is discussed in Section 4 of this paper. The third control layer is identified with the dynamic scheduling of production. The result of the operation of this layer is a production program - expressed as the slicing rate time function $Q(t)$ during the campaign.

From the practical point of view an important and special role takes the mass flows coordination system, also shown in Fig. 1. The intervention of this system takes place when due to some impairment a flow rate $Q_i(t)$ deviates from its desired value $Q_{io}(t)$ and the deviation can not be compensated by the first layer stabilizing controllers. The mass flows coordination system assures optimal changes of the flow rates and storages in those part-breakdown intervals and optimal return to the optimal steady state after the damage is removed.

In Fig. 1 two important parts of the control system are not shown. The first is adaptation of the models used in static op-

timization which shall be achieved by appropriate processing of current data. The second is dynamic optimization of the return to optimal steady state for the main controlled variables in the cases when large deviations exist due to damages (the same for mass flows $Q_1(t)$ was mentioned above).

3. Dynamic Scheduling

The sugar factory has available B tons of beets for processing. The sugar content in the beets and the cost of processing inclusive sugar losses change considerably during the campaign period [2]. This makes up the problem of dynamic optimization, where the objective function proposed is the total income

$$\max_{Q(t)} \left\{ Z = -\gamma_0 B + \int_0^T \gamma_1 z(t)\, Q(t)\, dt + \right.$$
$$\left. - \int_0^T \left[k_0(t) + k_1(t)\, Q(t) + k_2(t) Q^2(t) dt \right] \right\} \tag{1}$$

where: $z(t)$ - sugar concentration in the beets; γ_1, γ_2-prices; $k_0 + k_1 Q + k_2 Q^2$ - approximation to the production cost rate including the losses $\eta(Q, t)$ of the sugar.

Maximization of the income is subject to constraints

$$\int_0^T Q(t)\, dt \leqslant B \tag{2}$$

$$0 \leqslant Q(t) \leqslant Q_{max}(t) \tag{3}$$

A constraint generated by the plan of sugar production may also be considered:

$$\int_0^T \left[1 - \eta(Q, t) \right] z(t)\, Q(t)\, dt \geqslant C \tag{2a}$$

where C is the plan of sugar production and $\eta(Q,t)$ is coefficient of sugar losses in the processing.

For the application of (1) it is fundamental to find proper

approximations for coefficients $k_0(t)$, $k_1(t)$, $k_2(t)$. The initial data to find the numerical values is available from the balance sheets, comparisons of the prime cost and other records that were made during several past campaigns.

To emphasize the importance of considering the dynamic scheduling problem, the results of a numerical example might be given.

With certain simplifying assumptions, a maximum income $Z^o = 52.4 \times 10^6$ zloty was calculated as resulting from a schedule shown in Fig. 2, while $Q(t) = \text{const}$ would yield an income $Z = 50.0 \times 10^6$ zloty, for the same initial data.

4. Static Optimization

4.1. Objective Functions

If the production rate $Q(t)$ is given, the economic optimization reduces to minimization of cost. Objective functions pertinent to individual subsystems in the plant were proposed and they have the following properties:

(a) Their sum makes up the total production cost (strictly speaking , the part of the cost depending upon the controls).

(b) Each subsystem objective function. is suitable for the local optimization of the given subsystem.

The objective function (the cost rate in zloty/hour)for the extractor is set as

$$\varphi_1 = Q\left[\gamma_1 M_w c_{kw} + (\gamma_2 - \gamma_3) M \sum_{i=1}^{19} c_{Mi} K_{Mi}\right] \qquad (4)$$

where: Q - flow rate of sliced beet in tons/hour; γ_1 - price of sugar as left in pulp in zloty/ton; M_w -- relative flow rate of pressed pulp; c_{kw} - weight concetrations of sugar in pressed pulp; γ_2 - price of sugar as located in the juice at extractor outlet in zloty/ton; γ_3 - price of molasses in zloty/ton; M - water flow rate relative to beet flow in the extractor; c_{Mi} - weight concentration of the i-th non-sugar in the juice at the extractor outlet; K_{Mi} - sugar absorption coefficient of the i-th non-sugar.

It may be noticed that the first term in the objective function (4) represents sugar losses with the pulp while the second term represents losses due to molasses-forming properties of non-sugars in the juice.

In the objective function (4) several costs are omitted: electric energy, heating steam, water added to extractor etc. , etc., because they are low or practically independent from the operating conditions of the extractor.

Also in the objective function (4), the molasses-forming products of pectin dissociation are not taken into account, because very small quantities of these products pass into molasses. They are, however, taken into consideration as constraints, because they are colloidal, surface-active substances, and their salts contribute to building of foam and to making the filtration of the juice more difficult. Therefore, the pectin and its derivatives are treated as very detrimental and a limitation on their concentration in the raw juice is set:

$$c_p \leqslant c_{po}$$

For the juice clarifying processes the following objective function is taken

$$\varphi_2 = \gamma_2\left[Q_1 c_{k1} - Q_2 c_{k2}\right] + \\ - (\gamma_2 - \gamma_3)\left[Q_1 \sum_{i=1}^{19} c_{Mi} K_{Mi} - Q_2 \sum_{i=1}^{19} c'_{Mi} K_{Mi}\right] \qquad (5)$$

where the first term represents the value of sugar losses in clarifying processes (price of this raw sugar is γ_2 $\frac{\text{zloty}}{\text{ton}}$), and the second term represents the income due to the fact that less sugar passes into molasses thanks to the clarifying processes. In the equation (5) Q_1 and Q_2 are flow rates of the juice in ton/hour at the inlet and outlet of the clarifying installation, c_{Mi} is the weight concetration of the i-th non-sugar in the extractor juice, c'_{Mi} is the weight concentration of the i-th non-sugar in the thin juice.

The operation of the evaporating part of the plant is characterized by the following objective function

$$\varphi_3 = \gamma_4 Q_p + Q_2 \sum_{i=1}^{4} \gamma_{5i} T_i^2 \qquad (6)$$

where the first term represents the cost of the turbine exhaust steam fed to the evaporator, and the second term represents sugar losses and the decrease of its quality caused by too high temperature in the evaporator bodies. In equation (6) Q_p is the flow rate of the exhausted steam in ton/hour, Q_2 - flow rate of the juice, T_i - temperature in ^{o}C, γ_4 - price of the steam, γ_{5i} are loss coefficients of the sugar quality.

4.2. Method of Static Optimization

It is proposed to perform the static optimization of the plant discussed in a two-level structure [3]. The point is to present the global objective function (cost rate) as a sum

$$\varphi(\underline{u}, \underline{z}) = \varphi_1(\underline{u}^1, \underline{v}, \underline{z}) + \varphi_2(\underline{u}^2, \underline{v}, \underline{z}) + \varphi_3(\underline{u}^3, \underline{v}, \underline{z}) \qquad (7)$$

The objective (7) is dependent upon all control variables $\underline{u}$ and upon disturbances $\underline{z}$. Symbols $\underline{u}^1$, $\underline{u}^2$, $\underline{u}^3$ denote control vectors (they are disjoint, i.e. have no common components) of the individual subsystems, $\underline{v}$ is the vector of coordinating variables. Then the two-level optimization is based upon performing

$$\min_{\underline{u}} \varphi(\underline{u}, \underline{z}) = \min_{\underline{v}} \left[\min_{\underline{u}^1} \varphi_1(\underline{u}^1, \underline{v}, \underline{z}) + \min_{\underline{u}^2} \varphi_2(\underline{u}^2, \underline{v}, \underline{z}) + \min_{\underline{u}^3} \varphi_3(\underline{u}^3, \underline{v}, \underline{z}) \right] \qquad (8)$$

If the result of the optimal control at the first level is

$$\min_{\underline{u}^i} \varphi_i(\underline{u}^i, \underline{v}, \underline{z}) = \varphi_i^{o}(\underline{v}, \underline{z}) \qquad (9)$$

then for the second level one can set the following task

$$\min_{\underline{v}} \left[\varphi = \varphi_1^{o}(\underline{v}, \underline{z}) + \varphi_2^{o}(\underline{v}, \underline{z}) + \varphi_3^{o}(\underline{v}, \underline{z}) \right] \qquad (10)$$

It is most important to note, that independently of the optimality or nonoptimality of the subsystem operation (for instance a subsystem may be controlled manually) the upper-level optimization can still be performed according to

$$\min_{\underline{v}} \left[\varphi = \varphi^{*}_{1}(\underline{v}, \underline{z}) + \varphi^{*}_{2}(\underline{v}, \underline{z}) + \varphi^{*}_{3}(\underline{v}, \underline{z}) \right] \qquad (11)$$

where $\varphi^{*}_{i}(\underline{v}, \underline{z})$ is the cost function depending upon the coordinating variable $\underline{v}$, when the control is suboptimal and known and the disturbances are given.

As it is known, the success of the decomposition first of all depends upon the partition of equality and inequality relations which constraint, originally, the choice of $\underline{u}$. In the decomposed system it is necessary to have three sets of relations limiting the choice of $\underline{u}^1$, $\underline{u}^2$ and $\underline{u}^3$, and all that depends upon coordination variables forming the vector $\underline{v}$. The manner of dividing the objective function into a sum of components (7) is a rather secondary problem.

For the plant considered the partition was done according to the technological subsystems as it is shown in Fig. 3. It is important to note, that the subsystems interact by their output variable vectors ($\underline{y}^1$, $\underline{y}^2$). The classical approach to decomposition would consist in taking these as coordinating variables, but then their number would be too large for to make the solution of the problem feasible. That is why, as the result of many considerations the following coordinating variables (forming the vector $\underline{v}$) were chosen

Q - flow rate of sliced beet

M - water-to-beet ratio in the extractor

c_{po} - concentration of pectins in the juice at exctractor outlet

$c_{20} = \frac{c_{k2}}{Bx_2}$ - minimal clarity of the thin juice .

The flow rate Q is set as obtained from the dynamic scheduling and so only three coordination variables remain free. The fourth might be the density Bx_4 of the thick juice, but it is set fixed from other considarations.

The output variables, for instance $\underline{y}^1$, are now disturbances

for the static optimization problem of the second subsystem. The justification for accepting such a procedure is that the vector $\underline{v}$ has a considerable influence upon the variables $\underline{y}^1$, $\underline{y}^2$ and $\underline{y}^3$ and so the obtained solution can be close to optimal.

As the result of the choice of the coordinating variables, the exctractor optimization reduces to

$$\min_{T(1),n,pH} \varphi_1\left[T(1),\ n,\ pH,\ Q,\ M,\ \underline{z}^1\right] \tag{12}$$

subject to the constraint

$$c_p \leqslant c_{po} \tag{13}$$

where symbols are explained in Fig. 3.

The solution of the problem (12), (13) gives

$$\varphi_1^o = \varphi_1^o(Q,\ M,\ c_{po},\ \underline{z}^1) \tag{14}$$

and the output variables

$$\underline{y}^{10} = \underline{y}^{10}(Q,\ M,\ c_{po},\ \underline{z}^1) \tag{15}$$

With several simplifications (the values of some variables are determined by the technological tradition and experimental data) the problem of the optimization of the juice clarifying subsystem has the form

$$\min_{q_{mg},q_{ms}} \varphi_2\left[Q,\ M,\ q_{mg},\ q_{ms},\ c_{po},\ \underline{y}^1,\ \underline{z}^2\right] \tag{16}$$

subject to

$$c_2 = \frac{c_{k2}}{Bx_2} \geqslant c_{20} \tag{17}$$

where symbols are explained in Fig. 3.

Solving the problem (16), (17), gives

$$\varphi_2^o = \varphi_2^o(Q,\ M,\ c_{20},\ c_{po},\ \underline{y}^{10},\ \underline{z}^2) \tag{18}$$

and the output variables

$$\underline{y}^{20} = \underline{y}^{20}(Q,\ M,\ c_{20},\ c_{po},\ \underline{y}^{10},\ \underline{z}^2) \tag{19}$$

The evaporator optimization problem consists in obtaining

$$\min_{q_p, h_i, q_4} \varphi_3 \left[Q,\ M,\ q_p,\ h_i,\ q_4,\ Bx_4,\ \underline{y}^{20},\ \underline{z}^{3} \right] \tag{20}$$

under the conditions

$$Bx_4 = Bx_{40} \tag{21}$$

$$T_{4min} \leqslant T_4 \leqslant T_{4max} \tag{22}$$

where symbols are also explained in Fig. 3.

The solution of the problem (20), (21), (22) gives

$$\varphi_3^0 = \varphi_3^0 (Q,\ M,\ c_{20},\ c_{p0},\ Bx_{40},\ \underline{y}^{20},\ \underline{z}^{3}) \tag{23}$$

It is proposed to implement the optimal upper-level contro first, with the use of the empirical characteristics φ_1^*, φ_2^* φ_3^* which are known from the long experience.These character istics are either known or can be determined from proper ex periments. The exact solution of the local optimization prob lems is difficult because some of the mathematical models an their experimental verification is still lacking.

5. Dynamic Coordination of Mass Flows

The problem of mass flows coordination consists in control ling flow rates in several parts of the line to minimize los ses caused by temporary limitations of flow rates, what in volves overflows before the point of the limitation and defi ciency of the juice behind this point. The return to optima steady state flow rates after the elimination of disturbance can not be arbitrary. For one there are losses caused by tran sients in the line when flow rates of the juice change.That i why the problem of mass flows coordination is in fact a prob lem of optimal control of flow rates.

The technological line in the beet sugar factory is a ver complicated dynamic system which must be approximated by simpler model. The main elements of the line dynamics ar tanks (as integrating elements) and large time constants o the extractor and of the evaporator. This leads to the mode presented in Fig. 4. The model considers six tanks and seve

controlled flow rates. The differential equations are following

$$\dot{x}_i = \alpha_i(t)\, u_i; \qquad i = 1, \ldots, 7 \tag{24}$$

$$\left.\begin{aligned} \dot{x}_i &= x_{i-7}(t - h_{i-7}) - x_{i-6}(t);\ i = 8, 9, 10, 12 \\ \dot{x}_{11} &= x_{14} - x_5 \\ \dot{x}_{13} &= x_{15} - x_7 \end{aligned}\right\} \tag{25}$$

$$\left.\begin{aligned} \dot{x}_{14} &= \mu\left[x_4(t - h_4) - x_{14}\right] \\ \dot{x}_{15} &= \nu\left[x_6(t - h_6) - x_{15}\right] \end{aligned}\right\} \tag{26}$$

where

$x_i;\ i = 1, \ldots, 7$	flow rate in the i-th part of the line
$x_i;\ i = 8, \ldots, 13$	mass stored in the $(i - 7)$ tank
x_{14}, x_{15}	flow rates at the outlest of the extractor and the evaporator
h_i	transportation lags

Coefficients $\alpha_i(t)$ in the equation of flow dynamics (24) can be equal to 0 or 1 depending on the fact if the i-th flow rate can be controlled at time t or if it is temporary limited, Equations (25) show the mass balance in the individual parts of the line. Equations (26) show the inertial character of the flow rate at the outlet of the extractor and evaporator.

It is assumed that at time $t_o = 0$, when the line is in steady state, a disturbance of flow rate occurs in the part number k of the line. The expected duration of this disturbances is t_k. According to the value of t_k the total time $T > t_k > 0$ of the transient is assumed. In the interval $[0, t_k]$ the flow rate number i is uncontrolled, then

$$\alpha_k(t) = \begin{cases} 0, & t \in (0, t_k) \\ 1, & t \in [t_k, T] \end{cases}$$

The state equations are discontinuous at the instant t_k but this fact does not complicate the solution of the optimal control [6].

The problem of optimal control is formulated in the following way: (a) at time $t_o = 0$ the initial conditions $x_i(0) = z_i$,

$i = 1, \ldots, 15$, and initial functions $\varphi_i(t)$; $-h_i \leqslant t \leqslant 0$; $i = 1, \ldots, 6$ are given; (b) for the time $t = T$ final conditions $x_i(T) = \bar{x}_i$ are given; (c) the variables $x_i(t)$ are constrained

$$0 \leqslant x_i(t) \leqslant a_i \; ; \quad i = 1, \ldots, 7$$
$$b_i \leqslant x_i(t) \leqslant c_i \; ; \quad i = 8, \ldots, 13 \qquad (27)$$

(d) admissible controls $u_i(t)$; $t \in [0,T]$, $i = 1,\ldots,7$, $i \neq k$ and $u_k(t)$; $t \in [t_k, T]$ are to be found which give minimal value of the following performance index $J(\underline{u})$

$$J(\underline{u}) = -Z + \Delta K$$

where Z is the income associated with production of sugar, ΔK are additional losses connected with the decrease in product quality caused by transients in the line.

The term Z characterizes the quantitative aspect of production, while the term ΔK - the qualitative aspect which is completely omitted in the simplified mass flow model shown in Fig. 4.

It is a very difficult task to derive an accurate enough functional ΔK from the mathematical models of the processes. At the present stage of the investigation the functionals Z and ΔK are taken a priori in the form

$$J(\underline{u}) = \int_0^T \left[\sum_{i=1}^{7} \gamma_i x_i + \sum_{i=1}^{7} \beta_i u_i^2 \right] dt \qquad (28)$$

where $\gamma_i > 0$; $i = 1, \ldots, 6$; $\gamma_7 < 0$; $\sum_{i=1}^{7} \gamma_i \leqslant 0$; $\beta_i \geqslant 0$; $i = 1, \ldots, 7$.

It is assumed in the first term that the income grows linear with production. The second term represents the additional losses caused by changes of the flow rates. It is assumed that these losses are proportional to the squares of the derivatives of the flow rates.

The problem was solved using the maximum principle, without considering the constraints on state (27). This allows to obtain an analytical form of the solution. The optimal flow rates are following

$$x_i^{*}(t) = \frac{\bar{x}_i - z_i}{T_i} t + z_i + \frac{k_i}{4\beta_i} t(t - T_i) + y_i(t); \; i = 1, \ldots, 7$$

$$\text{for } t \in [0,\ T - h_i]$$

and $x^{*}_i(t) = \bar{x}_i;\ t \in [T - h_i,\ T]$, where

$$y_i(t) = \begin{cases} 0 \text{ for } i = 1, 2, 3, 5, 7 \\ k_8\left[\frac{t}{T_4}(1 - e^{-\mu T_4}) + e^{-\mu T_4}(1 - e^{+\mu t})\right];\ i = 4 \\ k_9\left[\frac{t}{T_6}(1 - e^{-\nu T_6}) + e^{-\nu T_6}(1 - e^{+\nu t})\right];\ i = 6 \end{cases}$$

where $k_1, \ldots, k_9$ are solutions to a set (9 x 9) of linear equations, resulting from conditions of optimality and conditions of mass balance.

The results are illustrated in Fig. 5. In this example it was assumed that the limitation occured in the juice clarifying station (part No. 5) and in a time t_5 it was equal to 20% of the steady flow rate.The plots show a considerable increase of the flow rate in the part No. 5 of the line.In order to decrease this top flow rate it is necessary to take a long time T ($T \approx 10t_5$). The rest of the flow rates change only slightly with the exception of the flow rate No. 6 (due to forcing the large time constant T of the evaporator).

The method discussed after some refinements,seems to enable the calculation of optimal flow rates for the transients in the line. This may be used to guide system operation in out--normal conditions.

6. Bibliography

1. I. Lefkowitz, Multilevel Approach Applied to Control System Design, Trans. ASME, 88, June 1966.
2. The Course of the Sugar Campaign in 1967/68, Gazeta cukrownicza, No. 6, June 1968 (in Polish).
3. W. Findeisen, Parametric Optimization by Primal Method in Multilevel Systems, Trans. IEEE on Systems Science and Cybernetics, August 1968.
4. P.M. Silin, Voprosy technologii sacharnych vieščestv,Moskva 1950.
5. S. Nikiel, Beet Sugar Technology, Warsaw 1958 (in Polish).
6. A. Wierzbicki, The Maximum Principle and Synthesis of Optimal Controllers, Archiwum Automatyki i Telemechaniki, No. 1 1968 (in Polish).
7. A. Manitius, Optimal Control of Processes with Delays of State Variables, Ph. D. Thesis, Technical University of Warsaw, 1968, and paper submitted to 4th IFAC Congress.

Summary

Changes of the beets quality, inaccuracy of the dosage of energy and materials streams, sudden oscillations of the mass flows, these are the main factors which cause the losses in the sugar production. To minimize these losses an optimizing control, structured as a multilayer system, is proposed.

The first layer consists of stabilizing control. The set points of the controllers are determined by local static optimizers. The losses in the whole technological line are minimized by the global static optimizer which coordinates the work of the local optimizers. The desired production rate is presented as a solution to a dynamic optimization problem - the scheduling problem.

If a temporary limitation of the desired production rate is caused by any reason, then a mass flows coordination system is called upon to control flow rates in different parts of the technological line, to minimize the loss. When the limitation is over, the coordination system brings the line to the previous optimal steady state leaves it to the static optimizers.

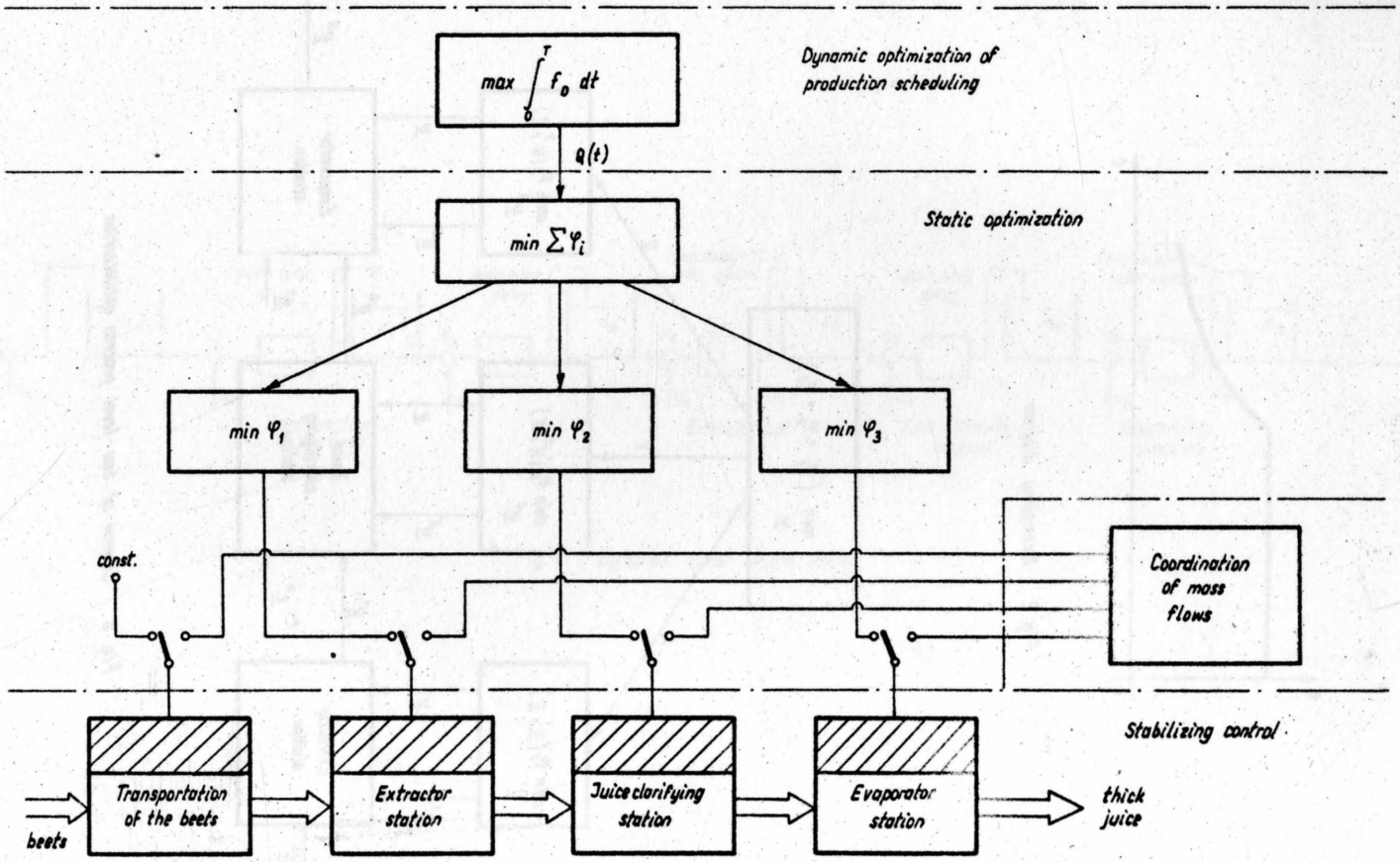

Fig. 1 Control in a beet sugar plant as a multilayer system

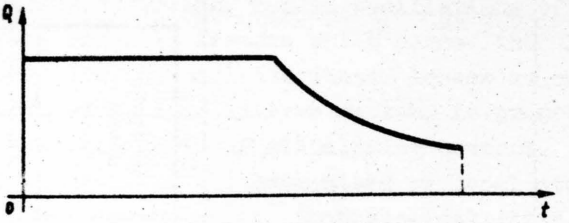

Fig. 2 Exemplary diagram

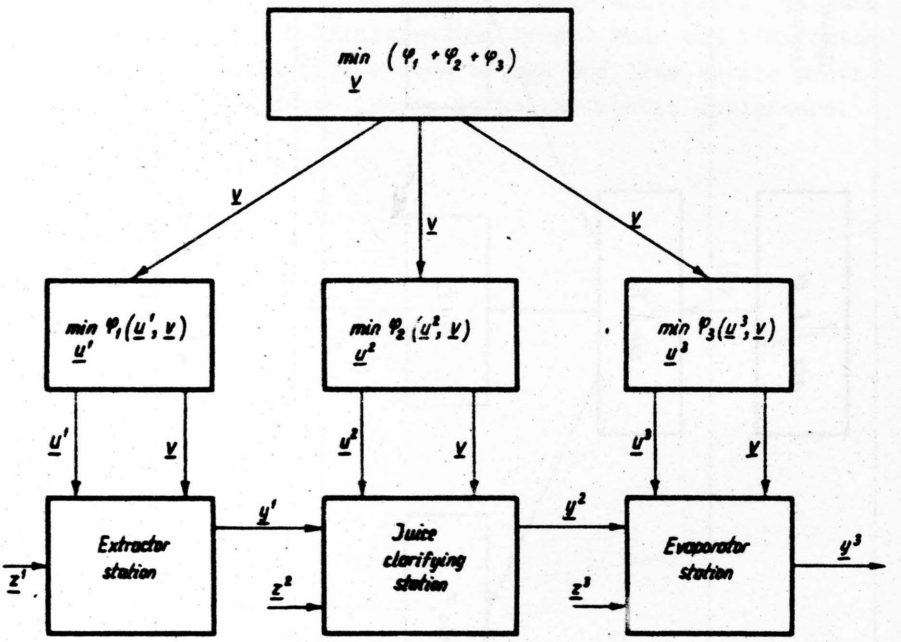

Fig. 3 Scheme of two-level process optimization

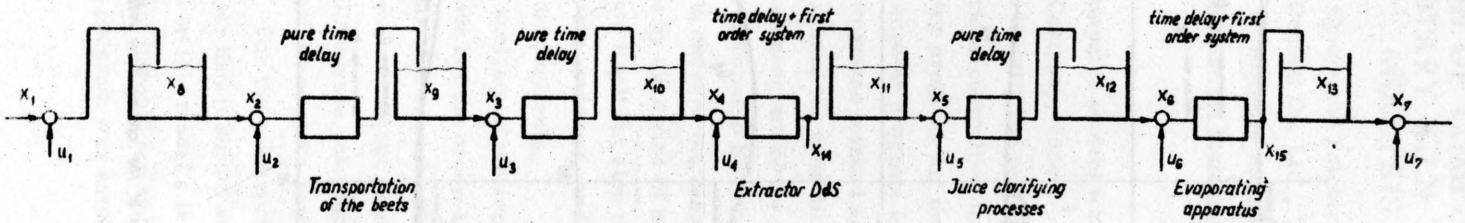

Fig. 4 Dynamic model of the plant

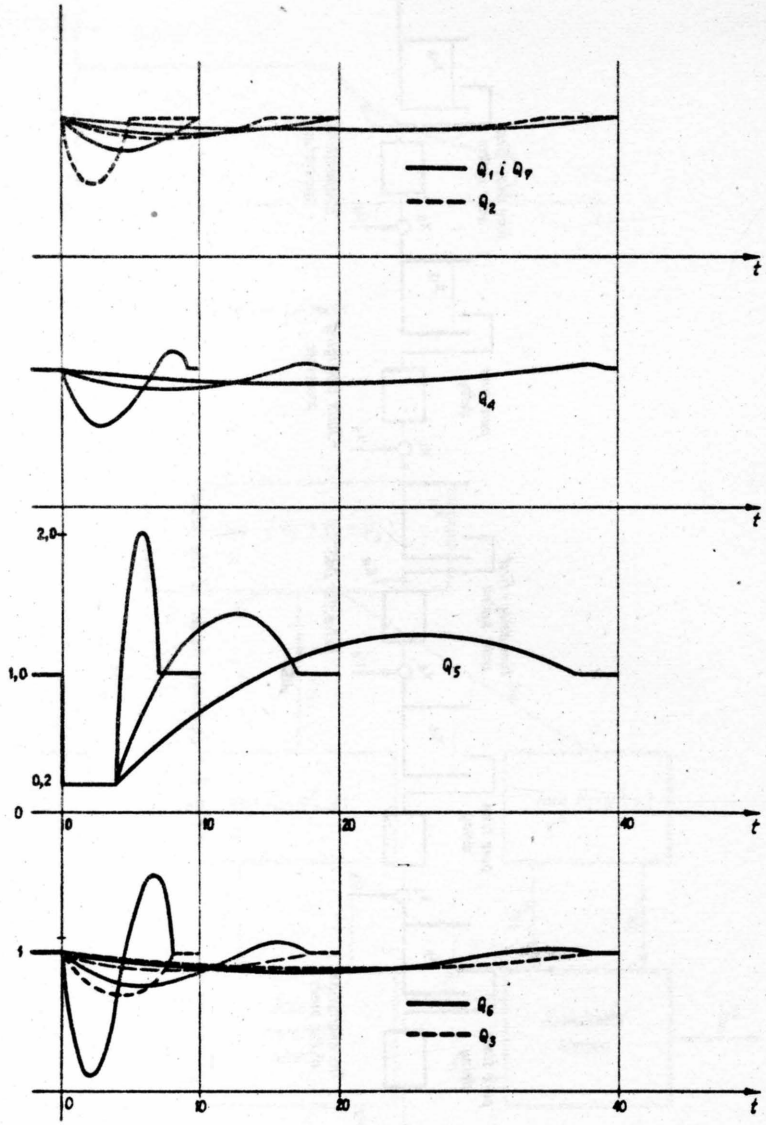

Fig. 5 Curves of the optimal flow rates

IMPLEMENTATION OF COMPUTER CONTROL OF A CEMENT ROTARY KILN THROUGH DATA ANALYSIS

Tsuneo Otomo and Toichiro Nakagawa
Chichibu Cement Co. Ltd., Tokyo, Japan
Hirotugu Akaike
The Institute of Statistical Mathematics, Tokyo, Japan

1. Introduction

In 1963, on-line computer control was introduced into Kumagaya plant of Chichibu Cement Company, Japan.[1] Before the introduction, experiments were made to identify the response characteristics of the kiln to artificial changes of various controlling inputs and a model of the kiln was constructed. A computer program for the kiln control was developed on this model. Another computer program for the blending control was also developed and these programs worked satisfactorily. Later as the rate of production was increased the dynamic behavior of the kiln changed significantly and the original program of the kiln control could not catch up with the change. Also it was found to be impossible to apply a significant artificial input to the kiln to observe the response, as the stationarity of the kiln behavior was only kept by the action of human operator. Thus it turned out that not only the program itself but also the philosophy of program construction had to be completely reviewed, and in 1965 we started to the somewhat lengthy road of data analysis.

Extensive spectral analysis of the records of the kiln under normal operating condition was made but the cross-spectral method failed to produce any definite result about this kind of system with significant feedback loop.[2] Various other approaches were tried but produced unsatisfactory results.[3] Along with these numerical analyses, careful study of various typically oscillatory records was performed and a rather qualitative model of the kiln behavior was adopted. For the construction of this crude model of the kiln we followed the principle that it should explain the significant situations within the records. Based on this model a tentative program was developed and carefully checked so that it would not aggravate the kiln condition. The result of application of the program was satisfactory but it lacked objective

proof of its effectiveness.

Recently one of the present authors proposed a general approach to the analysis of a noisy feedback system[4] and by this approach our kiln records produced quite understandable result which explains why the program was effective. Though our result is not yet perfect, it suggests the possibility to put the kiln control on a sound scientific foundation.

In this paper we shall historically describe our experiences and also discuss about possible further improvements of our computer control.

2. Results of spectrum analysis

Here we shall show some of the results of spectrum analysis of a kiln. The plant is wet process and we analyzed the behavior of kiln #2 of which dimension can be seen in Fig. 1. Since the blending control of raw material was almost perfect we guessed that the variation of the kiln behavior was due to the variation of material flow within the kiln. We had logging data of fuel rate, load of the main driving motor (kilowatt), exit gas temperature (T_{end}), intermediate gas temperature (T_{ig}), burning zone temperature (T_{bz}), temperature of the secondary air (T_{2nd}), speed of cooler grate, content of oxygen, draft damper position, under grate pressure of cooler (P_c), kiln speed, and feed rate of material. The time interval between observations was 10 minutes. Of these, fuel rate, feed rate, draft damper position, cooler grate speed and kiln speed are controlling variables and others are controlled variables. When the data was accumulated the kiln was being operated over the level of its design specification and the material flow was almost at the limit of the cooler capacity. Thus the cooler was at its full load and practically no control was applicable. Obviously under this circumstance a closed loop between the material flow and the burning condition was formed through draft variation. The power spectra of controlled variables showed significant peaks around the frequency of one cycle per 3 hours. A typical example is shown in Figs. 2 to 4. Also it has become clear that the powers of fluctuations of these controlled variables are mainly distributed within the frequency band from d. c. to one cycle per 1.5 hour. We further performed cross-spectral analysis of the related quantities. In Fig. 5 are illustrated observed sample coherencies between three main controlled variables and in Fig. 6 observed sample coherencies

between exit gas temperature and controlling variables. The coherency $\gamma^2(f)$ between the stationary time series x(t) and y(t) at frequency f is defined by

$$\gamma^2(f) = \frac{|p_{yx}(f)|^2}{p_y(f)\, p_x(f)} ,$$

where $p_{yx}(f)$ is the cross-spectral density between y(t) and x(t) and $p_y(f)$ and $p_x(f)$ are the power spectral densities of y(t) and x(t), respectively.[5] Generally it is considered that $\gamma^2(f)$ represents a degree of linear dependence between y(t) and x(t) at frequency f. From this standpoint we can see that the three controlled variables are showing very close linear relation at the frequency band where their power spectra have shown significant peaks. This fact suggests that there exists a definite relation between the behaviors of these three variables in that frequency band. Contrary to this, the coherencies between controlling variables and controlled variables were low. Even the results of much more complicated analysis of multiple coherency[6] which shows the simultaneous relation between the three main controlling variables and each controlled variable have shown very low coherencies between these variables. Is this result suggesting that the effect of controlling variables to the kiln behavior is quite low ? We can not generally say yes to this question when there is a negative feedback between the variables, as it can be shown that the coherency is generally low in the frequency band where negative feedback is effectively working. Thus it turned out that both high values and low values of coherency can be meaningful for our present problem. This fact and the fact that ordinary method of estimation of frequency response function through cross-spectrum is inapplicable to feedback systems made the spectral method almost useless for the present purpose of analysis.[2] Some alternative procedures have been investigated, but the results were discouraging.[3] We know that there is a pioneering work[7] on the correlation analysis of a heat exchanger, where a procedure proposed by Goodman and Reswick[8] was employed. But even this procedure is not applicable to our present situation where the related variables are far from whiteness.

3. Qualitative analysis of the data

We were also developing a qualitative analysis of the records. We

found that the typical pattern of one cycle of an oscillatory movement of the kiln was like the one schematically represented in Fig. 7, and we developed a hypothesis that kilowatt of the main driving motor represents the amount of material inside the burning zone. Thus if this quantity increases it generally means the increase of endothermic content within the burning zone and thus the need of thermal input. This assumption seemed to explain why the exit gas temperature goes down when the kilowatt goes up. Also it was observed that there was a definite relation between the kilowatt and the cooler pressure. This is quite understandable if the kilowatt is representing the amount of material within the burning zone, as it will finally appear as an input to the cooler. Further it was observed that the exit gas temperature was highly negatively correlated with the cooler pressure and these observations all appeared quite reasonable. Then was it able for us to locate the cause of the annoying fluctuations of these variables? This was almost impossible for us as there seemed to be a definite relation between the exit gas temperature and the kilowatt, which shows that the variation of the exit gas temperature produces a significant effect on the kilowatt after about one hour's delay. Thus a vicious circle of the type "Which is the first, the egg or the hen?" took place. As was stated before, the cooler speed was almost uncontrollable under the condition of over production beyond the cooler specification, and also it was well recognized that the controls by kiln speed and by damper position generally produce very much complicated after effects. Also it was observed that the exit gas temperature shows a quick response to the fuel input. Taking into account of these circumstances and the high coherencies between controlled variables we decided first to develop the control of the exit gas temperature by controlling fuel rate. A computer program was developed, where the difference between the adjacent values of exit gas temperature observed at every 6 minutes and that of kilowatt were used as main constituents of the program. Some kind of prefiltration was applied to the original data to reduce possible measurement noise. The structure of this main part of the program was as follows:

$$F(n) = F(n-1) + \Delta F(n)$$

$$\Delta F(n) = -\alpha(T_{end}(n) - T_{end}(n-1)) - \beta(T_{ig}(n) - T_{ig}(n-1)) - \gamma(T_{ig}(n) - T_{igsp}) + \delta(W(n) - W(n-1))$$

where

$F(n)$ = fuel rate at time n

$T_{end}(n)$ = exit gas temperature at time n

$T_{ig}(n)$ = intermediate gas temperature at time n

$W(n)$ = kiln load (kilowatt) at time n

T_{igsp} = set-point of intermediate gas temperature

and $\alpha, \beta, \gamma, \delta$ are positive constants and the time unit is 6 minutes. Adjustments of the parameters within the program were made by trial and error and the program produced satisfactory result. Thus it seemed that our qualitative analysis was a useful procedure but we could not make it a purely objective one.

4. Introduction of new model

Recently one of the present authors developed a procedure for the analysis of noisy linear feedback systems [4] and the procedure was applied to the analysis of our kiln data. We are going to discuss the result in this section.

We consider a set of K+1 observation points which are represented by $i=0, 1, \cdots, K$. We shall denote the measurement at i by $x_i(n)$. For the sake of simplicity we assume that the measurement is taken at integral multiples of a unit time Δt and $x_i(n)$ denotes the value at time $n\Delta t$. The basic model we are going to use is given by

$$x_i(n) = \sum_{j=0}^{K} \sum_{m=0}^{M} a_{ijm}\, x_j(n-m) + u_i(n) \qquad i=0, 1, \cdots, K,$$

where it is assumed that $a_{iim}=0$ $(m=0, 1, \cdots, M)$ and $u_i(n)$s are mutually orthogonal and satisfy the relation

$$u_i(n) = \sum_{\ell=1}^{L} c_{i\ell}\, u_i(n-\ell) + \varepsilon_i(n) \qquad i=0, 1, \cdots, K$$

where $\varepsilon_i(n)$ is a white noise satisfying the relations $E\,\varepsilon_i^2(n) = \sigma_i^2 (>0)$ and $E\,\varepsilon_i(n)\,\varepsilon_i(m)=0$ for $n \neq m$. Thus $\{a_{ijm}\}$ represents the impulse response from j to i and $u_i(n)$ the noise source, or driving input, at i. We further assume that $a_{ij0}=0$ $(j=0, 1, \cdots, i)$ and that the system is stable so that $\{x_i(n$ will be a stationary stochastic process. It should be noted that our last assumption of $u_i(n)$ is practically a very mild one and can be expected to hold in ordinary applications. Also it should be mentioned that if there is

a feedback loop from i to i which does not pass through other js its effect is included into all of $\{a_{ijm}\}$s and the effect of noise source within the loop is included into $u_i(n)$. This fact must be taken into account when we see the numerical result. Under the present assumption we first whiten the noise $u_i(n)$ to transform the original model into the form

$$x_i(n) = \sum_{j=0}^{K} \sum_{m=0}^{M+L} A_{ijm}\, x_j(n-m) + \varepsilon_i(n) ,$$

where

$$\begin{aligned} A_{ii0} &= 0 \\ A_{iim} &= c_{im} && m=1, 2, \cdots, L \\ A_{ij0} &= a_{ij0} \\ A_{ijm} &= a_{ijm} - \sum_{\ell=1}^{m} c_{i\ell}\, a_{ijm-\ell} && m=1, 2, \cdots, M+L \end{aligned}$$

and it is assumed that $c_{i\ell}=0$ for $\ell > L$ and $a_{ijm}=0$ for $m>M$. We consider the case where a set of data $\{x_i(n);\ i=0, 1, \cdots, K,\ n=1, 2, \cdots, N\}$ is given. Under our present assumption we can apply ordinary least squares method to obtain an estimate of $\{A_{ijm}\}$ and the consistency of the estimate is assured under very weak condition. Using the relation

$$\begin{aligned} c_{im} &= A_{iim} && m=1, 2, \cdots, L \\ a_{ij0} &= A_{ij0} \\ a_{ijm} &= A_{ijm} + \sum_{\ell=1}^{m} c_{i\ell}\, a_{ijm-\ell} && m=1, 2, \cdots, M \end{aligned}$$

where $c_{i\ell}=0$ for $\ell > L$, we can get estimates of $\{c_{im}\}$ and $\{a_{ijm}\}$ by substituting the estimated value of $\{A_{ijm}\}$ into the formulae. For the sake of typographical simplicity we shall not distinguish between the true values and their corresponding estimates. We can get an estimate of the frequency response function from j to i by

$$a_{ij}(f) = \sum_{m=0}^{M} a_{ijm} \exp(-2\pi\sqrt{-1}\, fm)$$

and that of the power spectral density function of $u_i(n)$ by

$$p(u_i)(f) = \frac{\sigma_i^2}{\left| 1 - \sum_{\ell=1}^{L} c_{i\ell} \exp(-2\pi\sqrt{-1}\, f\ell) \right|^2}$$

where

$$\sigma_i^2 = C(x_i, x_i)(0) - \sum_{k=0}^{K} \sum_{\ell=0}^{M+L} C(x_i, x_k)(\ell) A_{ik\ell}$$

and $C(x_i, x_j)(\ell) = \frac{1}{N} \sum_{n=1}^{N-\ell} x_i(n+\ell) x_j(n)$. Practically, we assume that the mean values or d. c. components of the related quantities are out of consideration and thus they are deleted from the data. The estimate of the closed loop frequency response function $b_{ij}(f)$ from j to i will be obtained by the matrix relation

$$\left[b_{ij}(f) \right] = \left[\delta_{ij} - a_{ij}(f) \right]^{-1} \qquad (i, j = 0, 1, \cdots, K)$$

where $\delta_{ii}=1$ and $\delta_{ij}=0$ $(i \neq j)$. The power contribution of the noise source $u_j(n)$ to the output $x_i(n)$ will be estimated by

$$q_{ij}(f) = |b_{ij}(f)|^2 p(u_j)(f) .$$

The quantity $\gamma_{ij}(f)$ given by

$$\gamma_{ij}(f) = \frac{q_{ij}(f)}{\sum_{k=0}^{K} q_{ik}(f)}$$

will give the relative contribution of $u_j(n)$ to the power of $x_i(n)$ at frequency f, and $R_{ij}(f)$ defined by

$$R_{ij}(f) = \sum_{k=0}^{j} \gamma_{ik}(f) \qquad j = 0, 1, 2, \cdots, K-1$$

will be useful for graphical representation.

Evaluation formulae for the statistical variation of these estimates are yet incomplete and we have decided to base our judgement on the results of repeated applications of the procedure.

We have applied our identification procedure to the data of kiln #2. We put K=2 and

$x_0(n)$=exit gas temperature, $x_1(n)$=kilowatt, $x_2(n)$=cooler pressure.

In Fig. 8 are shown estimates of the impulse response functions. The sampling time unit Δt was 10 minutes. We have selected the values L=4 and M=12 for computation. These values are not necessarily large enough but are limited by the computer capacity which was available at the time of analysis. Some of the results show quite noisy appearances due to

possible sampling fluctuations at higher frequencies, but they show fairly stable behavior after smoothing.

Some of the frequency responses are shown in Figs. 9-12, where the gain $|a_{ij}(f)|$ and the phase lag $\Phi_{ij}(f)$ are defined by the relation $a_{ij}(f) = |a_{ij}(f)|\exp(\sqrt{-1}\,\Phi_{ij}(f))$. We can see remarkable stabilities of phase relations at lower frequencies between exit gas temperature and kilowatt and between cooler pressure and kilowatt. From our estimate of the impulse response from cooler pressure to kilowatt we can see that the cooler pressure variation contributes integratedly to the kilowatt variation with negative sign. It was confirmed that this was in good agreement with the observation of an efficient kiln operator. Also our analysis gave steady response of cooler pressure to kilowatt, which was of transport lag type, and the phase relations between these two strongly suggested the contribution of this loop to the fluctuation with period of about 3 hrs and thus the importance of cooler control. An example of the set of graphs of $R_{ij}(f)$ is given in Fig. 13.

The estimates of the phase lag from cooler pressure to exit gas temperature were significantly different between the records. From the definition of our model, this may be explained by the fact that there existed some significant feedback loop at the site of exit gas temperature and that its characteristics had been changed significantly between the records. It is almost obvious that this means the contribution of feedback loop by human operator. Thus we turned our attention to the relation between fuel rate and exit gas temperature. In this case we adopted the values L=6 and M=18 and put $x_0(n)$=exit gas temperature and $x_1(n)$=fuel rate. The estimates of the impulse response from fuel rate to exit gas temperature are given in Fig. 14. It should be mentioned here that due to the limitation of computing time we are ignoring possible contributions from the damper position and the kiln speed and this may be introducing some bias into the present analysis. But these variables had usually been kept constant and the frequencies of change were much rarer than that of fuel rate. Thus our result will be giving a fairly reliable image of the response. In Fig. 15 are given the estimates of the gain and in Fig. 16 the estimates of the phase lag. Except for one example which corresponds to a non-stationary record these estimates of phase lag show good agreement between them. It is most remarkable that they pass the value $-\frac{\pi}{2}$ around the frequency one cycle per 3 hours and

are almost staying within the limit of $-\pi$ in the frequency range from 0 to one cycle per 1.5 hour, where the main part of the power of exit gas temperature fluctuation is distributed. Thus if we introduce a phase advance of $\frac{\pi}{2}$ into the negative feedback loop from exit gas temperature to fuel rate it will work efficiently in this critical frequency range. To verify the validity of this observation we have tested the control program with only the term of exit gas temperature, i.e., with $\beta = \gamma = \delta = 0$. The gain α was set very high and the result is illustrated in Fig. 17. It can be seen that the exit gas temperature shows only very low or very high frequency variations as was expected from the result of our data analysis. This confirms the practical utility of our analysis and partly proves why the former program could be useful. We are also developing a cooler control program based on the result of our analysis.

We have extended the analysis to another kiln #5 (see Fig. 1). The result has shown that the relations between the observation points are similar to those of kiln #2 but the noise characteristics, especially $R_{ij}(f)$, is different and the variation due to kilowatt noise is quite significant.

5. Further improvement of the program and related discussions

It has been pointed out that it is most necessary to keep the drying zone as stationary as possible to keep the burning zone load stationary.[9] Our success in stabilizing the kiln confirms this observation, as our program was mainly oriented towards the stabilization of the exit gas temperature which will be in close relation with the drying zone atmosphere. But, even when the drying zone was kept stationary there would unavoidably occur disturbances in the burning zone due to the fluctuation of material flow caused by the formation and falling of mud ring and coating. This kind of variation generally causes the variation of burning zone temperature and we have to control the fuel rate to compensate the latter. Though the measurement of burning zone temperature is quite difficult, the disturbance due to falling of mud ring or coating can clearly be recognized on kilowatt record.[10] Also it seems that, by using our present approach, we can eliminate from the variation of kilowatt the contributions from variations of exit gas temperature and cooler pressure and thus detect the disturbance originated in kilowatt. From the result of $R_{ij}(f)$ analysis of kilowatt of Fig. 13 we can expect that this kilowatt disturbance is relatively significant at higher frequencies

for this kiln #2. Thus it seems that the necessary control will be of high frequency characteristic and will be implemented without much interference to the exit gas temperature control. The kilowatt term in the original program was meant for this purpose and worked effectively when kilowatt was noisy. But its low frequency characteristic was somewhat unsatisfactory and our present observation suggests us to suppress the gain of this control loop at lower frequencies. We shall have to extend our analysis to the relation between the fuel rate, the kiln load, or kilowatt, and the burning zone temperature. In Fig. 18 is given a schematic representation of possible overall control system, attention being paid to the frequency characteristics of the components. G_{bz}, G_{kiln} represent conceptually the response characteristics of the burning zone with respect to heat transfer, of the kiln with respect to mass transfer, respectively. It is considered that the kilowatt noise is affecting G_{bz} through heat capacity variation induced by mass variation and through heat gain variation induced by profile variation of the flame and the T_{bz} compensation loop is to compensate for these effects. It is obvious that our original program may not cover the very low frequency range, say 1 cycle per 12 hours or lower. This very low frequency variation reflects the variation of the profile of the kiln. From our experiences, it seems quite possible to use the temperature of the wall as an index to detect this variation. The location of the thermo couple has been carefully chosen so as to keep it free from the noise due to the variation of coating condition. After the completion of the control of the exit gas temperature any variation of this wall temperature will suggest the variation of the kiln profile and we are expecting that we shall be able to regulate this by draft control. It may be necessary to relate our present observation with the static behavior of our kiln. There are many papers which treat the heat and material balance within a kiln [11, 12, 13, 14] and we have done the numerical analysis of the static profile of our kiln #2 following the procedure given by Stillman[11]. The result is given in Fig. 19.

It may be worth mentioning here that the control schemes hitherto developed on the static model have definite drawbacks. In Figs. 20, 21 are given some results of numerical analysis by our conventional lumped static equations.[15] The result suggests that by controlling the air flow rate we can regulate the content of oxygen. This kind of reasoning will only be

possible when we are dealing with d. c. components of the variables. As we have already shown, in our kiln #2, the cooler pressure which is in close relation with the air flow rate has shown a definite contribution to the kilowatt variation which shows the variation of burning condition. Thus without taking into account of this kind of dynamic relation between the variables and the spectral characteristics of noise sources we can hardly develop a control program for the stabilization of the kiln.

6. Conclusion

It has hitherto been considered that the cement rotary kiln is a very much complicated system and no one knows about the details of its dynamic behavior. Our present analysis and experiment have shown that if we carefully perform the data analysis we can get a fairly definite and objective description of a kiln behavior.

It seems reasonable to relate our result of data analysis and control experiment with a fundamental observation of material transfer within the wet process rotary kiln made by J. Rutle[10]. We focused our attention to the stabilization of exit gas temperature, and the result of experiment confirmed the validity of our approach. On this result we shall be further able to develop the overall control program following the general line of multi-input multi-output control system.[16]

It is our belief that, though there yet remain various difficulties and complexities, our result has shown that the kiln control can finally be based on a sound scientific foundation rather than on an art.

Acknowledgement

The authors express their deep appreciations of the efforts of Mr. S. Tsukata and Mr. Y. Yagihara of Chichibu Cement Co. Ltd. and of Miss E. Arahata of the Institute of Statistical Mathematics in programming and operating the computers.

References

1. T. Tashiro, T. Nakagawa & J. Hasegawa, "Chichibu cement company's new plant at Kumagaya — Japan is now under real time computer control," Quarterly of the Colorado School of Mines, vol. 59(1964), 465-492.
2. H. Akaike, "Some problems in the application of the cross-spectral method," Spectral Analysis of Time Series (B. Harris ed.), John Wiley

& Sons, Inc., (1967), 81-107.

3. H. Akaike, "On the use of non-Gaussian process in the identification of a linear dynamic system," Ann. Inst. Statist. Math., Tokyo, vol. 18 (1966), 269-276.
4. H. Akaike, "On the use of a linear model for the identification of feedback systems," Research Memo. No. 20, Inst. Statist. Math., Tokyo, April 1968.
5. H. Akaike et al, "Studies on the statistical estimation of frequency response functions," Ann. Inst. Statist. Math., Tokyo, Suppl. III (1964).
6. H. Akaike, "On the statistical estimation of the frequency response function of a system having multiple input," Ann. Inst. Statist. Math., Tokyo, vol. 17(1965), 185-210.
7. J. J. Florentin, B. D. Hainsworth, J. B. Reswick & J. H. Westcott, "Correlation analysis of a heat exchanger," Proc. Joint Symposium on Instrumentation and Computation in Process Development and Plant Design, Held at Church House, Westminster, London, 1959, Part A, 7-17.
8. T. P. Goodman & J. B. Reswick, "Determination of system characteristics from normal operating records," Tans. A. S. M. E. (1956), 259-271.
9. J. Rutle, "Investigation of material transport in wet-process rotary kilns by radio isotopes," Pitt and Quarry, July, 1955, 120-134.
10. T. Nakagawa, "On the prediction of kiln process by the pattern of kiln load record," Jour. Soc. Instr. Cont. Eng., Japan, vol. 11(1961).
11. R. Stillman, Paper presented at A. I. Ch. E. National Meeting, Calif., May, 1965.
12. H. S. Min et al, "Computer simulation of a wet process cement kiln operation," Paper presented at Fall Instrument and Automation Conf. U. S. A., Sept., 1961.
13. R. A. Phillips, "Automation of a portland cement plant using a digital control computer," Proc. 2nd IFAC Conf., Application and Components (1964), 347-357.
14. H. Gygi, "Thermodynamics of the cement kiln," Proc. of Symposium on Chemistry of Cement (1950).
15. T. Nakagawa, "Study on the control of cement rotary kiln," Ph. D.

Dissertation, Tokyo Univ. (1964).

16. K. Y. Wong et al, "Computer control of the Clarksville Cement Plant by state space design method" (to be presented at the Cement Industry Conference of IEEE in St. Louis, Mo., May, 1968).

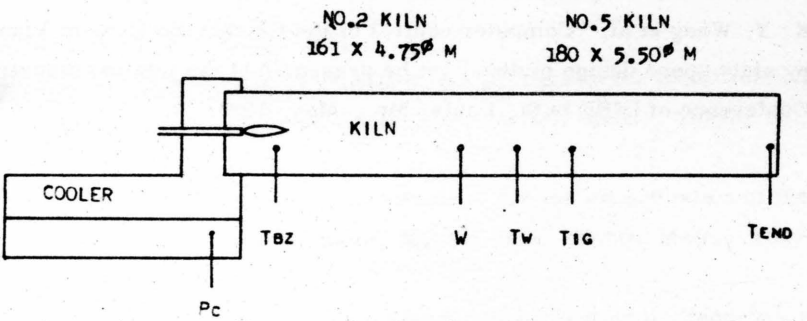

FIG. 1 KILN DIMENSION AND MAIN MEASURING POINTS

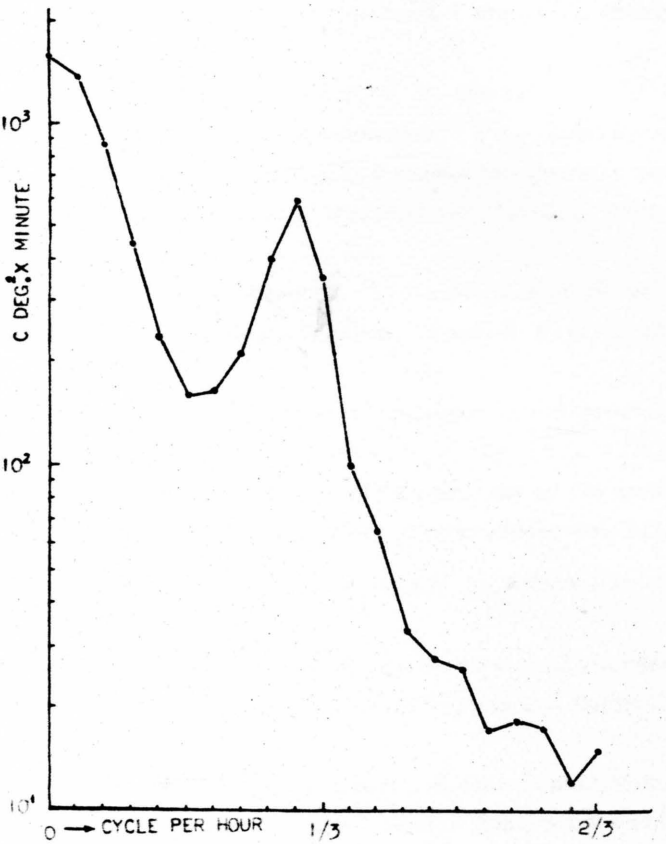

FIG. 2 POWER SPECTRUM OF EXIT GAS TEMPERATURE

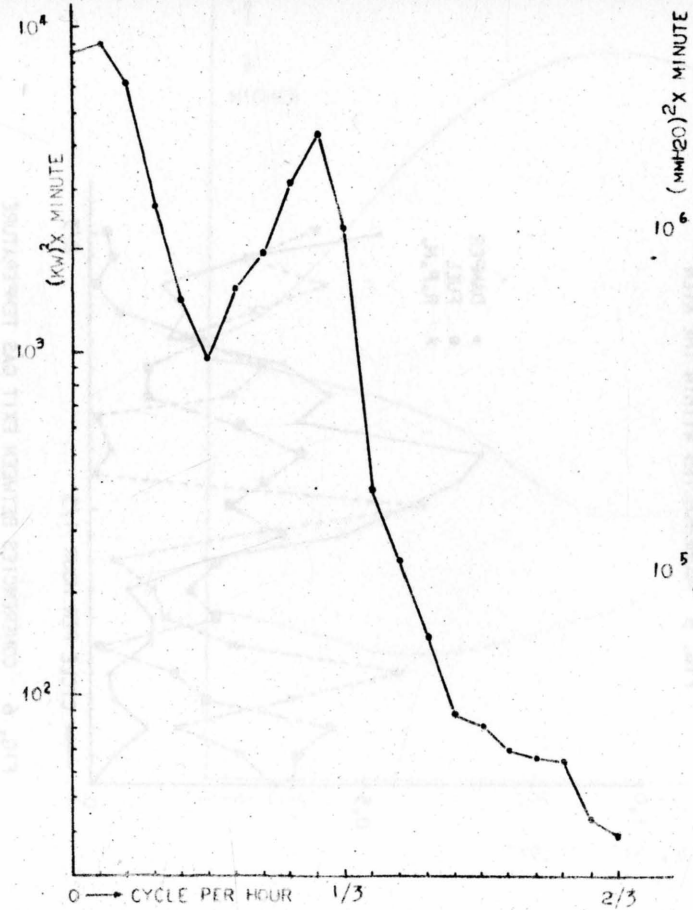

FIG. 3 POWER SPECTRUM OF KILOWATT

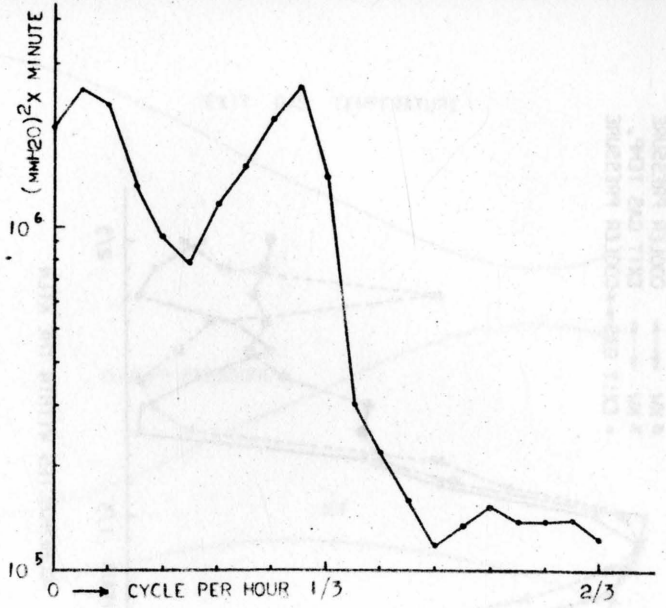

FIG. 4 POWER SPECTRUM OF COOLER PRESSURE

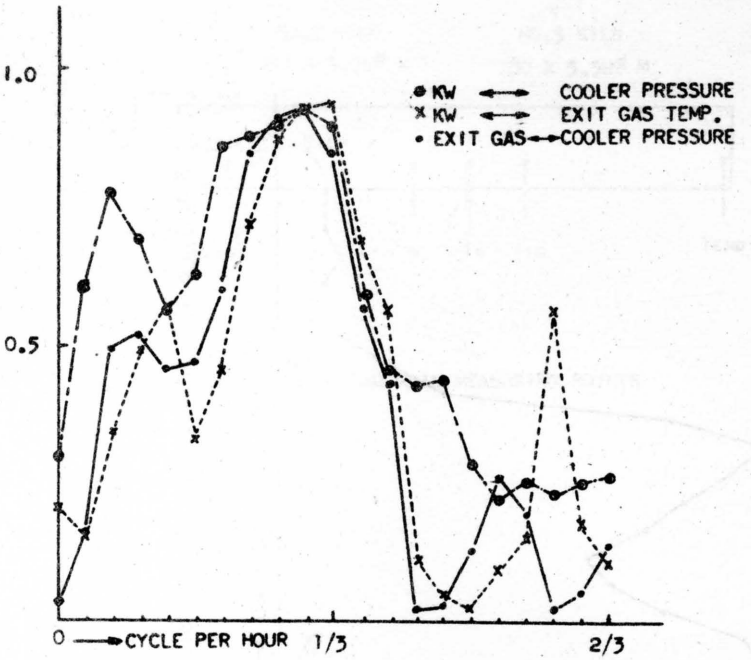

FIG. 5 COHERENCIES WITHIN THE KILN

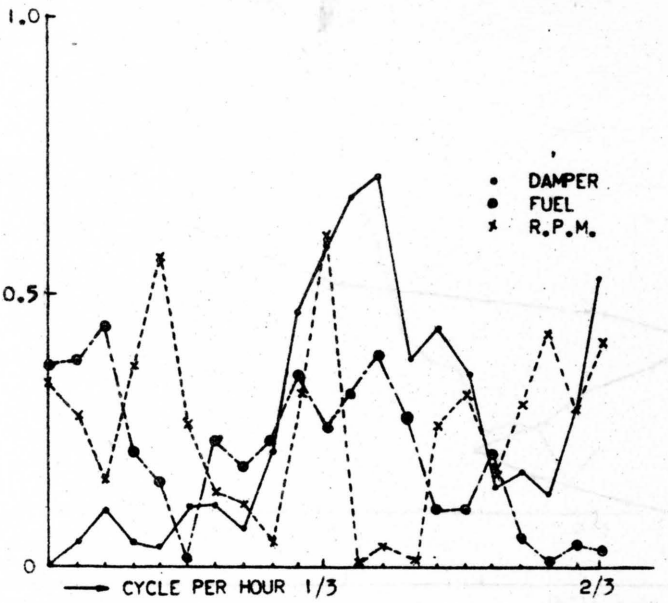

FIG. 6 COHERENCIES BETWEEN EXIT GAS TEMPERATURE AND CONTROLLING VARIABLES

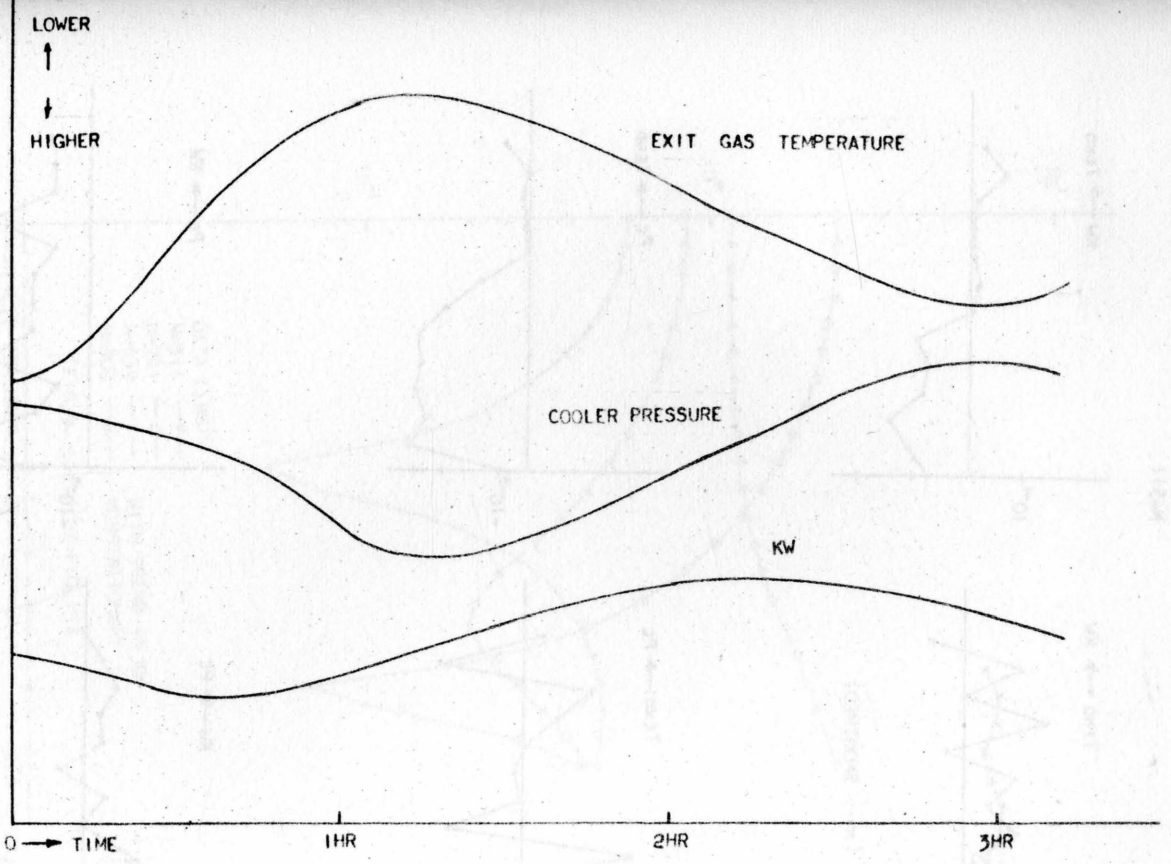

FIG. 7 TYPICAL PATTERN OF OSCILLATION

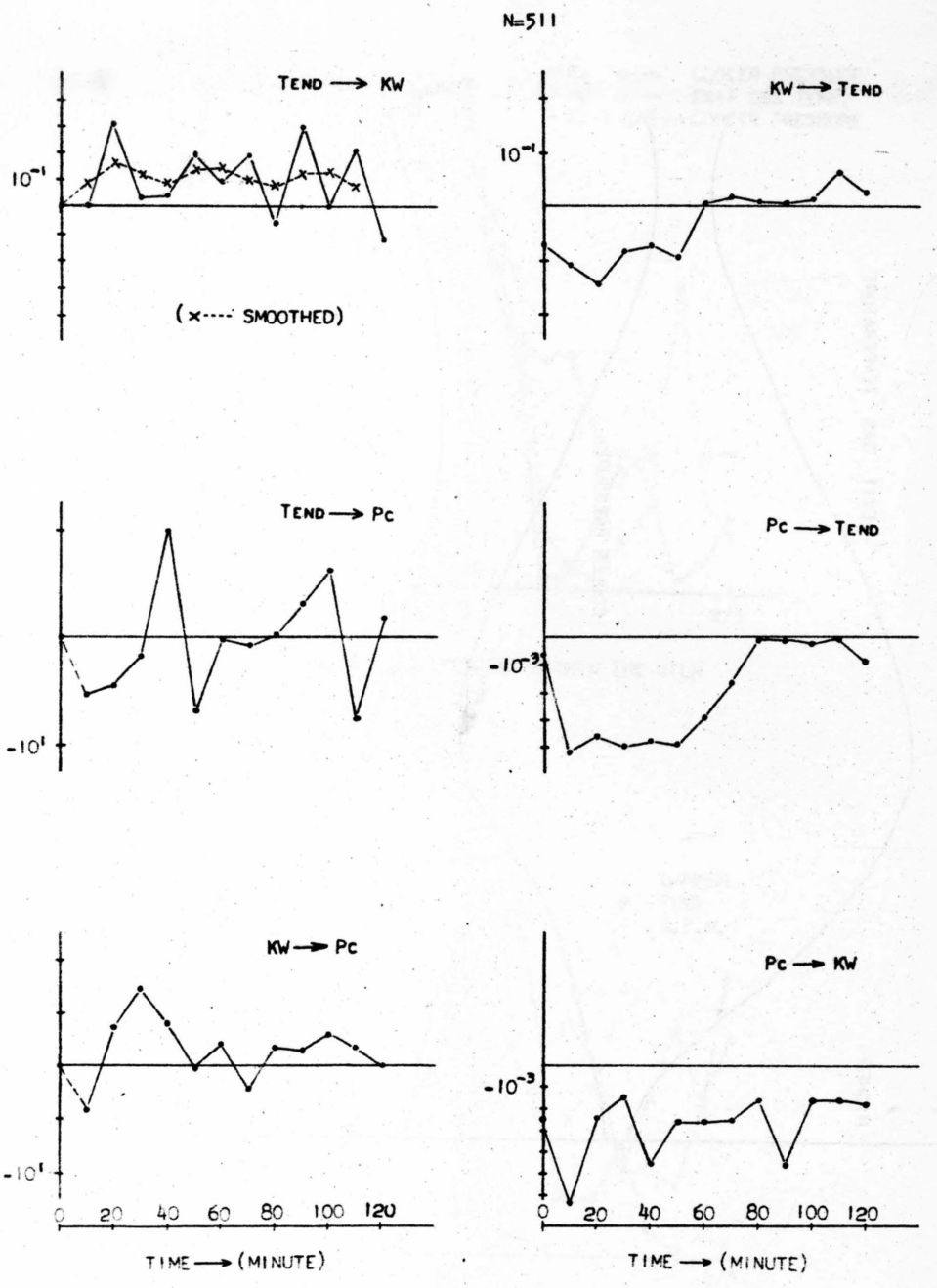

FIG. 8 ESTIMATES OF THE IMPULSE RESPONSES

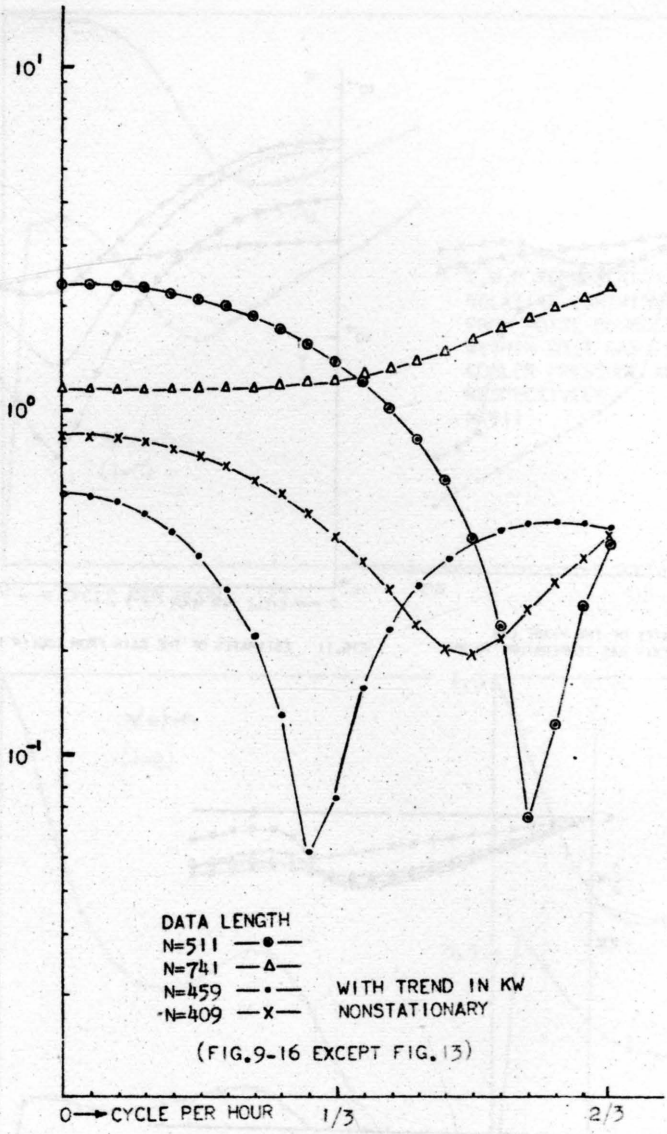

FIG. 9 ESTIMATES OF THE GAIN FROM EXIT GAS TEMPERATURE TO KW

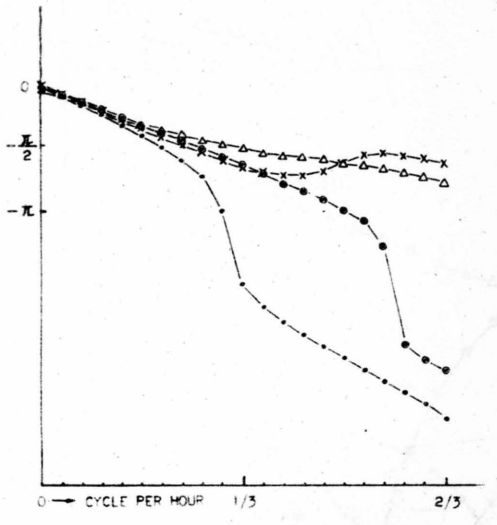

FIG. 10 ESTIMATES OF THE PHASE LAG FROM EXIT GAS TEMPERATURE TO KW

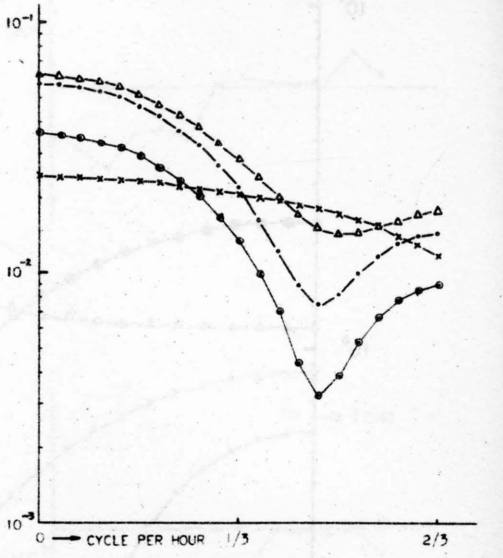

FIG. 11 ESTIMATES OF THE GAIN FROM COOLER PRESSURE TO KW

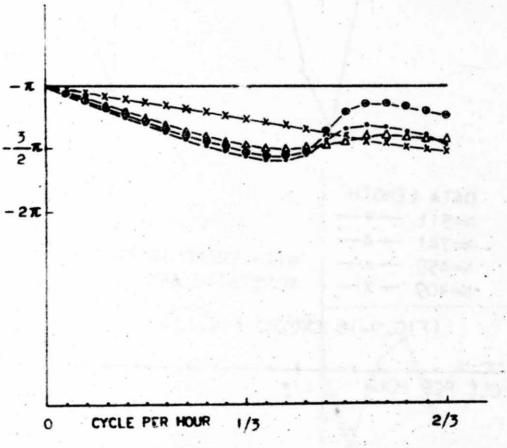

FIG. 12 ESTIMATES OF THE PHASE LAG FROM COOLER PRESSURE TO KW

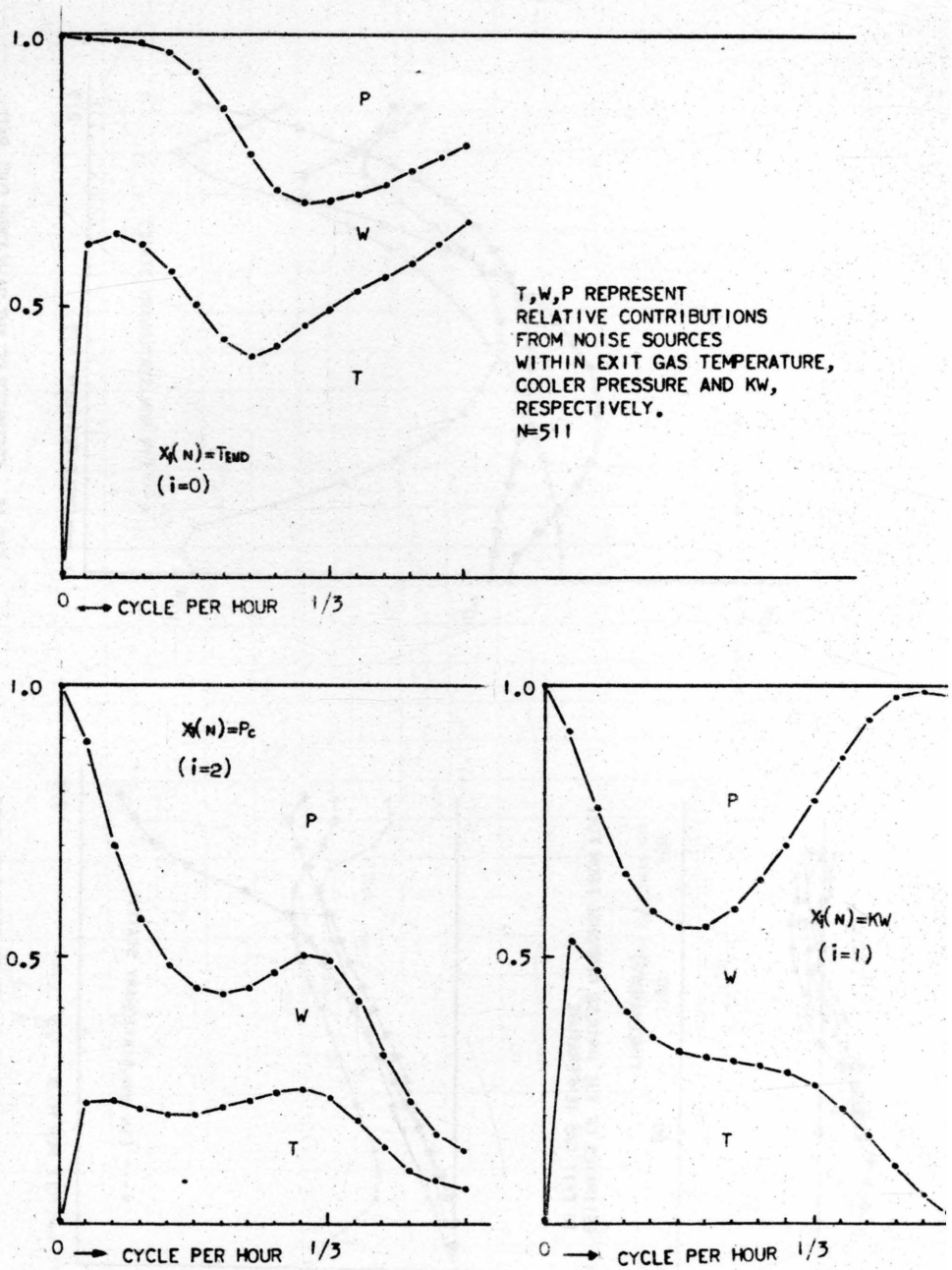

FIG.13 RELATIVE POWER CONTRIBUTIONS OF NOISE SOURCES TO Xi(N)

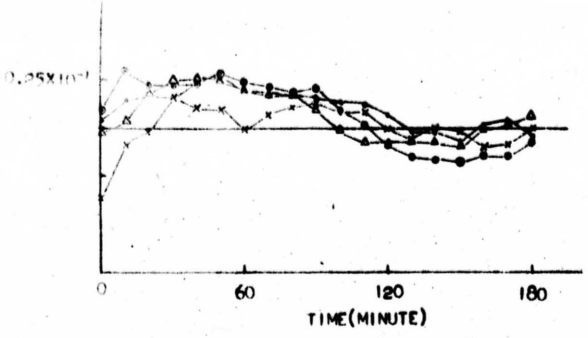

FIG. 14 ESTIMATES OF THE IMPULSE RESPONSE FROM FUEL TO EXIT GAS TEMPERATURE

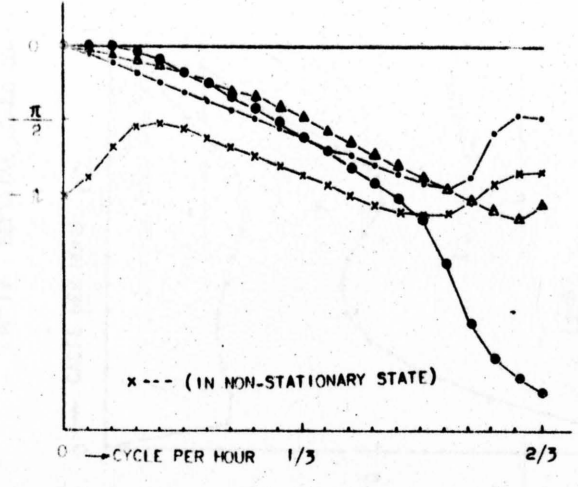

FIG. 16 ESTIMATES OF THE PHASE FROM FUEL RATE TO EXIT GAS TEMPERATURE

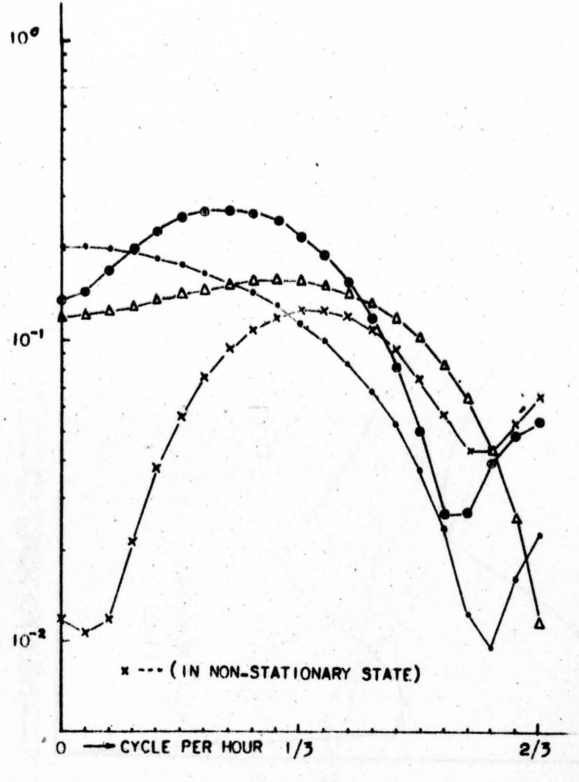

FIG. 15 ESTIMATES OF THE GAIN FROM FUEL RATE TO EXIT GAS TEMPERATURE

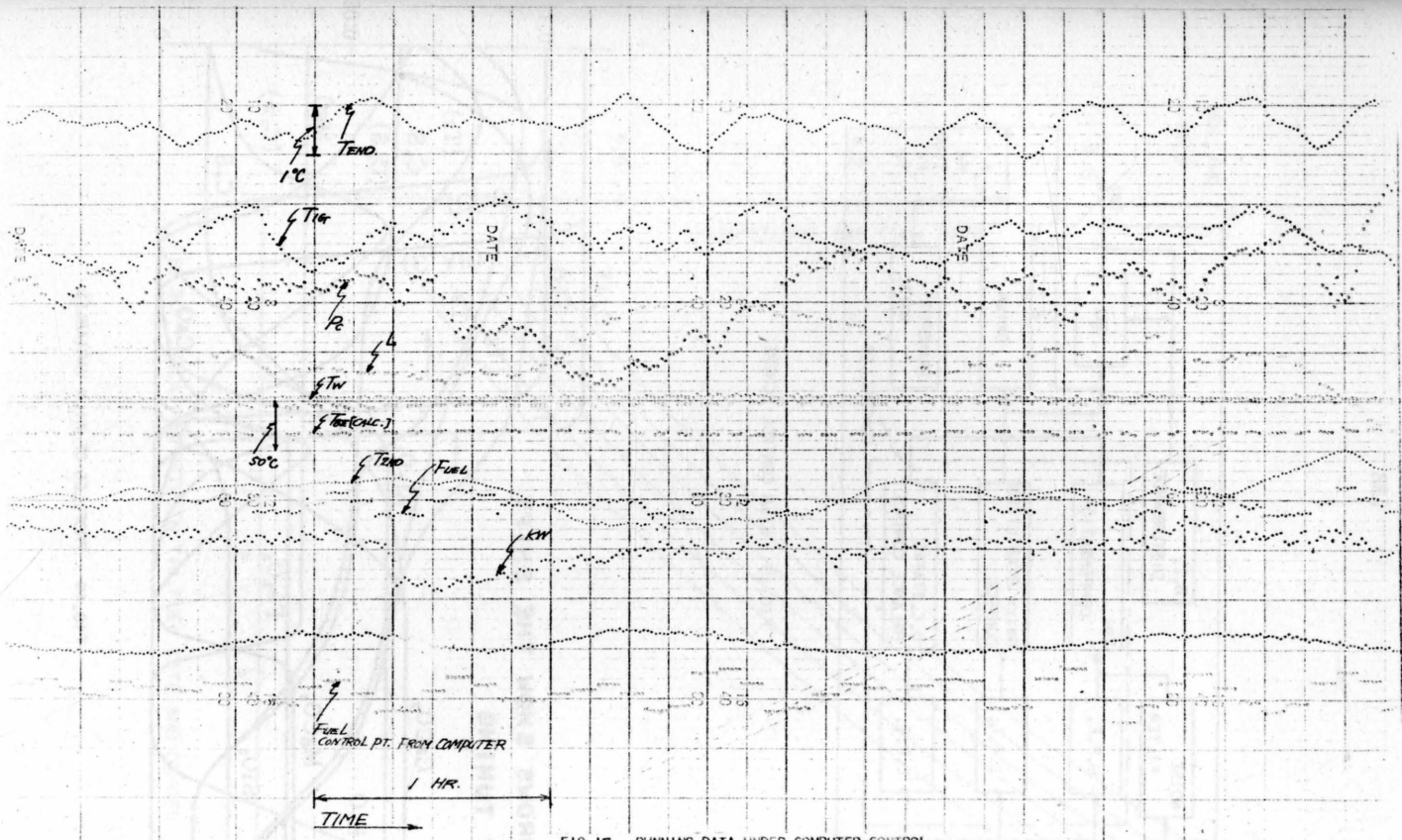

FIG. 17 RUNNING DATA UNDER COMPUTER CONTROL

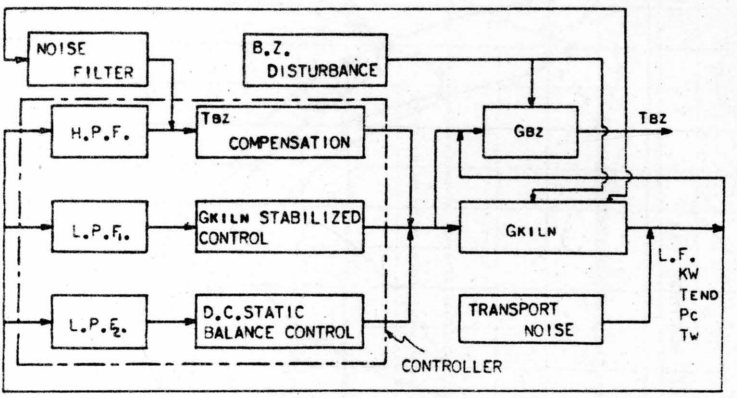

FIG.18 KILN CONTROL SCHEME

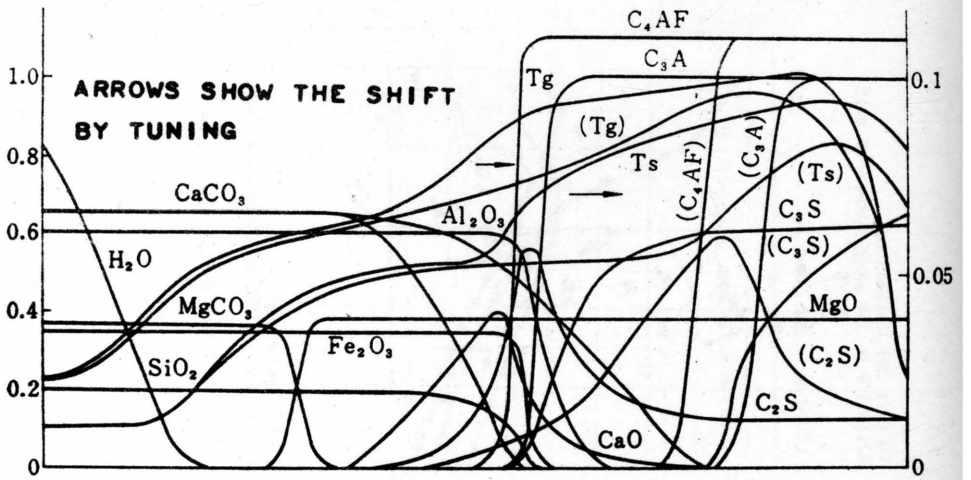

FIG.19 PROFILES OF KILN VARIABLES

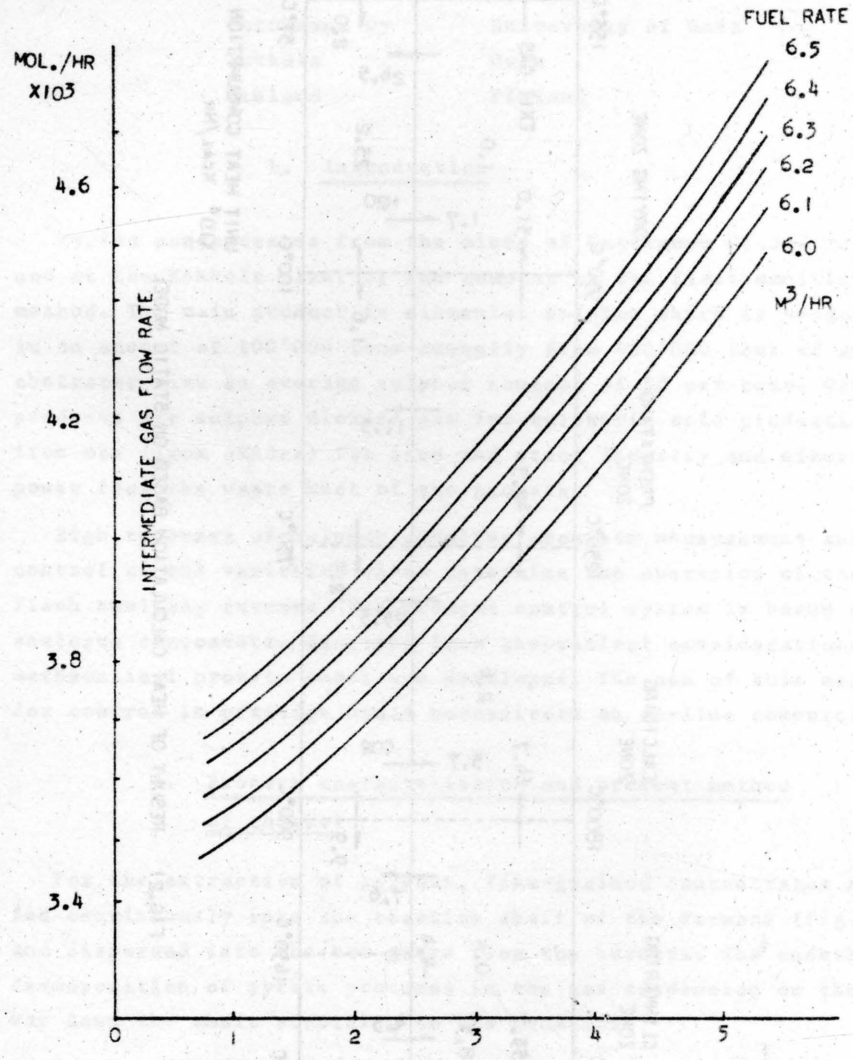

FIG.20 RELATION BETWEEN T_{IG}, FUEL RATE AND OXYGEN

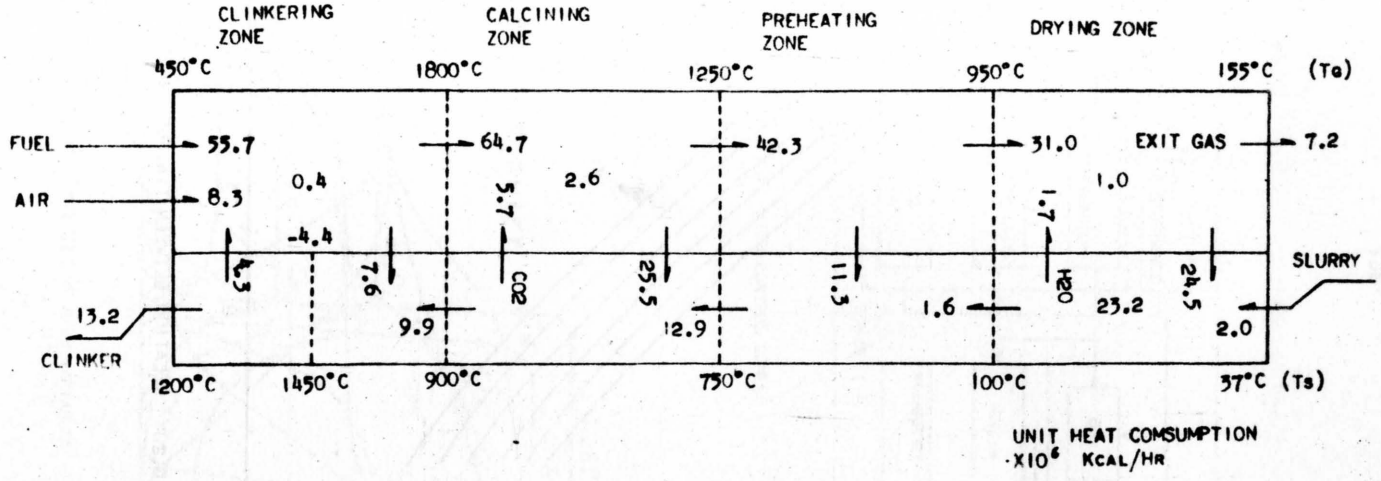

FIG.21 RESULT OF HEAT CALCULATION BASED ON STATIC MODEL

MODELLING OF A PYRITE SMELTING PROCESS

Timo Talonen
Outokumpu Oy
Kokkola
Finland

Antti Niemi
University of Oulu
Oulu
Finland

1. Introduction

Pyrite concentrates from the mines of Outokumpu Oy are refined at the Kokkola plant of the company by the flash smelting method. The main product is elemental sulphur which is produced in an amount of 100'000 tons annually from 450'000 tons of concentrates with an average sulphur content of 50 per cent. Other products are sulphur dioxide gas for sulphuric acid production, iron ore (iron oxides) for iron and steel industry and electric power from the waste heat of the process.

High recovery of sulphur requires accurate measurement and control of the variables which determine the operation of the flash smelting furnace. The present control system is based on analogue components. Starting from theoretical considerations, a mathematical process model was developed. The use of this model for control in practice would necessitate an on-line computer.

2. Process characteristics and present method of control

For the extraction of sulphur, fine-grained concentrates are fed continuously into the reaction shaft of the furnace (Fig.1) and dispersed into the hot gases from the burners. The endothermal decomposition of pyrite proceeds in the gas suspension on the way down the shaft according to the equation:

$$2\ FeS_2 \rightarrow 2\ FeS + S_2 \qquad (1)$$

The molten FeS droplets are separated from the gas stream at the bottom of the furnace and collected into the melt which is tapped for subsequent treatment by granulation and roasting. The hot gases, including the sulphur, are led from the furnace to a waste heat boiler for cooling and production of high pressure steam. This is followed by stages of purification and separation of the sulphur by condensation at a low temperature. A detailed description of the plant is available[1].

The recovery of sulphur depends essentially on the ratio of the flow rate of air to that of fuel oil used for smelting. The optimal point of operation is influenced also by the formation of carbon at low values of this ratio, since it impairs the purity of the main product. For these reasons special attention was given to the control of the individual burners and of the distribution of load among them and to the measurements required. The control system which was based on the use of conventional analogue controllers has been described in detail[2].

A complex gas atmosphere is produced, when the combustion products of fuel oil and sulphur transferred to the gas from the pyrite react with each other. Furthermore, the oxidizing and reducing constituents of gas react at relatively low temperatures down the plant producing elemental sulphur. This process is accelerated by catalysts. Thus the measurement of any single output variable is not sufficient for the control of the process for maximal productivity, but, instead, the analysis of the total gas composition would be required[2].

The ratio of the oxydizing and reducing gas components cannot be calculated simply, since a part of the oxygen from air is carried along by the molten droplets or matte. The analysis of the waste gas composition is now being measured by an on-line gas chromatograph which gives the needed information, and the flow ratio of air and fuel is adjusted on this basis. However, with an inherent delay of 10 min. in addition to the plant delay, the instrument is rather slow for closed loop control.

The amount of sulphur recovered through chemical reactions in the latter part of the plant depends on the difference of the content of sulphur dioxide and that of certain reducing components in the gas leaving the furnace:

$$D = SO_2 - \tfrac{1}{2}(H_2S + CO + COS + H_2) \qquad (2)$$

Only the above components participate signicantly in the later catalyzed reactions, which lead to the formation of elemental sulphur. The difference (2) in units of mass flow is not changed by these reactions and therefore it should have a low value after the furnace. From experience, the value corresponding to the maximal sulphur recovery differs somewhat from zero for probably nonlinear kinetics, since the reaction equilibria are not reached at the low temperature parts of the process.

A mathematical model of the furnace can be applied to the calculation of D on the basis of variables which are readily measurable, instead of using a rather slow gas analyzer. An experimental model for the latter part of the plant should be developed, or experimental optimization, based on the measurement of the composition of the waste gas, be used in order to find the exact location of the optimum and its dependence on the gas flow and the formation of carbon. This part of the process has some similarity with the corresponding part of the process used for recovery of sulphur from natural gases where the experimental optimization is based on the determination of the SO_2 and H_2S contents[3,4].

From the input variables of the furnace model the flow rates of air and oil are known by measurements. The concentrate feed cannot be measured accurately, because of the heavy construction of the feeders. However, this feed has an immediate influence on the gas temperature, which is measured and can be used as input data for the calculations. This dependence is currently used for the control of the furnace temperature at the level required for a sufficient fluidity of slag (cf. Fig.3). The compositions of the concentrate and oil change slowly and are known through sampling and off-line analysis.

3. Mathematical model

The model of the flash smelting process is based mainly on theoretical considerations. The temperature of the gas is at this stage so high, that the state of the thermodynamic equilibrium is reached and kinetics may be neglected. Because of the short residence time of the materials in the reaction shaft, the flash smelting can be considered as a process of zero capacity. A

semi-empirical relationship is used between the matte and gas compositions.

3.1. Basic equations

A group of equations is written according to the basic assumptions for computing the outputs from the values of input variables. The equations are listed in the Appendix.

The mass balance equations for a volume unit of gas are written for a mono- or diatomic form of each element present in the gas phase (equations A9-A13). The next equation (A14) sets the sum of all gas components or of their partial pressures equal to one.

The equations for eight reaction equilibria (A1-A8) are needed for the solution of the gas composition at a high temperature. The selection of the components is based on both thermodynamic considerations and experimental results. The equilibrium constants K are functions of temperature. They can be derived from the free energies of the reactions, obtained from the literature[5].

$$K = e^{-\Delta G^{o}_{T}/RT} \qquad (3)$$

ΔG^{o}_{T} free energy of the reaction (a function of temperature)
R gas constant
T absolute temperature

The heat balance equation (A15) for the heterogeneous suspension at the lower end of the shaft includes the heat brought into the process on the left and the heat leaving it on the right hand side. The heats of combustion were determined by assuming water as the oxydized state for hydrogen, CO_2 for carbon, SO_2 for sulphur and hematite for iron. The feed includes also some solid inert materials which melt without participating in the reactions and form a thin slag layer on the surface of the bath. Data for the expressions of the heat contents above the standard state were taken from the same source[5].

The composition of the matte is obtained from the equations (A16-A18) by means of the oxygen content of the gas and the temperature. The semi-empirical equation (A16) gives the ratio of the oxygen and sulphur contents of the matte[6]. The values of the para-

meters have been checked according to experimental results. The matte is considered as a mixture of FeS and Fe_3O_4, an assumption supported by the results of laboratory studies of matte samples.

The transfer of oxygen to the matte, and the transfer of sulphur to the gas are taken into account by the equations (A19-A21).

The compositions of the matte and gas can be calculated from this group of equations by means of the known values of the inputs and the parameters. Numerical iterative methods have to be used for the solution of the problem which can be stated in the general form:

$$f_i(x_1, x_2, \ldots, x_n) = f_i(X) = 0 \qquad (i=1,2,\ldots n) \tag{4}$$

3.2. Newton-Raphson and steepest descent methods of solution

While applying the Newton-Raphson method, a correction ΔX is sought for the initial estimate X^o so that the new point satisfies the equations

$$f_i(X + \Delta X) = 0 \qquad (i=1,2,\ldots,n) \tag{5}$$

The equations are expanded into Taylor series and all terms higher than the first order are neglected. A set of linear equations is obtained, giving the correction ΔX and a new estimate for X. The procedure is repeated until the difference between two successive solutions is under a chosen value.

For the use of the method of steepest descent the sum of the squares of the residuals is formed:

$$U = \sum_{i=1}^{n} \left[f_i(X) \right]^2 \tag{6}$$

The minimum of U, equal to zero, corresponds to the solution of the equations (4). A step is taken from the initial estimate X^o in the direction opposite to that of the gradient of U and the length of the step is chosen so that the minimum of U in this direction is reached. The direction of the gradient at the new point is determined and the procedure is repeated until the value of U is less than a chosen limit.

3.3. Rosenbrock's method

Several recently developed methods are more efficient than the ones previously used, especially if the function to be minimized is complicated. Rosenbrock's method[8] is, like the method of steepest descent, an optimization procedure, and it also applies to the solution of a set of equations.

Starting from the initial estimate, a step is taken in the direction of each variable. A succesful step length is selected by systematic trials. The total step is

$$A_1 = \sum_{i=1}^{n} d_i \xi^o{}_i \tag{7}$$

d_i step in direction i

ξ_i^o unit vector in direction i

Before the next step is determined, a new set of coordinates is selected. A set of vectors is set up as follows:

$$\begin{aligned} A_1 &= d_1\xi_1^o + d_2\xi_2^o + \ldots + d_n\xi_n^o \\ A_2 &= \quad d_2\xi_2^o + \ldots + d_n\xi_n^o \\ &\ldots\ldots \\ A_n &= \quad\quad\quad\quad d_n\xi_n^o \end{aligned} \tag{8}$$

The set of coordinates is now calculated by the Gram-Schmidt orthogonalization process from the vectors A_i, so that one of the new coordinates has the direction of the previous total step. The next step is taken along the new coordinates.

A considerable advantage of the Rosenbrock's method is that the partial derivatives of the objective function U need not be calculated. The iteration converges better than for earlier methods especially if the surface, defined by the objective function, forms a curved valley. One of the coordinate vectors takes the direction of the valley and the progress towards the minimum at the bottom of the valley is fast. The method of steepest descent is inefficient in cases like this. It requires that the contours of the function are more circular. The Newton-Raphson method converges only if the initial estimate is close to the correct solution.

For physical or practical reasons there are regions where the solution cannot lie, and often the best solution is to be found on the boundary of such a region. In order to find a maximum, Rosenbrock uses for each of these restrictions, a function ϕ_i with the following properties:

$$\phi_i = \begin{cases} 0 \text{ if } x_i \text{ is in the prohibited region} \\ 1 \text{ if } x_i \text{ is in the permitted region, except for a very narrow boundary region where } \phi \text{ changes from one to zero according to some suitable smooth function.} \end{cases} \quad (9)$$

Now the maximum of an objective function U' is to be sought, instead of that of U.

$$U' = \phi_1\phi_2.....\phi_m U \quad (10)$$

3.4. Solution procedure

While solving the furnace model given in the Appendix under typical operating conditions, it turned out that the iteration, according to the Newton-Raphson method, diverged. It was noticed, on closer study, to be improbable that a convergence could be achieved even through a mathematical modification of the basic problem, and therefore the application of this method was not developed further. Instead, the steepest descent method was tried, after the set of equations had been condensed analytically to three equations with three unknown variables. However, the convergence was so slow that no practical result was obtained.

Through a somewhat laborious analytical elimination, the model was reduced to the form of two equations with two unknowns viz. the partial pressures of diatomic sulphur and sulphur dioxide. The objective function consisted of the squared residuals of the mass balance equations for sulphur and oxygen. In this case the analytical calculation of the partial derivatives should have been abandoned and since much of practical evidence had been obtained of the known defincencies of the steepest descent method[8], this method was no longer applied.

Fig. 2 presents some contours of the objective function for a typical point of operation. It can be seen that the minimum is located at the lowest point of a curved valley. Thus it may be

expected that the Rosenbrock's method which was applied next would be superior to the other two, in the case considered.

The expression of the function U to be minimized includes square roots of some of the components. It was noticed that the method used by Rosenbrock for determination of the step length could lead to negative values of these variables. The solution is limited to the positive region of the variables, since negative partial pressures cannot exist, and so the programming for complex numbers is not motivated. It is also obvious that, because of the finite values of the equilibrium constants, the minimum of U cannot lie on the limit. Thus the artificial boundary region (9) is not required.

The procedure applied, in case the square root of a negative number was met, was to give U, without further calculations, the preceding value multiplied by ten. Consequently, the point beyond the frontier was rejected and the iteration was continued with shorter step lengths.

The solution of the problem by Rosenbrock's method was programmed for the Elliott 503 computer. The iteration converged well and the solution was obtained in 5-15 seconds for each set of input values, the time depending on the desired accuracy. In order to achieve reasonably accurate results for some of the most important outputs, the sum of the squared residuals had to be in an order of magnitude of 10^{-8} - 10^{-10} (cf. Fig.2). In addition to the quantities needed for the control, the values of several other output variables have been calculated, both of those listed in the Appendix and of their functions.

Applying the development of Rosenbrock's method by Davies, Swann and Campey, the value of the objective function is calculated at three points on the direction of each coordinate[9]. The step is taken to the minimum point determined by a parabola going through these three points. It was detected recently that negative partial pressures could be totally avoided by the use of this method[7].

4. Applications of the model

When the gas composition is known through the model calculations, a deviation of the quantity D (2) from the desired value can be used as the basis of the adjustment of the flow ratio of air and fuel. In Fig. 3, this type of control has been added to a scheme showing the present control method. A further development would be to consider the limit set to the total gas flow by the cooling capacity of the plant which is also a function of the gas composition.

If the equations (A16-A21) dealing with the matte composition are left out, the model could be applied for the process gas in other parts of the plant also. However, at lower temperatures down the plant the chemical equilibria are not reached and the model does not give the realistic results. Even the theoretical equilibrium calculations need some extra care at low temperatures, where the objective function is more difficult to deal with.

Up to now, the model has been used off line for preparing tables of composition corresponding to a variety of sets of inputs for the process operators. However, it is considered that the automatic control of the furnace, on the basis of the model, is expedient, so the on-line control computer has been suggested for this and some other tasks in the plant. It is expected that the model calculations would take an appreciable part of the computer time, since because of its sensitivity, the model obviously cannot be much simplified. The comparison of the results to the signals from the gas chromatograph gives a possibility of a continuous check of the values of parameters in the semi-empirical equation (A16).

The sulphur yield function is being studied, but it is not considered the final criterion, since also some other factors affect the economy of operation, although in a less degree. An expression has been somposed which insludes as the feed materials the concentrate and fuel oil and as products sulphur, SO_2 gas and iron ore produced from the matte through roasting and the high and low pressure steams from the boilers. The expression does not include new variables, and at present a procedure is being developed for detecting the air to oil ratio which would correspond to the

optimum of this criterion under typical operating conditions. The recently developed methods of mathematical optimization find application also here.

Acknowledgements

The authors wish to thank the Outokumpu Oy company, especially the Manager of the Kokkola works, Mr. H. Tanner for the opportunity of using plant data, and the Smelter Superintendent, Mr. E. Nermes for advice on the metallurgy of the process.

References

1. -, Outokumpu Process for the Production of Elemental Sulphur from Pyrites. Sulphur, Feb. 1964, 33-38.
2. Niemi, A., Regelung des Schmelzofens bei der Gewinnung von Schwefel in Kokkola (Finnland). Siemens-Z., 40(1966), 172-177.
3. Carmassi, M., Helein, J., Rouxel, R., Optimization of a Sulphur Recovery Plant. Proc. IFAC Tokyo Symp. 1965, 219-228.
4. Carmassi, M., Melennec, J., Rouxel, R., New Developments in the Optimization of a Sulphur Recovery Plant. Proc. 2nd IFAC/IFIP Int. Conf. Menton 1967.
5. Kubaschewski, O., Evans, E., Alcock, C., Metallurgical Thermochemistry, Pergamon, 1967.
6. Mäkipirtti, S., Internal Report, Outokumpu Oy, Pori, 1963.
7. Heikkilä, S., Internal Reports, Outokumpu Oy, Tapiola, 1968.
8. Rosenbrock, H., An Automatic Method for finding the Greatest or Least Value of a function, Computer J. 3(1960), 175-184.
9. Fletcher, R., Function Minimization without Evaluating Derivatives - a Review, Computer J. 8(1965), 33-41.

Appendix

Equations of the pyrite smelting furnace

$$CO_2 = K_1\sqrt{O_2} \cdot CO \qquad \text{(A 1)}$$

$$H_2O = K_2\sqrt{O_2} \cdot H_2 \qquad \text{(A 2)}$$

$$SO_2 = K_3\sqrt{S_2} \cdot O_2 \qquad \text{(A 3)}$$

$$H_2S = K_4\sqrt{S_2} \cdot H_2 \qquad \text{(A 4)}$$

$$COS = K_5\sqrt{S_2} \cdot CO \qquad \text{(A 5)}$$

$$S_4 = K_6(S_2)^2 \qquad \text{(A 6)}$$

$$S_6 = K_7(S_2)^3 \qquad \text{(A 7)}$$

$$S_8 = K_8(S_2)^4 \qquad \text{(A 8)}$$

$$\tfrac{1}{V}\Sigma C = CO_2 + CO + COS \qquad \text{(A 9)}$$

$$\tfrac{1}{V}\Sigma H_2 = H_2O + H_2 + H_2S \qquad \text{(A 10)}$$

$$\tfrac{1}{V}\Sigma S = SO_2 + H_2S + COS + 2S_2 + 4S_4 + 6S_6 + 8S_8 \qquad \text{(A 11)}$$

$$\tfrac{1}{V}\Sigma O_2 = SO_2 + CO_2 + 1/2(H_2O + CO + COS) + O_2 \qquad \text{(A 12)}$$

$$\tfrac{1}{V}\Sigma N_2 = N_2 \qquad \text{(A 13)}$$

$$1 = \sum_1^{13} Y_i \qquad \text{(A 14)}$$

$$(GH)_{conc} + (GH)_{oil} + (GH)_{air} = (GH)_{Fe_3O_4} + (GH)_{FeS} + (GH)_{slag} + V\sum_1^{13} Y_i H_i + Q \qquad \text{(A 15)}$$

$$\frac{N_O}{N_O + N_S} = A\left(\text{Log } O_2 + B + \frac{E}{T}\right) \qquad \text{(A 16)}$$

$$\frac{G_{Fe_3O_4}}{G_{conc}} = \frac{M_{Fe_3O_4}\, C_{Fe}}{M_{Fe}\left(3 + 4\frac{N_S}{N_O}\right)} \qquad \text{(A 17)}$$

$$G_{FeS} = \frac{4M_{FeS}N_S}{M_{Fe_3O_4}} G_{Fe_3O_4} \qquad \text{(A 18)}$$

$$O_{2matte} = \frac{22.4 \cdot 2G_{Fe_3O_4}}{M_{Fe_3O_4}} \qquad \text{(A 19)}$$

$$\Sigma O_2 = 0.210\left(\frac{G}{\rho}\right)_{air} - O_{2matte} \qquad \text{(A 20)}$$

$$\Sigma S = 22.4\left(\frac{G_{conc}C_S}{M_S} - \frac{G_{FeS}}{M_{FeS}}\right) \qquad \text{(A 21)}$$

Symbols

- Variables to be solved

Y_i $(i=1,2,\ldots,13) = S_2, S_4$ $S_6, S_8, SO_2, COS, CO, CO_2,$ $H_2S, H_2, H_2O, O_2, N_2$	Partial pressures or fractions of gas components
V	Flow of gas NTP
$\Sigma O_2, \Sigma S$	Total flow of gaseous oxygen, sulphur compounds
O_{2matte}	Oxygen transferred to matte in unit time
N_S/N_O	Ratio of atomic fractions of sulphur and oxygen in matte
G_{conc}	Feed of concentrate
G_{FeS}, $G_{Fe_3O_4}$	Production of FeS, Fe_3O_4

- Input data and parameters

C_{Fe}, C_S	Iron, sulphur content of concentrate
G_{oil}, G_{air}	Feed of fuel oil, air
T	Temperature of gas and matte
$T_{air}, T_{oil}, T_{conc}$	Temperature of air, oil, concentrate
$H_{oil} = f(T_{oil})$	Heat content above 25°C+ heat of combustion of fuel oil
ρ	Density
M	Molecular weight
A, B, E	Experimental parameters

- **Auxiliary variables**

K_i	$= f(T)$ $(i=1,2,\ldots,8)$	Equilibrium constant
$\Sigma C, \Sigma H_2$	$= f(G_{oil})$	Total flow of gaseous carbon, hydrogen compounds
ΣN_2	$= f(G_{air})$	Flow of nitrogen
$H_i, H_{FeS}, H_{Fe_3O_4}$	$= f(T)$ $(i=1,2,\ldots,13)$	Heat content 25°C + heat of combustion of a gas component, FeS, Fe_3O_4
H_{conc}	$= f(C_{Fe}, C_S, T_{conc})$	Heat content above 25°C + heat of combustion of concentrate
H_{air}	$= f(T_{air})$	Heat content of air above 25°C
H_{slag}	$= f(T)$	Heat content of slag above 25°C
G_{slag}	$= f(C_{Fe}, C_S, G_{conc})$	Feed of inerts
Q	$= f(T)$	Heat loss

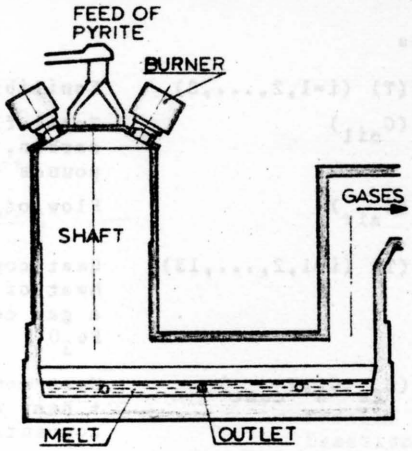

Fig. 1. Flash smelting furnace.

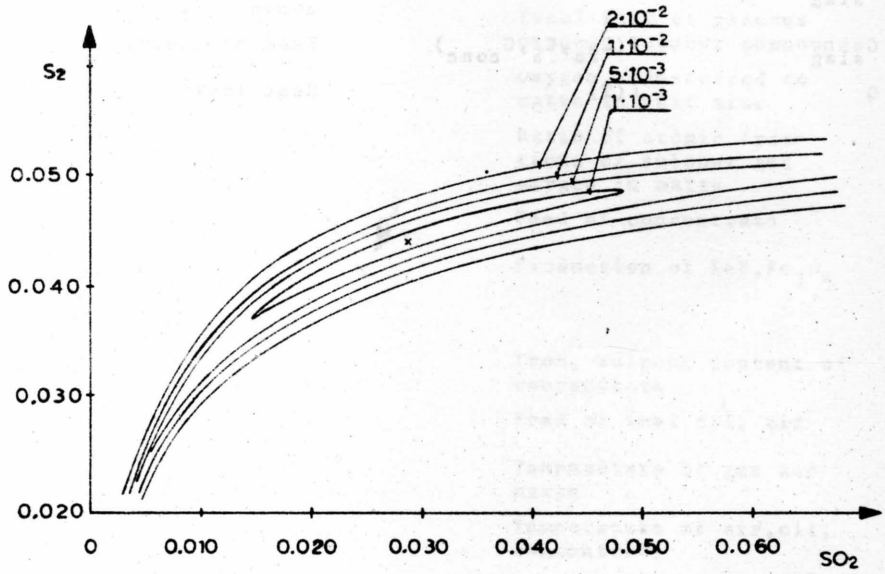

CONCENTRATE	= 75 ton/h	H_2	$= 1.127\cdot10^{-2}$	SO_2	$= 2.870\cdot10^{-2}$
OIL	= 8.7 ton/h	O_2	$= 1.710\cdot10^{-10}$	S_2	$= 4.414\cdot10^{-2}$
AIR	= 98000 Nm^3/h	N_2	$= 6.965\cdot10^{-1}$	S_4	$= 3.028\cdot10^{-6}$
TEMPERATURE	= 1219 °C	CO	$= 3.175\cdot10^{-2}$	S_6	$= 1.317\cdot10^{-10}$
		CO_2	$= 9.304\cdot10^{-2}$	S_8	$= 9.063\cdot10^{-15}$
		COS	$= 1.216\cdot10^{-3}$	H_2O	$= 8.476\cdot10^{-2}$
		H_2S	$= 8.663\cdot10^{-3}$		

Fig. 2. Contours of the objective function and coordinates of a point of operation.

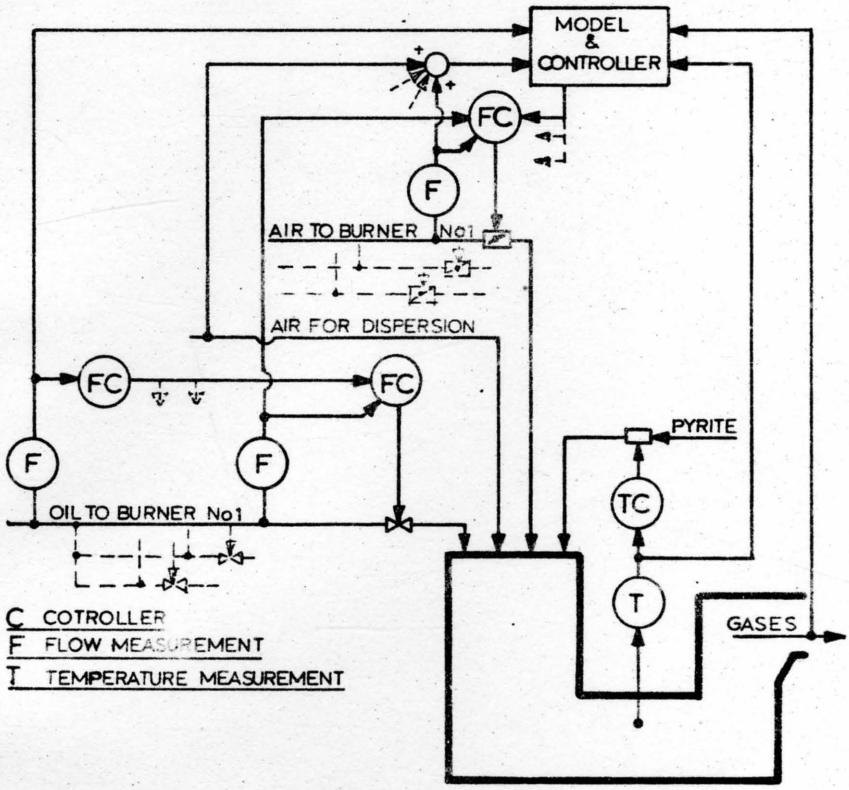

Fig. 3. A control scheme based on use of the furnace model.